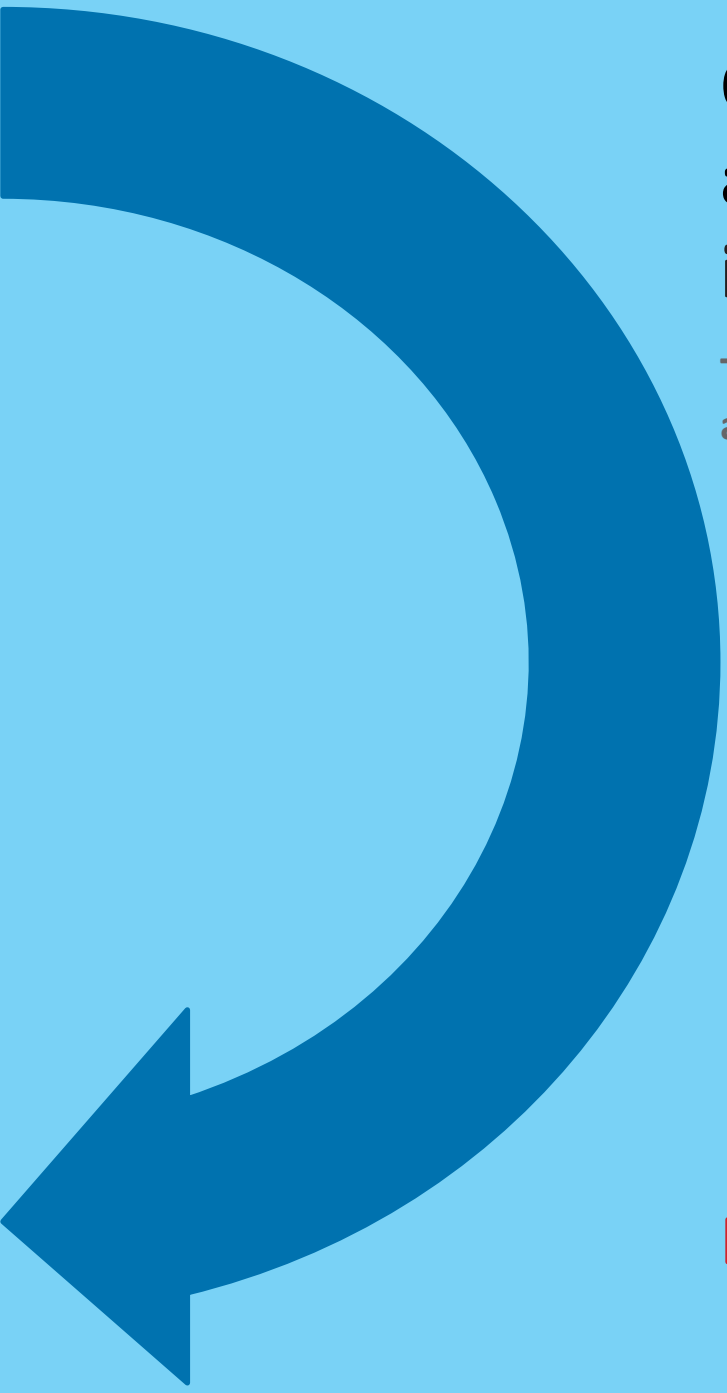

Organic Contaminants and Treatment Chemicals in Steam-Water Cycles

Thermal stability, decomposition products and flow-accelerated corrosion

David H. Moed

Organic Contaminants and Treatment Chemicals in Steam-Water Cycles

Thermal stability, decomposition products and flow-accelerated corrosion

Proefschrift

ter verkrijging van de graad van doctor
aan de Technische Universiteit Delft,
op gezag van de Rector Magnificus prof. ir. K.Ch.A.M. Luyben,
voorzitter van het College van Promoties
in het openbaar te verdedigen
op 17 november 2015 om 10:00 uur

door

David Hendrik MOED

civiel ingenieur

geboren te Amersfoort, Nederland

This dissertation has been approved by the promotors:

Prof. dr. ir. L.C. Rietveld
Prof. dr. ir. A.R.D. Verliefde

Composition of the doctoral committee:

Rector Magnificus	chairperson
Prof. dr. ir. L.C. Rietveld	promotor
Prof. dr. ir. A.R.D. Verliefde	Universiteit Gent, promotor
Independent members:	
Prof. dr. G.J. Witkamp	TNW, Technische Universiteit Delft
Prof. dr. ir. W.G.J. van der Meer	CiTG, Technische Universiteit Delf
Prof. dr. ir. K.M. van Geem	Universiteit Gent
Prof dr. ir. D.H. Lister	University of New Brunswick
Dr. ir. W. Hater	Kurita Europe

Prof. dr. ir. L.C. Rietveld (Technische Universiteit Delft) and prof. dr. ir. A.R.D. Verliefde (Universiteit Gent) have as supervisors contributed significantly to the preparation of this thesis.

The following organizations have contributed financially to the research:
Evides Industriewater (Main sponsor)
E4Water
EPRI
Shell Technology Centre Amsterdam

Copyright © 2015 by D. H. Moed

ISBN:	978-94-6203-951-3
Printed by:	CPI Koninklijke Wöhrmann
Written with:	LaTeX
Cover by:	D. H. Moed

An electronic version of this document is avaialable free of charge in the TU Delft Repository

Summary

Boiler feedwater and steam have to be of high purity, because of the susceptibility of the steam-water cycle to corrosion. Organic contaminants break down in boilers by hydrothermolysis, leading to the formation of organic acid anions, which are suspected to cause corrosion of steam-water cycle components. The impact and behavior of organic decomposition products in the steam-water cycle are not well understood. While guidelines for organic contaminants are becoming stricter, organic treatment chemicals are gaining popularity. Some alkalizing amines show potential for protecting steam-water cycles against corrosion, but their thermal stability is limited and acidic decomposition products are a concern. There are no official guidelines for the application of alkalizing amines in fossil-fired plants, because their thermal stability in the hottest sections of the plant is unknown.

This thesis aims to contribute to well-founded guidelines for organic contamination and amine application in steam-water cycles to facilitate effective water treatment and chemical dosing. It does so by investigating the thermal decomposition of organic contaminants and treatment chemicals and using results to conduct corrosion experiments.

To investigate hydrothermal reactions both batch and continuous flow reactors were tested, and it was concluded that the latter are better at investigating (hydro)thermolysis of organic treatment chemicals. A flow reactor gives precise control over retention time, temperature and pressure and these parameters can be changed much faster than with a batch reactor. The flow reactor was the basis for virtually all thermal stability and decomposition experiments described in this thesis.

It was found that lower heating rates give more organic acid anions as degradation products from organic carbon, both in quantity and variety. Thermal stability of the decomposition products determines which of these products is most prevalent. As boiler temperature increased, acetate became the dominant degradation product, due to its higher thermal stability. Shorter retention times led to more variety and quantity of organic acid anions, due to a lack of time for the thermally less stable ones to degrade.

The (hydro)thermolysis of monoethylene glycol and slurry oil produced up to a few hundred ppb acetate and formate. The (hydro)thermolysis of polyethylene glycol produced a high variety and quantity of organic acid anions, that could only partially be determined to be in the lower ppm range. The (hydro)thermolysis of the water dissolvable fraction of gasoil, naphtha and hydro wax did not lead to an increase in organic acid anions. Methyl ethyl ketoxime thermally degraded into several organic acid anions and nitrite in the higher ppb or lower ppm range.

By using the flow reactor to investigate amine thermal stability, it was concluded that thermolysis under superheater conditions was more rapid than hydrothermolysis under boiler conditions. Anionic decomposition products

increased linearly over time, while the thermal decomposition of morpholine followed first order kinetics. Metal catalysis of amine thermolysis caused by oxides on the inner surface of superheater tubes was investigated by using varying sizes and elemental composition. Kinetics of morpholine and ethanolamine thermolysis decreased as the tube size increased. The relation between the surface:volume ratio and the degradation rate constant was linear. Although results varied between the two applied tubing materials, there is no consistent trend that can link thermolysis kinetics to tube wall composition.

The thermolysis of five alkalizing amines and two organic acids was comprehensively tested at superheater conditions. Morpholine, ethanolamine, cyclohexylamine, dimethylamine, 3-methoxypropylamine and acetic acid were shown to undergo thermolysis according to first order kinetics. The activation energy, prefactor and activation volume were obtained from the experimental data for all investigated amines. Dimethylamine did not fully degrade, in spite of longer retention times being applied, suggesting synthesis may occur. Formic acid is very unstable under steam water cycle conditions. It is still found in high temperature and pressure steam-water cycles though, and therefore it is plausible that it is synthesized in the condensing stages. Acetic acid has higher thermal stability than all other tested compounds and is therefore the dominant organic acid anion at high temperatures. Cationic degradation products were ammonia and some amines, meaning that the complete thermolysis of an amine does not necessarily lead to acidic conditions, as the formed ammonia also provides protection. A model was constructed to predict the thermal stability of the amines in steam-water cycle. More plant data is necessary to fully validate the model.

Runs conducted with an experimental two-phase flow-accelerated corrosion loop showed a linear relation between liquid film pH and obtained corrosion rates for the same steam quality. The tested steam quality was not high enough to create the conditions in which ammonia provides insufficient protection against acetic acid, but expanding the liquid film pH model to higher steam qualities does give an idea of the dangers of high acetate concentrations in a steam-water cycle.

The models for calculating the pH of the liquid film in two-phase flow and amine thermolysis (if validated) could be connected to assess if alkalizing amine application is recommended for a specific steam-water cycle. In general, it can be concluded from the results that ethanolamine provides better protection against two-phase flow-accelerated corrosion in the presence of organic acid anions, so there is a maximum superheater temperature for each amine at which it can be applied. When ammonia is the only volatile treatment chemical protecting the steam-water cycle, organic acid anions in the plant should be reduced until theoretical pH drop of the two-phase liquid film is acceptable.

Samenvatting

Ketelvoedingswater en stoom moeten van hoge zuiverheid zijn, omdat de stoom-watercyclus zeer gevoelig is voor corrosie. Organische vervuilingen breken af in ketels door hydrothermolyse, waardoor organische zuren gevormd worden, welke ervan verdacht worden corrosie te veroorzaken. De impact en het gedrag van organische afbraakproducten in de stoom-water cyclus is onderbelicht. Terwijl richtlijnen voor organische vervuilingen strenger worden, winnen organische behandelingschemicaliën steeds meer populariteit. Sommige amines zouden de stoom-water cyclus kunnen beschermen tegen corrosie, maar hun thermische stabiliteit is beperkt en zure afbraakproducten zijn een risico. Er zijn geen officiële richtlijnen voor de toepassing van amines in fossiele krachtcentrales, omdat hun thermische stabiliteit in de heetste onderdelen van de centrale onbekend zijn.

Dit proefschrift heeft als doel bij te dragen aan goed onderbouwde richtlijnen voor organische vervuilingen en de toepassing van amines in stoom-water cycli om effectieve waterbehandeling en chemicaliëndosering mogelijk te maken. Dit wordt bewerkstelligd door de thermische ontbinding van organische vervuilingen en behandelingschemicaliën te testen en de resultaten te gebruiken voor corrosie-experimenten.

Om hydrothermische reacties te onderzoeken zijn zowel een batchreactor als een propstroomreactor getest, waarbij geconcludeerd is dat de laatste beter is voor het onderzoeken van de (hydro)thermolyse van organische vervuilingen en behandelingschemicaliën. Een propstroomreactor biedt nauwkeurige over retentietijd, temperatuur en druk en deze parameters kunnen veel sneller veranderd worden dan met een batchreactor. De propstroomreactor is de basis voor vrijwel alle ontbindings- en stabiliteitsexperimenten die in dit proefschrift beschreven worden.

Langzamere verhitting leidt tot meer organische zuren als afbraakproducten van organisch stof, zowel in kwantiteit als variatie. Thermische stabiliteit van de afbraakproducten bepaald welke van deze producten het meest voorkomt. Als keteltemperatuur toeneemt, wordt acetaat steeds dominanter, vanwege de hoge thermische stabiliteit van dit anion. Kortere retentietijden leiden tot meer variatie en kwantiteit van organische zuren, doordat er te weinig tijd is voor de afbraak van deze zuren.

De (hydro)thermolyse van ethyleenglycol en slurry-olie produceerde tot een paar honderd ppb acetaat en formiaat. De (hydro)thermolyse van polyethyleenglycol produceerde een hoge variatie en kwantiteit aan organische zuren, waarvan de concentratie in het lagere ppm bereik zat. Methylethyl ketoxime ontbond thermisch naar verschillende organische zuren en nitriet. Hiermee zijn en aantal in petrochemische stoom-water cycli voorkomende bronnen van anionen geïdentificeerd.

Door met de propstroomreactor de thermische stabiliteit van morpoline te onderzoeken, is geconcludeerd dat de superheater meer bijdraagt aan de afbraak van amines dan de ketel. Anionische afbraakproducten namen lineair toe met de tijd, terwijl morpholine afbraak beschreven kon worden met een eerste orde relatie. Katalyse van amine thermolyse door de binnenkant van een

superheater buis was onderzocht door verschillende buisformaten toe te passen. De kinetiek van morpholine en ethanolamine thermolyse nam af naar mate de buisdiameter toenam. De relatie tussen de oppervlakte:inhoud verhouding en the afbraakconstante was lineair. Hoewel de resultaten ietwat varieerde tussen de twee toegepaste materialen, was er geen consistente trend die thermolyse kinetiek aan de samenstelling van de buiswand kan koppelen.

De thermolyse van vijf amines en twee organische zuren is uitvoerig getest onder superheater omstandigheden. Morpholine, ethanolamine, cyclohexylamine dimethylamine, 3-methoxypropylamine en azijnzuur ondergingen thermolyse volgens eerste orde kinetiek. De activatie-energie, prefactor en het activatievolume is bepaald met behulp van de experimentele data. Dimethylamine brak niet volledig af, ondanks het feit dat langere retentietijden toegepast werden, wat suggereert dat synthese plaats vindt. Mierenzuur is zeer onstabiel onder hoge temperatuur en druk en toch wordt het gevonden na blootgesteld te zijn aan extreme omstandigheden. Het is waarschijnlijk dat mierenzuur tijdens condensatie gevormd wordt uit andere afbraakproducten. Azijnzuur heeft de hoogste thermische stabiliteit van alle geteste stoffen, wat verklaart waarom azijnzuur het meest voorkomt in hoge druksystemen. Kationische afbraakproducten waren ammonia en wat andere amines, wat betekent dat de thermolyse van een amine niet altijd tot zure omstandigheden leidt. Een model was ontwikkeld om de stabiliteit van amines te voorspellen, maar voor validatie is meer praktijkdata nodig.

Acknowledgements

When starting my PhD research, I consciously decided to delve deeper into industrial water, but the actual scope of my studies had no yet been determined. I was given a lot of freedom by both the TU Delft and Evides Industriewater to choose my own subject, for which I am very thankful. It has given me the opportunity to investigate a very specific and very interesting field of water research: power plant chemistry. While doing my own research I have become intrigued by many aspects of industrial water treatment and have had the pleasure to meet and work with a lot of knowledgeable people.

First of all I thank my two promotors, prof. Luuk Rietveld and prof. Arne Verliefde. They have each taken a different role in supervising me, in doing so giving me all the help I needed (and more). Especially their expertise in the publishing process has been vital to successfully completing my PhD. Apart from our professional relationship, Luuk and Arne have also been incredibly kind and warm to me and our meetings have always been both fun and effective.

I have had the pleasure of performing high-end corrosion experiments at the University of New Brunswick in Canada under the supervision of prof. Derek Lister and with the help of many others. Derek, the reception I got from you at your department was exceptional and I am still amazed by what we have achieved in only 5 months. This would not have been possible though without Sarita (Som-O) Weerakul, Naravit (Nich) Leaukosol and Noel Kippers, my Canadian colleagues and friends that have pulled me through a line of research that was new to me.

My whole project would not have existed without the extensive contributions of Evides Industriewater. Not in the least because of the financial commitment, but also for all the technical input. Jacques van Agtmaal has had faith in my efforts and ideas from the start and has been extremely supportive on several levels. The initial inspiration for my research came from Hans Paardenkoper and along the way Peter van Hartingsveldt, Wilbert van den Broek and Martin Pot have all contributed to the final output. A big thank you goes out to all Evides Industriewater employees who have directly or indirectly made my thesis possible. Part of the financial contributions of my project have come through the E4Water Consortium, in which both Evides Industriewater and the TU Delft are active, and I am grateful that the European Commission has been willing to support this project.

I want to thank EPRI and Shell for also providing financial and technical support. At EPRI, specific gratitude goes out to James (Jim) Mathews and Michael Caravaggio. They have steered my research into the right direction and your ideas about amine decomposition were inviable to my thesis. Michael has also facilitated the collaboration with the University of New Brunswick. At Shell I thank Edwin Muller for providing me with a fresh idea on investigating petrochemical contaminants and giving advice while doing experiments and writing a publication on the results.

Through IAPWS and PPChem I have met a small army of knowledgeable and intelligent water experts and

chemists. I need to thank all of you for providing me with ideas and constructive criticism. The events we attended were inspirational and fun and I hope to see many of you in the near future. Specific gratitude goes out to James (Jim) Bellows from Siemens for unselfishly helping me out with all sorts of chemistry questions. Wolfgang Hater from Kurita Water has helped me by always being critical of my work and results, which has greatly improved the quality of my thesis.

At the TU Delft I want to thank my colleagues for the interesting and fun years we have had together. I hope our paths cross again and maybe even work together again. I thank my officemates for the laughs and for providing some frustration relief. In the laboratory special thanks go to Tonny Schuit and Armand Middeldorp for all the help Ive had during my experiments.

Last but not least, I want to thank my family, friends and Suéllen for supporting me on this journey. Without your friendship, love and company I would be lost, regardless of my newly obtained title. Of all those wonderful people one person deserves explicit acclaim: Joost Döbken, for pulling me through the layout process during the production of this thesis.

Table of Contents

Summary **v**

Samenvatting **vii**

Acknowledgements **ix**

1 Introduction **1**

2 Organic Acid Formation from Organic Carbon Decomposition **13**

3 Thermolysis of Morpholine in Water and Superheated Steam **27**

4 Role of Metal Surface Catalysis in the Thermolysis of Amines **39**

5 Effects of Temperature and Pressure on the Thermolysis of five Alkalizing Amines **49**

6 Anionic Organic Contamination in Petrochemical Steam-Water Cycles **65**

7 Ethanolamine and Two-Phase Flow Accelerated Corrosion **77**

8 Concluding remarks **103**

List of publications **113**

Curriculum Vitae **115**

1

Introduction

1.1 An introduction to steam-water cycles

Steam-water cycles are mainly found in electricity generation and the (petro)chemical industry. Although the designing of a power plant is complex, the concept behind the steam-water cycle is simple. High-purity water is heated to high temperatures in pressurized vessels (boilers). Lower pressure downstream of the boiler causes the hot liquid water to rapidly expand to high temperature steam. The kinetic energy that is released can be used to drive large turbines, allowing energy stored in fuel to be converted to electricity. According to the International Energy Statistics of the U.S. Energy Information Administration thermal power plants were responsible for 78.2% of the world's electricity production, of which 67.3% resulting from fossil fuel and 10.9% from nuclear fuels. Coal is responsible for 40.4% of the world's electric energy from fossil fuel. There are also gas- and oil-powered plants which utilize the steam-water cycle for electricity production, as does the geo-thermal plant. This thesis primarily deals with conditions found in fossil-fired plants, because of their higher possible operating temperatures and pressures, although these can range from only 200 °C and 2.0 MPa to supercritical conditions. A schematic drawing of a steam-water cycle for a conventional fossil-fired plant is shown in Figure 1.1.

Power plants can apply several variations to this basic concept to improve efficiency. A power plant will usually contain several turbine stages (i.e. high, intermediate and low pressure). The dimensions of each turbine stage are optimized to match the volume of the steam at the corresponding temperature and pressure. Because condensation can be dangerous for a turbine, reheating of the steam can be applied after passing through the high pressure turbine, to regain steam at superheat temperature. Economizers can be placed in between the feedwater pump and heater to preheat the working fluid, by utilizing the excess heat at the end of the turbine stage. Boiler blowdown is not always discharged, but can also be treated and recycled. Boilers come as drum boilers (which recirculate the water) and once-through boilers.

Fossil-fired plants are either conventional or combined cycle plants with a Heat Recovery Steam Generator (HRSG). The plant upstream of an HRSG utilizes gas powered turbines, of which the exhaust is used to produce steam, which in turn is used to drive steam turbines. A conventional plant instead uses fuel to directly heat water to produce steam. The temperature in an HRSG is typically much lower (around 580 °C) than in a conventional plant (around 1300 °C), which has consequences for the way the plants are designed. In an HRSG, positioning and apportioning of heat transfer surfaces is more important and these plants operate on a triple pressure format. This means that water-steam conversion takes place at three different pressure levels in three interconnected circuits.

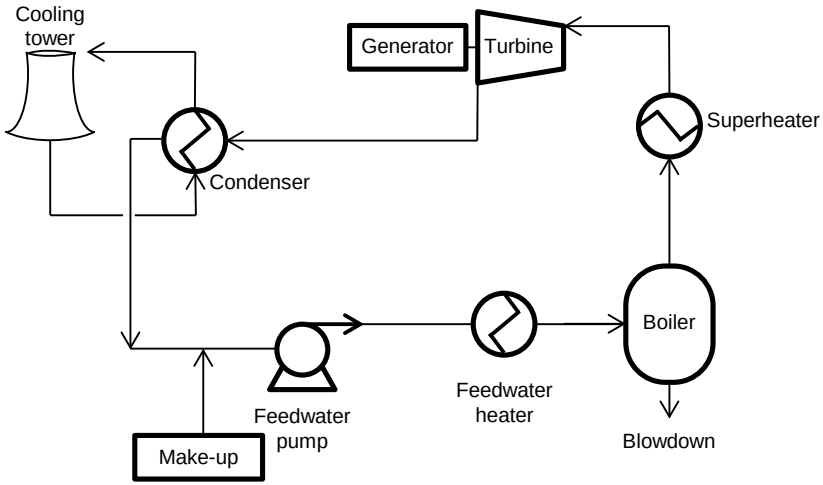

Figure 1.1: Schematic drawing of a steam-water cycle

1.2 Water quality in steam-water cycles

Although the majority of water in power generation is used for cooling, which is of a relatively lower quality, the demineralized water in steam-water cycles is of high-purity. Therefore extensive treatment is required, making boiler feedwater far more expensive. This treatment is necessary to prevent a variety of corrosion issues that can emerge due to insufficient water quality. Basically, corrosion is the natural process of metal turning back into its thermodynamically favored state, which is ore (usually oxide) and is a temperature, oxygen and pH dependent process. In the United States alone, the annual direct cost of corrosion during the production of electricity is $ 6.9 billion (Virmani, 2001). The International Association for the Properties of Water and Steam (IAPWS) lists the following major failure mechanisms for water-side corrosion (Petrova & Dooley, 2013).

- Under-deposit
- Corrosion fatigue
- Pitting corrosion
- Stress corrosion cracking
- Flow-accelerated corrosion

Under-deposit corrosion is caused by corrosion products or an excess of dissolved solids depositing on metal surfaces. Underneath and around those deposits, hydrogen damage and caustic gouging (only when NaOH is added to boiler water) may occur. Corrosion fatigue results from repetitively applied stress that causes damage to the protective oxide layer. Pitting corrosion is the formation of corrosion cells on the surface, which does not

occur under normal plant conditions, but during (inadequate) shutdown, due to exposure to oxygen. Stress corrosion cracking is caused by the presence of impurities, such as hydrogen, sodium and chloride, while tensile stress is applied to the material (Sieradzki & Newman, 1987). As small cracks occur, the ions will lead to localized caustic or acidic conditions in the crack causing the cracks to grow even faster. Alternatively, hydrogen can move through the metal lattice, leading to intergranular stress corrosion cracking. Because of its inconspicuous nature, stress corrosion cracking can remain unnoticed until a failure occurs, like an incident at the Hinkley Point power plant in the United Kingdom (1969), where a steam turbine rotor suddenly burst. Flow accelerated corrosion (FAC) is the accelerated removal of the protective oxide layer on the surface of carbon steel components caused by highly turbulent flow. This can happen in both single-phase (water only) and two-phase (water and steam). This corrosion mechanism is notorious due to major FAC related incidents like the Surry pipe rupture in 1986 which resulted in the death of four workers and huge damage to the plant.

Which corrosion mechanism most frequently occurs in a power plant depends on many factors like design, used materials, operating temperature and pressures and water qualities. FAC for instance, affects mostly low alloy carbon steel and occurs in regions where temperatures are between 100 and 200 °C and where turbulent flow occurs. In response to the Surry accident, an overview of FAC related failures and incidents was made (EPRI, 1998) . FAC is the most dominant failure mechanism in fossil-fired plants, due to the (usually) lower alloy construction materials applied Dooley (2008). Because of their compact design with many bends in which turbulent conditions and localized high flow occur, HRSGs are especially susceptible to FAC. Single-phase FAC is mostly found around feedwater heater drains, although there are ten other potentially critical zones. Of special concern are zones in power plants where flashing and condensation occurs, as condensates typically contain the majority of (in)organic impurities from the bulk steam. Areas of power plants where wet steam is found, like HRSG piping, feed-water heaters, turbine casings, de-aerators and air-cooled condensers are the most prone to two-phase FAC (Dooley, 2008). When FAC, or any other corrosion mechanism, occurs in condensing areas of a plant, this is can also be referred to as first condensate corrosion or early condensate corrosion.

By setting guidelines for water and steam quality, an attempt is made to slow-down corrosion as much as possible. The Electrical Power Research Institute and VGB PowerTech provide such guidelines at a cost, while IAPWS has more recently started providing open source guidelines for chemical conditioning, feedwater and steam quality (Daucik & Dooley, 2011; Friend & Dooley, 2010; Petrova & Dooley, 2013). For example, to prevent some of the previously discussed corrosion processes, chloride, sulfate and sodium guidelines for feedwater and steam quality are lower than 5 g/L, while the oxygen concentration is typically between 0 and 100 g/L.

1.3 Make-up water treatment and chemical conditioning

In order to meet the aforementioned guidelines for boiler feedwater quality, water from any source will be treated

and demineralized until all concentrations, of mainly dissolved solids, are below the required limit. Demineralization is conventionally achieved through ion exchange, but membrane technology is gaining popularity. When steam is released from a drum boiler, the concentration of all non-volatile substances in the liquid phase increases. Therefore, the boiler needs to release some of its water through blowdown to avoid a too high increase in dissolved solids concentration and thus increased corrosion risks. This blowdown is compensated for by adding make-up water. Since the actual concentrations in a boiler and in the steam are a function of make-up water quality, boiler blowdown rate and the volatility of the individual dissolved compounds, concentrations found in boiler water and steam are therefore more complicated to predict than those of the make-up water. The volatility in turn is influenced by the compound's dissociation characteristics and the temperature and pressure in the boiler. Concentrations of most dissolved solids in a boiler are higher than those in the steam. However, organic acids are an exception to this, because of their more volatile nature. Organic acids present can lower the pH of the liquid and can therefore increase the probability of corrosion.

Because water in itself is corrosive, chemicals additives are used to raise the pH of the feedwater to 8.5 10, regardless of the quality of the make-up water treatment. In order to protect both feedwater and condensate, volatile bases such as ammonia are needed (Friend & Dooley, 2010). Although ammonia is commonly applied in steam-water cycles, it is a weak base. Because ammonia is more volatile than water, it offers limited protection to corrosion in areas where flashing occurs or the first droplets of condensate are formed (Miller, 1997; Svoboda, 2009). The application of ammonia therefore requires high feedwater purity (Dooley et al., 2002). It also directly reacts with any copper that might be present in a steam-water cycle. Therefore, organic alternatives with higher basicity and lower volatility are also available. Organic alternatives to ammonia are alkalizing amines, which are discussed in more detail in Section 1.5.

1.4 Organic contamination of steam water cycles

In the 1980s, the first papers expressing concerns regarding organic acid formation from organic matter present in boiler feedwater appeared (Flint & McIntosh, 1986; Jonas, 1982). These papers indicate that pH is lowered and steam cation conductivity is raised by the breakdown of organic matter, pointing towards the formation of organic acid anions. The link between cation conductivity and organic carbon has been emphasized (Heijboer et al., 2006; Huber, 2003), because cation conductivity is the main operational parameter used to monitor the power plant's water chemistry status. Although the relation between cation conductivity and contamination is clear, it has also been pointed out that cation conductivity is not necessarily the best descriptor and even can give a wrong impression of the state of a plant. High cation conductivity does not necessarily imply that the plant is prone to failure due to corrosion (Bursik, 2010; Carvalho et al., 2008; Svoboda et al., 2000). For instance a rise in cation conductivity can also be caused by CO_2, which is not detrimental to the steam-water cycle, unless

concentrations are high enough to cause pH depressions in the feedwater or condensate return lines.

Some case studies have shown that organic acids can indeed cause damage to plants (de Wispelaere, 2004; Savelkoul et al., 2001). Because of this, the manufacturers of turbines tend to be conservative when it comes to limits of organics in steam water cycles (Svoboda et al., 2005). However, in these cases, high acetic acid concentrations were measured, due to the incorrect application of organic treatment chemicals, not as a result of organic contamination from Natural Organic Matter. Denk & Svoboda (2006) claim that the prevention of corrosion due to organic contaminants is just a matter of keeping pH of the two-phase liquid film in check. No specific effect of acetic acid on stress corrosion cracking and FAC was found. In addition, lab-scale corrosion studies with conflicting findings are reported, one in which acetic acid led to an increase in stress corrosion cracking susceptibility (Maeng & Macdonald, 2008) and another in which the presence of acetic acid had no effect on stress corrosion cracking at all Nakane et al. (2010).

Two reviews on organic carbon in steam-water cycles state that experimental data to come to a solid, well-founded total organic carbon guideline is not available (Bursik, 2008; Mathews, 2008). Neither the organic acid formation (quantity and quality) nor the impact on corrosion (especially FAC) in two-phase zones is well understood. In addition, no work has been published on the sources of anionic contaminants found in petrochemical steam-water cycles, dealing with steam in contact with (for instance) oil refining in steam crackers for the production of olefins.

1.5 Organic treatment chemicals

Alkalizing amines like morpholine and ethanolamine offer a less volatile alternative to ammonia (Cobble & Turner, 1992), making the steam-water cycle more resilient to corrosion, especially in zones where first condensate is formed (Kluck et al., 2010; Lertsurasakda et al., 2013; Robinson et al., 2009). Because ammonia corrodes copper, amines can also be a good chemical water treatment solution for systems with mixed metallurgy. Amines have been applied in nuclear power plants for decades and some guidelines on how these should be applied are available (Miller, 1997). However, their use in fossil fired plants is under debate, due to the higher operating temperatures and pressures used in these plants. Indeed, because amines are known to have limited thermal stability, they may decompose and form organic acid anions which lower pH and thereby increase the probability of corrosion (Bellows, 2004; Denk & Svoboda, 2006; Svoboda, 2009).

Potential organic acid anion formation during amine thermolysis currently prevents the general acceptance of amines for application in steam-water cycles. Excessive breakdown of morpholine has been reported to cause two-phase FAC in the turbine exit steam line to the condenser of a 12.5 MPa industrial steam system (Savelkoul et al., 2001). Other bad cases of amines application were investigated by de Wispelaere (2004), where again morpholine breakdown was responsible for high acetic acid concentrations, especially in the first condensate. Therefore, given the effect of organic acid formation on pH (and thus potential corrosion), knowledge about the rate of amine degradation at a certain temperature and/or pressure is

therefore crucial in understanding the applicability of alkalizing amines in steam-water cycles.

Some experimental data for the thermal degradation of amines is available, focusing on conditions found in nuclear and fossil-fired plants. Domae & Fujiwara (2009) investigated the thermal stability of 10 ppm 3-methoxypropylamine in water at 280 °C and 6.3 MPa by using an autoclave and observed 6% decomposition after 1.5 hours. The autoclave took 2.4 hours to warm-up and 15 hours to cool down, which points out one of the problems with using autoclaves for kinetic studies. Shenburger et al. (1992) studied the stability of six amines at 286 °C and 6.9 MPa with a high pressure test boiler system, thereby more accurately simulating the conditions found in a power plant. They observed morpholine decomposition only up to a few percent and also observed that the addition of oxygen does not lead to an increase in decomposition rate. Decomposition kinetics for all tested amines were higher in the feed water heater than in the boiler itself, indicating the importance of heat flux at the water-metal interface. An attempt was made to determine rate constants for the amine decomposition, but with the low decomposition percentages there was a large degree of uncertainty in the results. Feron & Lambert (1992) used a combination of batch autoclave and loop tests to investigate the thermolysis of three amines, including morpholine. They applied much longer retention times in the autoclave than Domae & Fujiwara (2009), observing 50% morpholine decomposition after 21 days at 300 °C, but were unable to determine the decomposition kinetics. In the loop test, which operated at 295 °C, the morpholine decomposition percentage was below detection, indicating that a 21 day retention time might not be relevant to the actual application of amines and might lead to overestimation of amine decomposition. Gilbert & Lamarre (1989) also studied morpholine decomposition in an autoclave at 260, 280 and 300 °C, showing that breakdown kinetics were of first order with an activation energy of 131.9 $kJmol^{-1}$. Mori et al. (2012) tried to simulate the thermolysis of six amines at fossil-fired plant conditions at higher temperatures with a boiler-superheater test loop. This is the only study that considered the influence of the superheater on thermolysis, by varying the superheater exhaust temperature. They concluded that morpholine breakdown in the boiler was undetectable and starts only from 500 °C onwards in the steam phase. The retention time was not mentioned, making any calculation of kinetics impossible. However, they were able to show the importance of the superheater in the applicability of alkalizing amines in fossil-fired plants. The importance of the superheater temperature in the applicability of alkalizing amines in fossil-fired plants was also pointed out by Bull (2013), in a report detailing the results from a fossil-fired plant survey on the use of amines. The retention time had again not been taken into consideration though, making it hard to extrapolate the data in the report to other case studies.

In short, the kinetics of amine thermolysis at superheater conditions have not been sufficiently investigated. When the degradation characteristics of amines are better understood, the results can be used as input for a predictive degradation model. Using this input two-phase FAC experiments, like those performed by Lertsurasakda et al. (2013), can be performed. This should provide more insights into the effect of amine decomposition on two-

phase FAC, which helps assess the applicability of amines in steam-water cycles.

1.6 This thesis

The on-going discussion around organic contaminants and treatment chemicals in steam-water cycles, cannot come to a conclusion due to a lack of evidence from refereed literature. This thesis aims to fill in some of the most prominent knowledge gaps, with a strong emphasis on practical applications. Based on the information provided in the introduction, a main objective and six sub-objectives have been defined.

1.6.1 Main objective

Contribute to well-founded guidelines for organic contamination and amine application in steam-water cycles to facilitate effective water treatment and chemical dosing

1.6.2 Sub-objectives

To reach the main objective, this study aims to:

1. Investigate the influence of temperature, oxygen, organic carbon concentration and retention time on organic acid formation (Chapter 2)
2. Assess suitability of a flow reactor to investigate amine (hydro)thermolysis kinetics and to determine model possibilities (Chapter 3)
3. Investigate the influence of temperature, amine structure, surface:volume ratio and metal surface composition on the kinetics of the thermolysis of amines at superheater conditions (Chapter 4)
4. Determine the Arrhenius constants of the temperature and pressure dependent thermolysis of morpholine, ethanolamine, 3-methoxypropylamine, cyclohexylamine and dimethylamine for modelling purposes (Chapter 5)
5. Quantify organic acid formation from petrochemical contaminants and the thermal stability of acetic and formic acid (Chapter 6)
6. Investigate the effect of different ethanolamine, ammonia, acetic and formic acid concentrations and mixtures on (two-phase) FAC and establish a link with the pH of the liquid film in two-phase flow (Chapter 7)

1.6.3 Thesis outline

Although it is not the main goal of the chapter, Chapter 2 firstly compares and evaluates two practical methods and set-ups that can be used for investigating thermolysis in dilute aquatic solutions in a laboratory setting. The most relevant method (the flow reactor) has then been used to investigate the influence of temperature, oxygen, organic carbon concentration and retention time on organic acid formation. The chapter ends with comparing obtained laboratory results to results from a case study.

Chapter 3 continues to use a flow reactor, and determines whether this reactor is suitable for investigating amine (hydro)thermolysis kinetics. The chapter deals with both

boiler and superheater conditions and confirms that thermolysis in the superheater is much faster. Additionally, it looks into amine thermolysis model possibilities. Chapter 4 considers the influence of temperature, amine structure, surface:volume ratio and metal surface composition on the kinetics of the thermolysis of amines at superheater conditions. Chapter 5 takes what has been learned from the previous two chapters to determine the activation energy and activation volume of the temperature and pressure dependent thermolysis of morpholine, ethanolamine, 3-methoxypropylamine, cyclohexylamine and dimethylamine in order to build a model. This model can predict amine thermolysis kinetics, to assist assessing the possibility for amine application in steam-water cycles.

Special attention is given to organic contaminants found in steam-water cycles in the petrochemical industry in Chapter 6. Five common contaminants and an oxygen scavenger are thermolyzed to determine to what extent these contaminants can lead to an increase in organic acid anions. This chapter also describes the thermal stability of acetic and formic acid, which have proven to be the most prevalent organic anionic contaminants in the previous chapters.

Chapter 7 deals with the FAC studies, which combine the obtained knowledge on amine thermolysis and organic acid anions formation to determine the impact on two-phase FAC. The effect of acetic acid on two-phase FAC, in the presence of ammonia and ethanolamine at different steam qualities is evaluated. Subsequently the change in two-phase FAC rate when acetic acid, formic acid and ethanolamine are added to water containing only ammonia is determined. A model to calculate the pH of the liquid film in two-phase flow is presented and extrapolated to higher steam-qualities.

Figure 1.2 summarizes the relation between the chapters and the sub-objectives they deal with. Chapter 8 discusses the extent to which the research has been able to meet the objectives and what the results mean for the practice of water treatment in steam-water cycles.

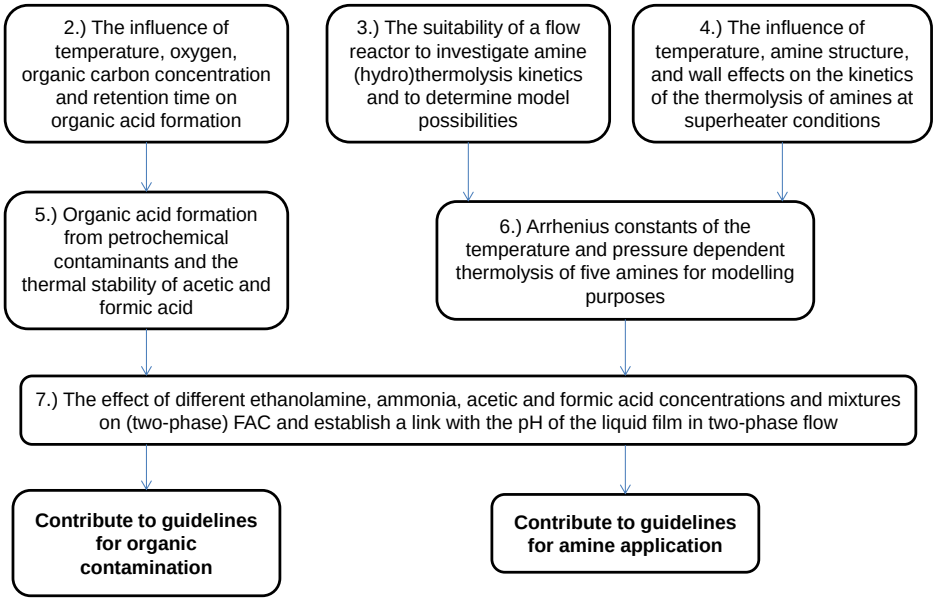

Figure 1.2: The relation between the sub-objectives and how they lead to the main objective of this thesis

References

Bellows, J. C. (2004). Hazards of amine use in boiler systems. *International Water Conference*, Pittsburgh, PA.

Bull, A. (2013). Dimethylamine as a replacement for ammonia dosing in the secondary circuit of an advanced gas-cooled reactor power station. *16th International Conference on the Properties of Water and Steam*, London, United Kingdom.

Bursik, A. (2008). Carbon is not Equal to Carbon. *2nd International Conference on the Interaction of Organic and Organic Plant Cycle Treatment Chemicals with Water, Steam and Materials*, Lucerne, Switzerland.

Bursik, A. (2010). Degassed cation conductivity - a key parameter for steam quality surveillance? *PowerPlant Chemistry*, *12*(4), 224-231.

Carvalho, L., James, T., & Hunter, W. (2008). Questioning the relevance of cation conductivity monitoring in modern combined cycle power plants. *17th Conference on Electric Power Supply Industry*, Macao, China.

Cobble, J., & Turner, P. (1992). PWR advanced all-volatile treatment additives, by-products, and boric acid. *EPRI Report*, *TR-100755*, Palo Alto, CA.

Daucik, K., & Dooley, R. (2011). Phosphate and NaOH treatments for the steam-water circuits of drum boilers of fossil and combined cycle/HRSG power plants. *IAPWS Report*, Plzen, Czech Republic.

Denk, J., & Svoboda, R. (2006). Stress corrosion cracking due to carbon dioxide and organic impurities in the steam/water cycle. *PowerPlant Chemistry*, *8*(7), 401-408.

de Wispelaere, M. (2004). Early condensate in a fossil power plant using organic treatment. *14th International Conference on the Properties of Water and Steam*, Kyoto, Japan.

Domae, M., & Fujiwara, K. (2009). Thermal decomposition of 3-methoxypropylamine as an alternative amine in PWR secondary systems. *Journal of Nuclear science & Technology*, *46*(2), 210-215.

Dooley, R. (2008). Flow-accelerated corrosion in fossil and combined cycle/HRSG plants. *PowerPlant Chemistry*, *10*(2), 68-89.

Dooley, R., Shields, K., Aschoff, A., Ball, M., & Bursik, A. (2002). Cycle chemistry guidelines for operators and chemists: All-volatile treatment, revision 1. *EPRI Report*, *1004187*, Palo Alto, CA.

EPRI. (1998). Flow-accelerated corrosion in power plants. *EPRI Report*, *TR-106611-R1*, Palo Alto, CA.

Feron, D., & Lambert, I. (1992). Thermal stability of three amines in pressurized water reactor secondary systems. laboratory and loop experiments. *Journal of Solution Chemistry*, *21*(8), 919-932.

Flint, W. G., & McIntosh, R. J. (1986). Operating experience in correcting severe secondary chemistry upsets by controlling makeup water organics. *International Water Conference*, Pittsburg, PA.

Friend, D., & Dooley, R. (2010). Volatile treatments for the steam-water circuits of fossil and combined cycle/HRSG power plants. *IAPWS Report*, Niagara Falls, Canada.

Gilbert, R., & Lamarre, C. (1989). Thermal stability of morpholine additive in the steam-water cycle of CANDU-PHW nuclear power plants. *Canadian Journal of Chemical Engineering*, *67*(4), 646-651.

Heijboer, R., van Deelen-Bremer, M. H., Butter, L. M., & Zeijseink, A. G. L. (2006). The behaviour of organics in a makeup water plant. *PowerPlant Chemistry*, *8*(4), 40-46.

Huber, S. A. (2003). Sources and behaviour of organics, in particular polysaccharides, in boiler feedwater preparation and in water-steam cycles. *PowerPlant Chemistry*, *5*(5), 105-116.

Jonas, O. (1982). Beware of organic impurities in steam power systems. *Power*, *126*(9), 103-107.

Kluck, R., Torres, J., Antompietri, A., & Rivera, J. (2010). Experiences using neutralizing amines to control pH and minimize FAC in a combined cycle plant. *International Water Conference*, San Antonio, TX.

Lertsurasakda, C., Srisukvatananan, P., Liu, L., Lister, D., & Mathews, J. (2013). The effects of amine on flow-accelerated corrosion in steam-water systems. *PowerPlant Chemistry*, *15*(3), 181-189.

Maeng, W., & Macdonald, D. (2008). The effect of acetic acid on the stress corrosion cracking of 3.5NiCrMoV turbine steels in high temperature water. *Corrosion Science*, *50*(8), 2239-2250.

Mathews, J. (2008). Organics in the power plant cycle. *2nd International Conference on the Interaction of Organic and Organic Plant Cycle Treatment Chemicals with Water, Steam and Materials*, Lucerne, Switzerland.

Miller, A. (1997). Pwr advanced amine application guidelines - revision 2. *EPRI Report*, *TR-102952-R2*, Palo Alto.

Mori, S., Sato, T., & Shimura, Y. (2012). Characterization of amines under high temperature conditions and their use for boiler water treatment. *Corrosion*, Salt Lake City, UT.

Nakane, T., Niu, L. B., Oishi, S., & Takaku, H. (2010). Influence of organic acids on corrosion behavior of boiler tube steels in simulated avt waters coexisted with chloride ions. *Journal of the Japan Institute of Metals*, *74*(9), 565-571.

Petrova, T., & Dooley, R. (2013). Technical guidance document: Steam purity for turbine operation. *IAPWS Report*, London, UK.

Robinson, J., Kluck, R. W., Rossi, A., & Carvalho, L. (2009). Organic chemical treatment of high-purity boiler feedwater - advantages and limitations. *PowerPlant Chemistry*, *11*(11), 690-699.

Savelkoul, J., Janssen, P., & Verhoef, H. (2001). Monitoring of first condensate corrosion in industrial systems. *PowerPlant Chemistry*, *3*(6), 326-330.

Shenburger, D., Zupanovitch, J., & Walker, J. (1992). Loop testing of alternate amines for all-volatile treatment control in pwr's. *EPRI Report*, *TR-100756*, Palo Alto, CA.

Sieradzki, K., & Newman, R. C. (1987). Stress-corrosion cracking. *Journal of Physics and Chemistry of Solids*, *48*(11), 1101-1113.

Svoboda, R. (2009). The effect of carbon dioxide and organics in a steam turbine. *PowerPlant Chemistry*, *11*(1), 20-29.

Svoboda, R., Bodmer, M., & Sandmann, H. (2000). Impact of organic impurities on steam turbine operation. *PowerPlant Chemistry*, *2*(9), 530-534.

Svoboda, R., Gabrielli, F., Hehs, H., Seipp, H.-G., Leidlich, F.-U., & Roberts, B. (2005). Organic impurities an organic conditioning agents in the steam-water cycle: A manufacturers point of view. *International Conference on Interaction of Organics and Organic Cycle Treatment Chemicals with Water, Steam and Materials*, Stuttgart, Germany.

Virmani, Y. (2001). Corrosion cost and preventive strategies in the united states. *FHWA Report*, United States.

2

Organic Acid Formation from Organic Carbon Decomposition

This chapter is based on:

Moed, D.H., Verliefde, A.R.D., Rietveld, L.C. and Heijman, S.G.J. (**2014**) Organic acid formation in steam-water cycles: influence of temperature, retention time, heating rate and O2. *Applied Thermal Engineering*, 65(1-2), 194-200

Abstract

Organic carbon breaks down in boilers by hydrothermolysis, leading to the formation of organic acid anions, which are suspected to cause corrosion of steam-water cycle components. Prediction of the identity and quantity of these anions, based on feedwater organic carbon concentrations, has not been attempted, making it hard to establish a well-founded organic carbon guideline. By using a batch-reactor and flow reactor, the influence of temperature (276-352°C), retention time (1-25 minutes), concentration (150 to 2400 ppb) and an oxygen scavenger (carbohydrazide) on organic acid anion formation from organic carbon was investigated. By comparing this to data gathered at a case-study site, the validity of setups was tested as well. The flow reactor provided results more representative for steam-water cycles than the batch reactor. It was found that lower heating rates give more organic acid anions as degradation products of organic carbon, both in quantity and species variety. The thermal stability of the organic acid anions is key. As boiler temperature increases, acetate becomes the dominant degradation product, due to its thermal stability. Shorter retention times lead to more variety and quantity of organic acid anions, due to a lack of time for the thermally less stable ones to degrade. The absence of oxygen increases the thermal stability of organic acid anions.

2.1 Introduction

Several authors report on the link between Total Organic Carbon (TOC) concentrations and formed organic acid concentrations in steam-water cycles at specific sites (de Wispelaere, 2004; Heijboer et al., 2006; Svoboda, 2009; Svoboda & Bodmer, 2004). The main degradation products found in these studies are mainly acetic acid, formic acid and CO_2. Others have attempted to simulate boiler TOC hydrothermolysis experimentally, in batch autoclave experiments (Lepine & Gilbert, 1995). In the study of Lepine and Gilbert, actual boiler make-up water was concentrated by reverse osmosis (RO) to 16.5 ppm TOC and used to identify the potential organic degradation products by heating the concentrate in two separate runs at 260 and 300 °C for 7 days. With ion chromatography, 3.58 / 5.20 ppm acetic and 1.38 / 2.30 ppm propionic acid were identified as the main degradation products at 300 and 260 °C respectively, with lower concentrations of glycolic (0.289 ppm) and formic acid (0.101 ppm) only present at 260 °C. Those results however do not match the findings of the aforementioned case studies, where propionic and glycolic acid were quite rare.

The differences between laboratory and case-study results indicate that a good understanding of TOC hydrothermolysis under different conditions is still lacking, despite indications that breakdown of TOC might affect steam-water cycle operation. The aim of this chapter is to investigate the influence of several process parameters such as temperature, (absence of) oxygen, TOC concentration and retention time, on organic acid formation. By comparing this to case study results, it was assessed whether the laboratory methods applied were suitable for simulating TOC hydrothermolysis in steam-water cycles.

2.2 Methods & Materials

Two types of setups have been used. A batch autoclave as used by Lepine & Gilbert (1995) and an adaptation

of the flow reactor as described in a schematic by Brill & Savage (2004). In addition, samples were taken from a 13.0 MPa/331 °C steam-water cycle at an ammonium plant in North-Western Europe to compare to the results from the lab setups.

Experiments were performed at both mildly oxidizing and reducing conditions. Ammonia is used to raise pH and oxygen is kept below 20 ppb, like in many conventional steam-water cycles. Because some steam-water cycles operate at reducing conditions carboyhydrazide was dosed to create reducing conditions. These two conditions were chosen, because they are the most sensitive to impurities in the system (Dooley, 2008) and reducing chemistry was applied at the case study site mentioned above.

2.2.1 Autoclave experiments

The autoclave was a 1.8 L, SS316-L Parr Instrument Company (Frankfurt am Main, Germany) pressure vessel, equipped with pressure transducer, thermocouple, rupture disk, steam vent and sample collection vessel. This sample collection vessel was water cooled and had a volume of 10 mL. Gaseous nitrogen was used to clear the sample lines after sample collection. The vessel was placed inside a heating mantle, which was connected to a 4838 Parr temperature controller, providing temperature control and stability. The autoclave took 80 minutes to get to the desired temperature, for which 331 °C was chosen, because this was also the boiler temperature at the site (described in Section 2.2.3).

Before starting an experiment, the autoclave and its sample lines were flushed with ultrapure water to get rid of any remaining organic material. Then 1 L of the RO concentrate was added to the vessel, which was sparged with nitrogen to remove oxygen down to below 20 ppb O_2. To create a pH of 10 and reducing conditions, 35 ppm (1 mL of 1 molar (M)) NH_4OH (Sigma Aldrich 99,9% trace metals basis) and 0.1 mg of carbohydrazide (Sigma Aldrich 99% trace metal basis) were added, the vessel closed and again sparged for 1 minute to remove any oxygen that might have been added during the ammonia and carbohydrazide dosing. Then the heating mantle was switched on and samples were taken from 130 °C to 331 °C at 40 °C intervals. The vessel was kept at 331 °C for another two hours after reaching the set temperature, before switching off the heating mantle. Prior to cooling and while cooling down, additional samples were taken.

2.2.2 Flow reactor experiments

Figure 2.1 shows a schematic of the flow reactor used in this study. A glass vessel containing the TOC solution of interest was equipped with a pH and oxygen meter, to keep close watch on the influent quality. The vessel also contained a tube for nitrogen sparging and an HPLC pump inlet equipped with a filter. This HPLC pump provided the pressure to send the water through a steel bath at an accurate flow rate. The steel bath itself was a 2L SS316-L cylinder, containing small (¡ 1mm) steel balls for heat transfer. Heat was provided and controlled by the same mantle and controller used in the batch experiments. The water was sent through 6 meters of 1/8 stainless steel tubing inside the steel bath. Outside the reactor the water was immediately cooled in a cooling spiral that was emerged in beaker with water, which was kept at 20(±2) °C. Back pressure was controlled by an

adjustable relief valve from Swagelok (Waddinxveen, the Netherlands). The volume of the tubes inside the reactor was 8 mL, but water increases in volume at higher temperatures, making the actual retention time a function of both pump velocity and steel bath temperature (which was verified by measuring retention time for several temperatures). Tubing was purged with nitrogen and flushed with ultrapure water with NH_3 after each experiment. The concentrate of the RO system (described in Section 2.2.3) had a TOC concentration of 2.4 ($\pm$ 0.05) ppm and has been used as input for the laboratory experiments.

At the beginning of each flow reactor experiment, the relief valve was first set to 0.5 MPa above the pressure that corresponds to the set temperature's boiling point (i.e. for 331 °C, 13.5 MPa instead of 13.0 MPa). This was done to prevent steam flashing. The glass vessel was filled with the solution of interest and sparged until oxygen was below 20 ppb O_2. Ammonia was added to get to pH = 10 after which the solution was again briefly sparged. In the case of an experiment under reducing conditions, carbohydrazide (Sigma Aldrich 99% trace metal basis) was dosed at 1 ppm. In the meantime, the steel bath was heated to the desired temperature. Just before the experiment started, the solution was pumped through the system, after which the tubing was purged with nitrogen. When temperature was stable again, the experiment started and two 4 mL samples were created at the desired contact time, after which the tubing was purged with nitrogen again. This was repeated for all the conditions listed in Table 2.1.

2.2.3 Case-study

At a production site, two ion exchanger based demineralization plants produce boiler make-up water for (amongst others) a 112 MW HRSG, which consists of a feedwater heater, an economizer, a superheater and three waste heat boilers operating at 330 °C and 13.0 MPa. The feedwater tank contains a mixture of the water from these two treatment plants and the condensate return coming from the low pressure turbines. There are no condensate polishers. After switching from potable to surface water for feedwater production, the plant experienced degassed cation conductivity values higher than 0.2 μS/cm in the steam, thereby exceeding the maximum value for operation. TOC was identified as the source of the problem, which consisted of neutrally charged Natural Organic Matter (NOM) from the surface water source. To lower the feedwater TOC concentration, one of the demineralization treatment trains was followed by a reverse osmosis (RO) system, with LE400 Dow Filmtec membranes, that was there for TOC removal only. At the time of sampling, the influent TOC concentration was 200 ppb and there was 25 ppb left in the effluent. The RO system ran at 93% recovery, which matched the 2.4 ppm TOC measured in the concentrate.

When during this study the RO system was bypassed the feedwater TOC concentration, steam degassed cation conductivity and organic acid anion concentration went up. Samples were taken for analysis, before and during the bypass test, in order to determine the organic acid anions in the system based on the incoming TOC concentration from the make-up water plant. The data provides a real-world reference for TOC hydrothermolysis.

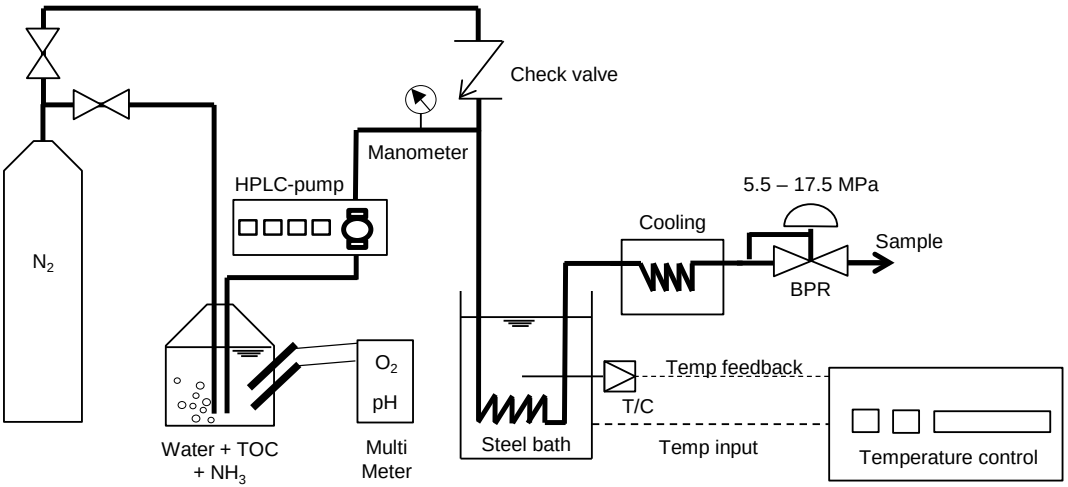

Figure 2.1: Schematic of the flow reactor used for the hydrothermolsyis of NOM

Table 2.1: Tested experimental conditions

Parameter	**Tested values**	**Unit**
Temperature	276, 286, 295, 303, 311, 318, 325, 331, 337, 342, 347, 352	°C
Retention time	1, 2, 5, 10, 25	minutes
TOC Concentration	2400, 1200, 600, 300, 150	ppb
Oxygen	0, 20	ppb

2.2.4 Water quality analysis

Analysis of organic acid anions was performed using a Metrohm (Schiedam, The Netherlands) 881 ion chromatography system. A Metrohm A Supp 16 4.0/250 anion column was operated at 67 °C and the eluent used contained 7.5 mM Na_2CO_3 + 0.75 mM NaOH in ultrapure water. The suppressor was regenerated with 50 mM H_2SO_4 and the limit of detection was 1 ppb. All ultrapure water used was purified by an Elga Purelab Ultra, delivering water with a 18.2 MΩ resistivity and <1 ppb TOC.

TOC was measured as Non-Purgable Organic Carbon (NPOC) and was performed on a Shimadzu ('s-Hertogenbosch, the Netherlands) TOC-V analyzer with high sensitivity catalyst. The online measurements for O_2 and pH were done with WTW (Weilheim, Germany) probes and multi-meter.

2.3 Results

2.3.1 Batch experiments

The results for two identical batch experiments have been summarized in Figure 2.2. As can be seen from the temperature curve, it took 82 minutes to get to 331 °C. In this time the majority of reaction products were formed. Lactate was the first considerable degradation product detected when the reactor had reached 120-130 °C. It continued to be formed, until the autoclave got to its maximum temperature, from where it started disappearing, most likely because it was degraded. While cooling down lactate concentrations remained more or less constant, probably because neither degradation nor formation occurred. Formate seems to favor temperatures between 200 and 300 °C. At higher temperatures formate was decreasing in concentration. Unlike lactate, formate concentrations started increasing again when the autoclave was cooling down. Glycolate was not detected in significant concentrations until temperatures exceeded 250 °C and kept being formed even when the autoclave was fully warmed up, but was eventually degraded as well. Levulinate was formed in low concentrations at temperatures higher than 300 °C and did not change in concentration after that. The pH was measured in samples gathered in the first run and fluctuated between 9.5 and 10. Theoretically, 17 ppm of NH_3 in ultrapure water gives a pH of 10.08. In combination with the highest measured concentrations of organic acid anions, this would become 10.05, which made further pH measurements redundant.

Acetate was formed until after the heating mantle was turned off, remained stable in concentrations at the highest temperatures and had the highest final concentration amongst all organic acid anions. Propionate was formed at higher temperatures and decreased in concentration only after the autoclave started cooling down.

The final production of organic acid anions was 506 (±5) ppb acetate, 296 (±11) ppb glycolate, 117 (±1) ppb lactate, 96 (±31) ppb propionate, 50 (±7) ppb formate, and 30 (±2) ppb levulinate. Expressed as total organic acid anions that is 17.0 (±1.2) μmol/L and in total carbon 448 (±48) ppb, meaning 18.7% of initial TOC was found to have been converted to organic acid anions after the batch experiments had ended. NPOC analysis revealed 1.76 (±0.08) ppm organic carbon was left, meaning 27%

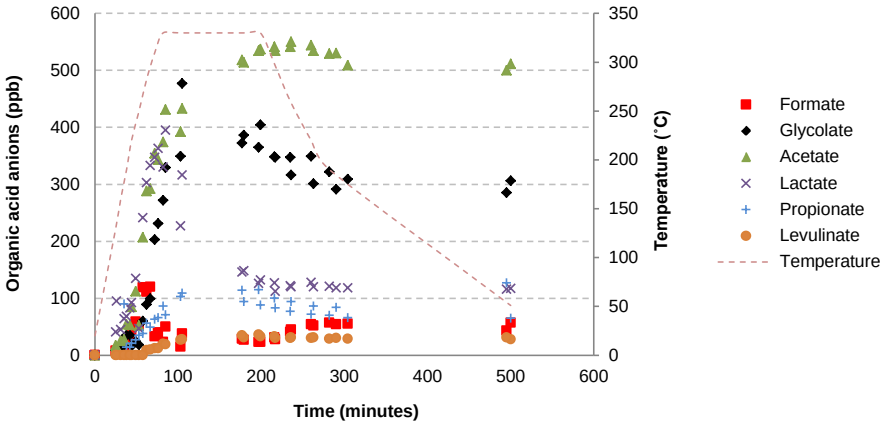

Figure 2.2: Organic acid anions formed in time while running the autoclave at 331 °C for 120 minutes with 2.4 ppm TOC in the form of make-up water concentrate under reducing conditions (Data from two identical experiments)

had been converted to inorganic carbon. The remaining 54.3% of initial organic carbon was assumed to consist of low molecular weight neutrals.

2.3.2 Flow reactor experiments

By loading the flow reactor with 2.4 ppm TOC as make-up water concentrate under mildly oxidizing and reducing conditions, using a fixed retention time (5 minutes) and a range of temperatures, the data sets shown in Figure 2.3 and Figure 2.4 have been produced. Each graph shows the data of two experimental series. Under oxidizing conditions, acetate was the main degradation product over the whole range of temperatures, although at the lowest investigated temperature formate had about the same concentration by mass. Acetate concentrations increased slightly with temperature, whereas formate concentrations decreased as temperature went up. There were small quantities of lactate in most samples and glycolate was not formed at all. Propionate was found in all samples, although in slightly higher concentrations at higher temperatures. Expressed in μmol/L total organic acid anions, lower temperatures resulted in higher concentrations, which decreased linearly from 8.2 to 5.8 μmol/L as temperature increased from 276 to 352 °C. Expressed in ppb carbon, organic acid anions represented 130 ($\pm$10) ppb TOC under oxidizing conditions, meaning around 5% of ingoing TOC was converted to organic acid anions. Sample size made NPOC detection difficult, but by producing bigger samples for 276 and 352 °C, organic carbon concentrations of 2.21 ($\pm$13) and 2.09 ($\pm$5) mg/L respectively were found, meaning 8% and 13% of initial organic carbon was converted to inorganic carbon or very volatile organic carbon species.

Under reducing conditions a similar trend for the formation of formate and acetate as under oxidizing conditions

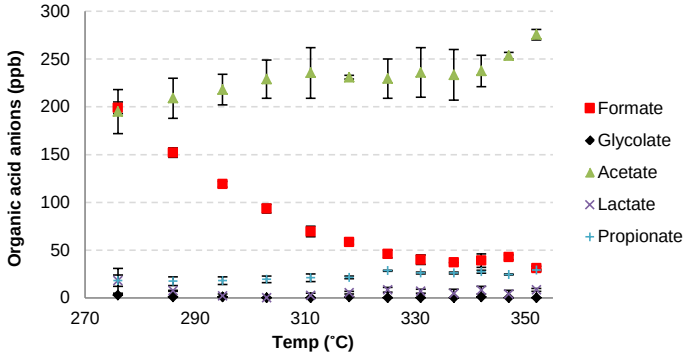

Figure 2.3: Organic acid anions formed from ultrapure water with 2.4 ppm TOC (make-up water concentrate) as a function of temperature in the flow reactor under mildly oxidizing conditions with a 5 minute retention time)

was seen, with formate concentrations decreasing as temperature went up and vice versa for acetate. However, the relative concentration of formate was much higher between 276 and 242 °C than in the previous experiments. At the highest temperatures this was not the case. In the same way there was less acetate being formed between 276 and 342 °C under reducing conditions. Although there was no glycolate found under oxidizing conditions, glycolate was formed under reducing conditions at temperatures up to 318 °C. Lactate was a breakdown product between 276 and 325 °C, whereas it was almost absent in the oxidizing experiment. From 331 °C and up, propionate was (by mass) as abundant as formate and reached its highest concentration at 325 °C. At the conditions found in the autoclave and the case-study, the average concentrations found were 192 (±16) ppb acetate, 91 (±10) ppb formate, 80.5 (±8.5) ppb propionate, 26.5 (±8.5) ppb lactate and 4.5 (±0.5) ppb glycolate resulting in 6.73 μmol/L organic acid anions. From 2.4 ppm TOC, 154 ppb became organic acid anions within a 5 minute retention time, which represents 6.5% of initial organic carbon. After 5 minutes at 276 and 352 °C, 2.25 (±0.1) and 2.15 (±0.11) ppm NPOC were detected respectively, meaning 6% and 10% of TOC was degraded to inorganic carbon.

Figure 2.5 shows for both oxidizing and reducing conditions the measured acetate and formate concentrations as a function of the retention time, with the flow reactor set at 331 °C (because of the case study) and an influent TOC concentration of 2.4 ppm. As the retention time increased, acetate concentrations increased as well. For formate longer retention times decreased its concentration. This might indicate again that formate is only formed while the water is being heated and is then degraded again when temperatures reach 331 °C. The difference in formate concentrations between oxidizing conditions and experiments with carbohydrazide dosed decreased as retention time increased. Apparently, the hydrothermolysis of formate is stimulated by the presence of (low

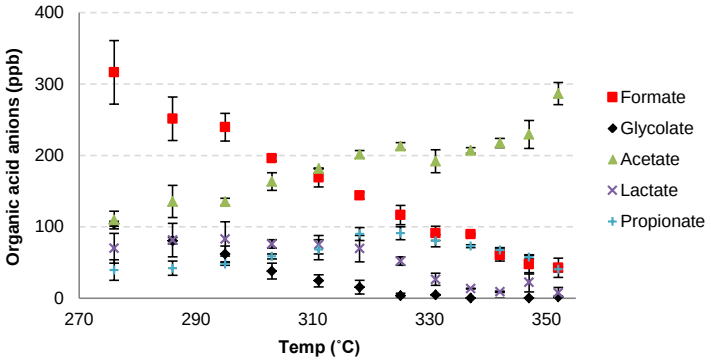

Figure 2.4: Organic acid anions formed from feedwater with 2.4 ppm TOC (make-up water concentrate) as a function of temperature in the flow reactor under mildly reducing conditions with a 5 minute retention time

concentrations of) oxygen. Lactate and glycolate disappeared with high contact times and propionate stayed more or less constant (data not shown).

To test the influence of TOC concentration on the quantity of degradation products, the make-up water concentrate was diluted with ultrapure water 1:1 in 5 steps. These experiments were only performed under reducing conditions. Figure 2.6 shows the relation between the TOC concentration going into the flow reactor and the resulting formate and acetate concentrations after a 5 minute retention time at 331 °C. Table 2.2 shows the ratios of acetate:formate, acetate:TOC and formate:TOC. The acetate:formate ratio stayed constant around 6, except for the second highest ingoing TOC concentration, where it was 8. As the TOC concentration goes down, it appears there is more acetate and formate being formed. This could also be caused by an increasing influence of small amounts of TOC contamination (from the laboratory atmosphere or plastic parts like the pump membrane).

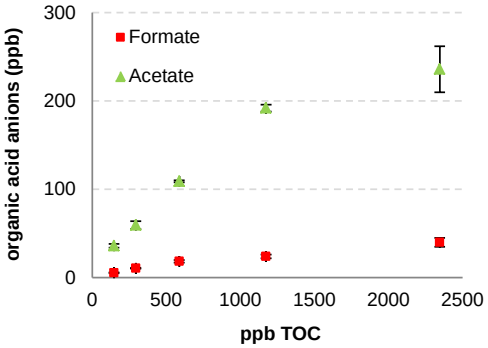

Figure 2.5: Acetate and formate formed as a function of the TOC concentration under reducing conditions at 331 °C and 13.5 MPa

2.3.3 Case study results

The presented data show the average organic acid anion concentrations in the boiler blowdown and steam from

Table 2.2: Ratios for TOC and resulting acetate (Ac) and formate (For) concentrations

TOC (ppb)	**Formate** (ppb)	**Acetate** (ppb)	**ratio** Ac:For	**ratio** For:TOC	**ratio** Ac:TOC
143	6	36	6.55	0.038	0.25
298	11	60	5.67	0.035	0.20
560	19	109	5.89	0.033	0.19
1,213	24	192	8.00	0.020	0.16
2,346	40	236	5.90	0.017	0.10

triplicate sampling (Figure 2.7). The TOC concentration in the feedwater (a mix of water from two demineralization plants and condensate return) went up from 45 ppb before bypassing the RO, to 75 ppb during the RO bypass at the time of sampling (a 67% increase). Boiler TOC was 3 times higher than in the feedwater, as boiler concentrations are a function of feedwater input, steam output, blowdown and the volatility of the organic compounds, resulting in TOC cycles of concentration.

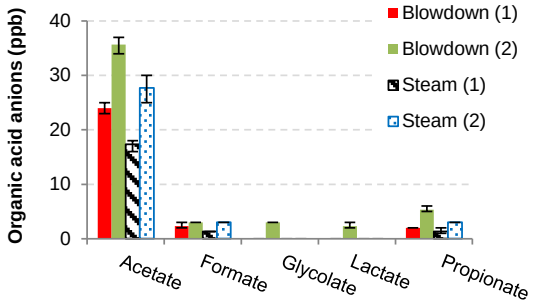

Figure 2.6: Average organic acid anions measured in blowdown and steam before (1) and during (2) the RO stop test at the case study site

The measured concentrations of acetate went up from 24 to 36 ppb in the blowdown and from 17.3 to 27.6 ppb in the steam when the RO was bypassed, which are increases in concentration of 50% and 62% respectively. For both blowdown and steam, the relative increase in acetate is lower than the relative increase in TOC. Because all other organic acid anion concentrations were very low (<10% of the acetate concentration) and the measuring accuracy was ±1 ppb for all compounds of interest, no significant statements about proportionality can be made.

It can be seen that for all organic acid anions the concentration increased during the RO bypassing. Both propionate and formate go up in both blowdown and steam. Glycolate and lactate were below detection in all parts of the system before the test, but after the increase in feedwater TOC 2 to 3 ppb could be measured in the blowdown. From the differences between the concentrations in blowdown and steam, it can be seen that formate is more volatile than acetate and propionate.

2.4 Discussion

2.4.1 Influence of process parameters

The batch reactor had most of the reaction occurring during the warming-up of the reactor, which led to results deviating from both the flow reactor and case-study. Apparently the reaction pathway is of vital importance for the end product, which indicates a strong influence of heating rate. Although explanations can be found for differences in results, the autoclave as a batch reactor for hydrothermolysis studies is probably not very effective when used in the way described in this paper. The flow-reactor results are a better match with the case-study, probably due to the more representative heating rate. Increasing the retention time in the lab reactor from 5 to 25 minutes also produced more representative results.

The higher the temperature in a system, the more prevalent acetate becomes. A higher variety of organic acid anions can be found when the water is brought to the set temperature more slowly, as was seen in the batch-reactor experiments. The high heating rate is therefore a plausible explanation for the relatively high acetate concentrations measured in the case-study. Acetate is more stable at the high temperatures than other organic acid anions found in high pressure steam-water cycles. Meyer et al. (1995) investigated acetic acid stability under supercritical conditions between 425-600 °C in the absence of oxygen to determine an Arrhenius global rate law. Applying this global rate law at 331 °C, would mean that after 10 minutes, 10% of acetate would have degraded. In the retention time experiments, a contact time of 25 minutes still did not result in observable acetate hydrothermolysis, indicating that either the global rate law overestimates degradation at lower temperatures, or that flow reactor conditions (the material, pH or presence of ammonium ions) prolong acetate life-span.

Longer contact times at higher temperatures have a negative influence on formate concentrations, as could be seen in both the batch-reactor and flow reactor. Actually, when looking at the kinetics of formate breakdown determined by Maiella & Brill (1998) in stainless steel cells, it is surprising there is any formate in any experiment at all. With an activation energy of $E_a = 113$ kJmol^{-1} and prefactor $A = 10^{8.7}$, formic acid hydrothermolysis at 331 °C should be a matter of seconds. Maiella & Brill (1998) however, did not take the oxygen concentration into consideration and sparged with argon before chemical addition only. A lack of oxygen is probably responsible for the reduction in formate degradation kinetics in this study. This is the case for acetic acid as well (Meyer et al., 1995), for which the degradation kinetics greatly decrease with decreasing oxygen levels. No experimental data were found for glycolate, lactate and propionate hydrothermolysis in literature.

A lack of oxygen (reducing conditions) either changes reaction pathways, resulting in higher concentrations of formate, glycolate and lactate, or these products persist due to a lack of oxygen. It has been mentioned before that oxygen promotes degradation kinetics for both acetate and formate. Depending on the stability of the compound, a longer retention time results in a lower concentration.

A decrease in feedwater TOC going into the flow reactor, led to relatively higher concentrations of organic acid an-

ions. A similar trend is seen in the increase in acetate during the RO bypass at the case-study site. The use of higher concentrations TOC to simulate a process with lower concentrations in the feedwater is therefore not recommended from a quantitative point of view.

2.4.2 Consequences for steam-water cycles

The presented results show that the higher the boiler temperature, the more acetate will be the dominant degradation product. At lower boiler temperatures, more formate, propionate or even glycolate and lactate can be expected. At lower temperatures there will be more mols of organic acid anions, which means that the economizer and feedwater heater will experience the biggest pH drop. Longer retention times in high temperature areas of the steam-water cycle, will further degrade unstable organic acid anions to a certain extent, meaning that more acetate will be found in systems with higher boiler retention times (i.e. fossil fired recirculating boilers). There is currently not enough knowledge on the degradation of formate, glycolate, propionate and lactate under boiler conditions.

In order to make more accurate predictions for full-scale steam-water cycles, several other parameters that could influence organic acid anion formation need to be investigated. TOC is a group name for a variety of organic molecules. Changing the origin of the TOC (which could be from the demineralization plant, lubricants, ion exchange resins, steam contamination or even treatment chemicals) can change the quantity and variety of organic acid anions formed after thermal degradation. The composition of the metal surface and volume-surface ratio might have an effect and the influence of the superheater still needs to be evaluated. When both organic acid anion formation and corrosion are well understood, a well-founded TOC guideline can be established.

2.5 Conclusions

The use of three different ways to gain understanding of TOC hydrothermolysis in steam-water cycles, has led to the following new insights:

- The flow reactor as proposed by Brill and Savage provided results more representative for steam-water cycles than the batch reactor used by Lepine and Gilbert.
- A lower heating rate gives more organic acid anions as degradation products, both in quantity and variety.
- The thermal stability of the organic acid anions is key.
  - As boiler temperature increases, acetate becomes the dominant degradation product, due to its thermal stability.
  - Shorter retention times lead to more variety and quantity of organic acid anions, due to a lack of time for the thermally less stable ones to degrade.
- Reducing conditions (or the absence of oxygen) increases the stability of organic acid anions.
- As the feedwater TOC concentration decreases, there are relatively more organic acid anions formed.

References

Brill, T., & Savage, P. (2004). Kinetics and mechanisms of hydrothermal organic reactions. In D. Palmer, R. Fernandez-Prini, & A. Harvey (Eds.), *Aqueous systems at elevated temperatures and pressures* (p. 643-675). London, United Kingdom: Elsevier Publishing.

de Wispelaere, M. (2004). Early condensate in a fossil power plant using organic treatment. *14th International Conference on the Properties of Water and Steam*, Kyoto, Japan.

Dooley, R. (2008). Flow-accelerated corrosion in fossil and combined cycle/HRSG plants. *PowerPlant Chemistry*, *10*(2), 68-89.

Heijboer, R., van Deelen-Bremer, M. H., Butter, L. M., & Zeijseink, A. G. L. (2006). The behaviour of organics in a makeup water plant. *PowerPlant Chemistry*, *8*(4), 40-46.

Lepine, L., & Gilbert, R. (1995). Characterization and fate of natural organic matter in steam-condensate cycles of fossil and nuclear power plants. *12th International Conference on the Properties of Steam*, New York, Wallingford.

Maiella, P. G., & Brill, T. B. (1998). Evidence of wall effects in decarboxylation kinetics of 1.00 m HCO_2X (X = H, Na) at 280-330 °C and 275 bar. *Journal of Physical Chemistry A*, *102*(29), 5886-5891.

Meyer, J. C., Marrone, P. A., & Tester, J. W. (1995). Acetic acid oxidation and hydrolysis in supercritical water. *AIChE Journal*, *41*(9), 2108-2121.

Svoboda, R. (2009). The effect of carbon dioxide and organics in a steam turbine. *PowerPlant Chemistry*, *11*(1), 20-29.

Svoboda, R., & Bodmer, M. (2004). Investigations into the composition of the water phase in steam turbines. *14th International Conference on the Properties of Water and Steam*, Kyoto, Japan.

3

Thermolysis of Morpholine in Water and Superheated Steam

This chapter is based on:

Moed, D.H., Verliefde, A.R.D., Heijman, S.G.J. and Rietveld, L.C. (**2014**) Thermolysis of Morpholine in Water and Superheated Steam. *Industrial & Engineering Chemistry Research*, 53(19), 8012-8017

Abstract

Amines show great potential for protecting steam-water cycles against corrosion, but their thermal stability is limited and acidic decomposition products are a concern due to increased corrosion risk. In this study, morpholine (hydro)thermolysis is simulated at boiler (352 °C 17.5 MPa) and superheater (490 °C 17.5 MPa) conditions with an experimental stainless steel flow reactor. Thermolysis under superheater conditions was more rapid than hydrothermolysis under boiler conditions. Organic acid anion decomposition products increased linearly over time, while the thermal decomposition of morpholine followed first order kinetics. Further experiments under superheater conditions were performed at 470, 490 and 510 °C, with pressures of 9.5, 13.5 and 17.5 MPa. With the kinetic rate constants for morpholine thermolysis in dry steam derived empirically, the activation energy of the decomposition reaction was 160.0 (±2.0) $kJmol^{-1}$, the pre-exponential factor was $e^{21.7(\pm 0.66)}$ s^{-1} and the activation volume was 896 (± 36) cm^3mol^{-1}. Care must be taken when using the model results to calculate morpholine stability in the steam-water cycle, because wall effects during (hydro)thermolysis require further investigation.

3.1 Introduction

The information provided in Section 1.5 of this thesis shows that a better understanding of the behavior of amines at high temperatures is crucial for the use and acceptance of their application in fossil-fired plants. Most of the previous studies focused on trying to mimic a full boiler system and determining degradation products and mechanisms. However, because the thermolysis of any amine in steam depends on different parameters, of which temperature, pressure, time and catalytic effects due to wall surface composition are the most important, the effect of variations in each of these parameters needs to be investigated individually, in order to come to a better understanding of the mechanisms behind amine thermolysis in a full-scale steam-water cycle.

In this chapter, morpholine was selected to investigate the influence of time, pressure and temperature on the kinetics of the thermolysis of amines under boiler and superheater conditions. As was shown in Section 1.5, morpholine has been studied the most in the past, due to its application in nuclear power plants. First the comparison between thermolysis under boiler and superheater conditions was made, to confirm the influence of the superheater. The water/steam was sampled and analyzed for organic acid anions that were formed during thermolysis. Parameters that introduced uncertainty such as oxygen and heat-up/cooling issues, were minimized. The experimental data were used to propose and validate a model for morpholine degradation rate constants that include temperature and pressure as variables.

3.2 Methods & Materials

3.2.1 Flow reactor

The flow reactor used in this study is an adaptation of the flow reactor shown in Section 2.2 of this thesis. The biggest change was the replacement of metal balls with liquid salts to improve heat transfer and temperature

uniformity. The salt bath was a 2 L SS316-L cylinder, containing a 1:1 molar ratio $NaNO_2$:KNO_3 salt mixture for heat transfer, which melts at around 180 °C. The salt mixture was continuously stirred. A heating mantle around the vessel controlled temperature by a 4838 Parr (Frankfurt am Main, Germany) temperature controller. Temperature feedback was provided by a thermocouple from the salt solution to the controller. The water was sent through 6 meters of 1/16" 316 stainless steel tubing inside the salt bath. The volume of the tubes inside the reactor was 3.5 mL, but since water density decreases at higher temperatures, the actual retention time was a function of both pump velocity and steel bath temperature.

At the beginning of each experiment, the relief valve was set to the desired pressure and the temperature controller at the right temperature. The glass vessel was filled with ultrapure water (Elga Purelab Ultra, Veolia WS, Ede, The Netherlands) and sparged with nitrogen until oxygen was below 20 ppb O_2, after which 9 mL of a 1000 ppm morpholine solution (Sigma Aldrich) was added, which led to a pH of 9.2. Then carbohydrazide (Sigma Aldrich, 99% trace metal basis) was dosed at 1 ppm to scavenge any oxygen, after which the solution was again briefly sparged. The remainder of the experiment, the solution was kept under a nitrogen blanket, to prevent oxygen intrusion. When temperature was stable, the experiment was started and 4 mL samples were collected at the desired contact times. This was repeated for all conditions listed in Table 3.1 and executed in duplicate.

3.2.2 Analyses

Analysis of organic acid anions was performed using a Metrohm (Schiedam, The Netherlands) 881 ion chromatography system. A Metrohm A Supp 16 4.0/250 anion column was operated at 67 °C with eluent containing 7.5 mM Na_2CO_3 + 0.75 mM NaOH in ultrapure water. The suppressor was regenerated with 50 mM H_2SO_4 and the limit of detection was 1 ppb. For cation analysis a Metrohm C5 cation column was used, with 3 mM HNO_3 as an eluent, for which the limit of detection of morpholine was 5 ppb.

3.2.3 Modelling

First order isobaric degradation kinetics as a function of absolute temperature were modeled according to the following equations (Laidler, 1987):

$$r = k(T)\,[C] \tag{3.1}$$

$$k(T) = Ae^{\frac{-E_a}{RT}} \tag{3.2}$$

where:

r	=	degradation rate ($\mathrm{molL^{-1}s^{-1}}$)
$k(T)$	=	degradation rate constant ($\mathrm{s^{-1}}$)
$[C]$	=	concentration of the degrading compound ($\mathrm{molL^{-1}}$)
A	=	pre-exponential factor ($\mathrm{s^{-1}}$)
E_a	=	activation energy ($\mathrm{Jmol^{-1}}$)
T	=	temperature (K)
R	=	universal gas constant ($\mathrm{Jmol^{-1}K^{-1}}$)

The latter equation can be written as:

Table 3.1: Tested experimental conditions

	Temperatures (°C)	Pressures (MPa)	Retention times (s)
In water	352	17.5	80 – 350
In steam	470	9.5, 13.5, 17.5	
	490	9.5, 13.5, 17.5	7 – 65
	510	9.5, 13.5, 17.5	

$$\ln(k) = \ln(A) - \frac{E_a}{R}\frac{1}{T} \tag{3.3}$$

Meaning that in an Arrhenius plot of $\ln(k)$ vs. $1/T$ the slope of the regression line represents E_a/R, while the true y-intercept will correspond to $\ln(A)$.

Nguyen (2011) studied the temperature-pressure relation for the degradation of 5-methyltetrahydrofolic acid solutions and obtained first order kinetics over a pH range of 3-9.2. The activation energy (E_a) and activation volume (V_a) were proven independent of both temperature and pressure. Nguyen used the fact that when the natural logarithm of the degradation rate constant (k) is plotted as a function of pressure at constant temperature, the activation volume can be derived from the slope.

$$\ln(k) = \ln(k_{ref}) - \frac{V_a}{RT_{ref}}(P - P_{ref}) \tag{3.4}$$

where:

k_{ref}	=	degradation rate constant corresponding to T$_ref$ and P$_ref$ (s^{-1})
T_{ref}	=	reference temperature (K)
P_{ref}	=	reference pressure (MPa)
V_a	=	activation volume (m^{3}mol^{-1})

The calculated values for Va should be independent of the chosen values for T_{ref} and P_{ref}. The integrated first-order rate law is:

$$C = C_0 e^{-kt} \tag{3.5}$$

In which C_0 is the initial concentration of the degradation compound. Therefore the reaction rate constant k can be found by plotting C/C_0 against time and calculating the exponential regression function $y = e^{(-kx)}$. Subsequently A and E_a can be found by plotting $\ln(k)$ against $1/T$ for each pressure as described above. Lastly, V_a is determined by plotting $\ln(k)$ against P for each temperature and determining the slope of the regression line. The experimentally obtained k from each experimental run can be compared to the value for k calculated from the E_a, A and V_a that were obtained from the Arrhenius plots.

3.3 Results

3.3.1 Boiler vs. superheater

The results for hydrothermolysis of 9 ppm morpholine at 352 °C 17.5 MPa are summarized in Figure 3.1 and the

results for thermolysis at 490 °C 17.5 MPa are shown in Figure 3.2 to illustrate the difference in amine decomposition between the boiler and the superheater. Both figures also present the resulting formate and acetate concentrations. After 343 seconds, morpholine thermolysis at the chosen high-pressure boiler conditions was still below 5%, whereas the same amount of morpholine thermolyzed for more than 75% in 61 seconds at the chosen superheater conditions. This is also reflected by the increase in organic acid anion species, although, unlike the exponential decomposition of morpholine, this seems to be linear in time. This indicates that the organic acid anion species were not formed directly from the decomposition of morpholine, but from the further decomposition of other products. At boiler conditions, 0.44 ppm thermolyzed morpholine led to 17 (± 1.5) ppb of both acetate and formate. At 490 °C, 6.8 ppm decomposed morpholine led to 334 (±2) ppb acetate and 46 (±2) ppb formate. Gilbert & Lamarre (1989) identified glycolate as the dominant anionic degradation product, but in this study only small traces of glycolate were measured.

Temperatures in this study are higher though. It has previously been shown in Chapter 2 that at higher temperatures acetate becomes the dominant degradation product. Besides these anionic degradation products, 75% morpholine thermolysis produced 246 (±15) ppb ethanolamine and 1.6 (±0.1) ppm ammonia, of which about 0.35 ppm ammonia was produced by the thermolysis of 1 ppm carbohydrazide (determined from blank run). Because most of the nitrogen in the thermolyzed morpholine molecule became ammonia (which is a stronger base than morpholine) the thermolysis of morpholine would have raised the pH of the sample to

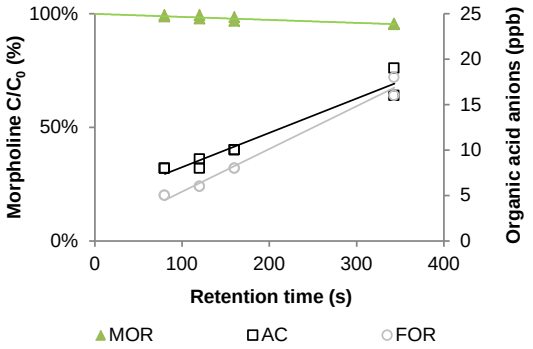

Figure 3.1: Hydrothermolysis of 9 ppm morpholine (MOR) and formation of acetate (AC) and formate (FOR) at 352 °C and 17.5 MPa

9.4 (at 25 °C), although this does not consider the production of CO_2. It is unlikely that pH has an influence on thermolysis in dry steam, because of the lack of ionization of molecules in steam. pH during hydrothermolysis under boiler conditions did not change noticeably. Organic degradation products without charge were outside the scope of this study and were therefore not measured.

The above shows that morpholine degraded faster in the superheated steam, as was also shown by Mori et al. (2012). Comparing the hydrothermolysis data from tests at boiler conditions to existing literature is difficult, due to differences in temperature, pressure, retention time and the ratio of the water volume and the metal surface area. Over the timespan of 343 seconds, hydrothermolysis of morpholine followed first order degradation kinetics. Thermolysis of morpholine in steam was well described by first order degradation kinetics as well, which will be further supported by data in the next section.

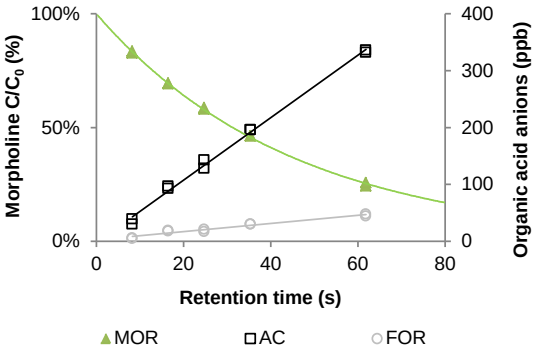

Figure 3.2: Thermolysis of 9 ppm morpholine (MOR) and formation of acetate (AC) and formate (FOR) at 490 °C and 17.5 MPa

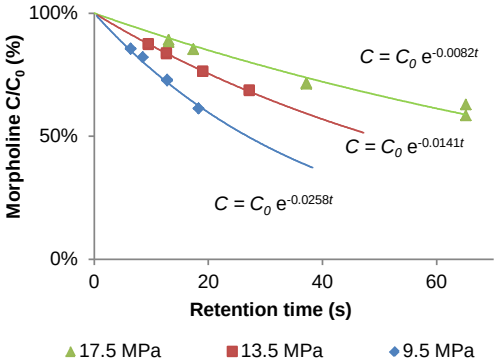

Figure 3.3: Thermolysis of morpholine in superheated steam at 470 °C for 9.5, 13.5 and 17.5 MPa

3.3.2 Temperature-pressure relation

The results for thermolysis of 9 ppm morpholine in superheated steam at 9.5, 13.5 and 17.5 MPa have been plotted for each of the tested temperatures. Figure 3.3, Figure 3.4 and Figure 3.5 show results for 470 °C, 490 °C and 510 °C respectively. Morpholine thermolysis in steam increased with temperature and decreased with increasing pressure. All results follow first order degradation kinetics and the exponential regression lines for the data points are given. At 470 °C, conversion kinetics increased from 40% in 65 seconds to 32% in 27 seconds to 39% in 18 seconds as pressure decreased. At 490 °C, conversion increased from 76% in 62 seconds to 82(±2)% in 45 seconds to 87(±2) in 31 seconds as pressure decreased. At 510 °C, conversion increased from 36% in 34 seconds to 60% in 18 seconds to 69% in 12 seconds as pressure decreased.

The Arrhenius plot of the obtained data is presented in Figure 3.6, with a curve for each tested pressure. The slope of the regression lines has been used to determine E_a and the true y-intercept equals $\ln(A)$. The average calculated E_a is 160 kJmol^{-1}, which is an 18% difference from the 131.9 kJmol^{-1} calculated by Gilbert & Lamarre (1989). The average calculated $\ln(A)$ is 21.7 s^{-1}, a value that Gilbert and Lamarre did not mention. Judging from extrapolation of their data to higher temperatures, morpholine degradation in their setup was slower, which might have to do with the difference between hydrothermolysis and thermolysis. Within the temperature and pressure range tested, errors of 1.28% and 3.02% for the average E_a and $\ln(A)$ were calculated respectively.

In Figure 3.7 $\ln(k)$ has been plotted against pressure for 470, 490 and 510 °C. The slope of the regression lines is equal to $V_a/(RT_{ref})$ for each temperature, which in case V_a and E_a are independent of both temperature and pressure should give a constant value. The average calculated value for V_a was 896 cm^{3}mol^{-1}, with an error of 3.98%,

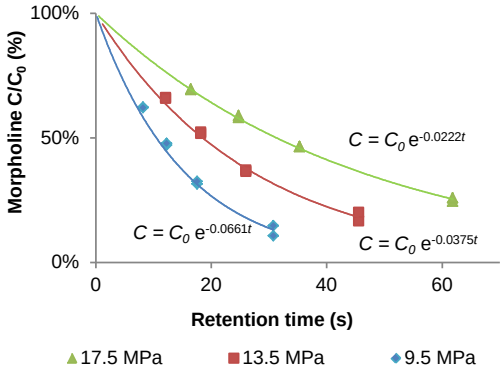

Figure 3.4: Thermolysis of morpholine in superheated steam at 490 °C for 9.5, 13.5 and 17.5 MPa

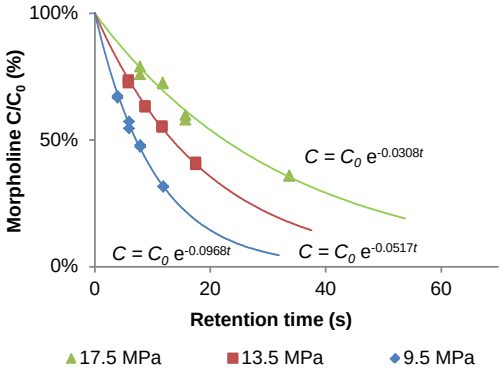

Figure 3.5: Thermolysis of morpholine in superheated steam at 510 °C for 9.5, 13.5 and 17.5 MPa

so the assumed temperature and pressure independence is plausible.

The degradation rate constants k were found by using the calculated value of E_a, A and V_a as input for Equations 3.3 and 3.4. The reference pressure that led to the smallest differences between calculated and measured k values was chosen. The reference pressure was determined by finding the smallest solution for the Mean Square Error of the modeled k value as a function of P_{ref}, from which a P_{ref} of 13.6 MPa was determined. When applying the acquired model to the results obtained at 352 °C and 17.5 MPa, the calculated hydrothermolysis was 4%, whereas the measured thermal decomposition was 5%. This could mean that the model can be extrapolated to lower temperatures to some degree and does not only fit the results for thermolysis in dry steam, but hydrothermolysis as well. The calculated k values are plotted against the empirical data in Figure 3.8. The predicted k does differ from the calculated values and is systematically lower for 490 °C and higher for 510 °C. The explanation for this difference could lie in the fact that the experiments at 490 °C were conducted first and the experiments at 470 and 510 °C were initiated a month later. Meanwhile, the thermal stability of other, more acidic substances was tested, which might have changed the metal surface composition of the tubing. Rossiter et al. (1985) investigated the thermal stability of ethylene glycol on several materials and concluded that the surface composition has a strong influence on degradation rates and products. Another explanation is that the prefactor is inherently valid over a limited temperature range. Therefore calculated values for k will become increasingly inaccurate as they deviate from the mean temperature.

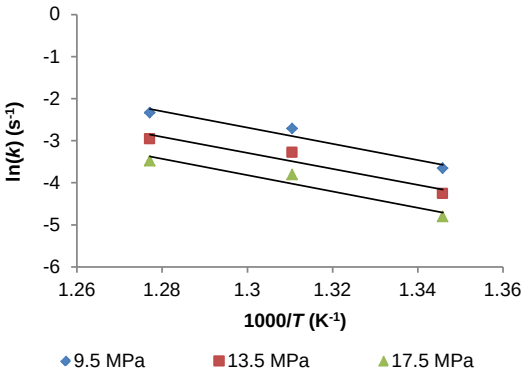

Figure 3.6: Arrhenius plot for morpholine degradation at 470, 490 and 510 °C for 9.5, 13.5 and 17.5 MPa

3.4 Discussion

Based on the comparison of the experiments and the modeling efforts, predictions of amine thermolysis in superheaters should be possible when system parameters are known. Morpholine hydrothermolysis in boilers seemed to be less important due to the lower temperatures, although the applied retention time of six minutes in the experiments was 10 times lower than in most fossil boilers. This six minutes retention time is a factor of two lower than most Heat Recovery Steam Generators though and three times higher than that of a nuclear recirculating PWR. Thermolysis in the superheater appeared to account for a much greater percentage of thermal degradation, but superheater retention times tend to be less than 10 seconds in an actual plant, which is close to the lowest retention times applied in the experiments described in this study. In addition, the steam remains heated in the high pressure turbine before being often reheated, increasing the time during which thermolysis in dry steam can occur. Therefore the visual interpretation of the graphs should not be directly translated to the real situation. Instead, the model results could be used for predictions by using the retention time, temperature and pressure in the superheater.

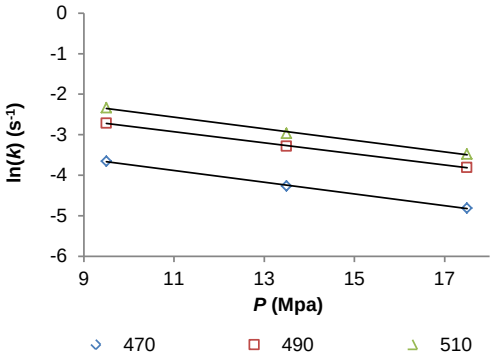

Figure 3.7: ln(k) plotted against pressure in MPa for 470, 490 and 510 °C. The slope of the regression lines is equal to $V_a/(RT_{ref})$

When considering a steam-water cycle consisting of a 352 °C - 17.5 MPa boiler and a superheater exhaust temperature of 510 °C with retention times of 20 minutes and 5 seconds respectively, thermal degradation in the boiler and superheater would be, based on the acquired model, 15% for both. However, a 17.5 MPa system will be likely to have a higher superheater exhaust temperature like 540 °C, which would cause 32% morpholine thermolysis in the steam phase, based on extrapolation of the acquired model. Much higher boiler pressures (beyond supercritical) and only slightly higher superheat temperatures are applied in fossil-fired power plants, which could mean that there are situations in which hydrothermolysis of amines in the boiler drum exceeds thermolysis in

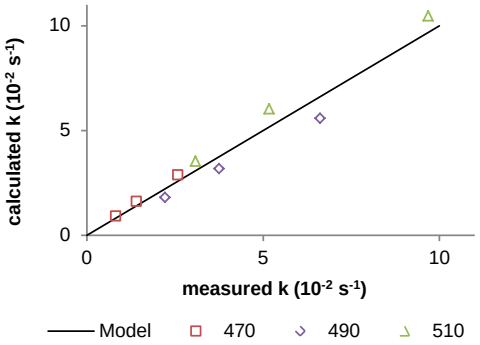

Figure 3.8: Model results of k values vs. the measured k values sorted by temperature in °C

the superheater. There are many industrial steam-water cycles though that operate at lower pressures and apply superheating. Shenburger et al. (1992) found almost no hydrothermolysis of morpholine at 286 °C - 6.9 MPa, but if this were to be followed by a 510 °C superheater, thermal degradation and degradation products could become high.

It is common for steam-water cycles to be classified by their pressure and, because of this, amines are applied up to a certain amount of MPa, depending on the compound. Results in this study showed that the applicability of an amine should not only depend on boiler pressure, but also on superheater temperature. In addition, the retention time in the boiler should be considered as well; a Once-Through Steam Generator with a water retention time of 25 seconds will react quite differently to amine based volatile chemical treatment than a fossil-fired steam-water cycle with a boiler retention time of 60 minutes. What should be considered as well is how much of the condensate is returned and what the blow-down rate is.

When it comes to maintaining sufficient pH to protect the steam-water cycle, the results are specific for morpholine. Because of the low pKa of morpholine, a measured 75% drop in concentration would not cause a large drop in pH (from 9.18 to 8.88 at 25 °C). With all nitrogen atoms becoming either part of ammonia or ethanolamine, the pH could rise, even when considering the produced organic acid anions, but unfortunately no data on CO_2 production is available which makes pH calculation for the condensate difficult. The hypothetical first moisture droplets, which would contain the remaining morpholine, ethanolamine and organic acid anions and almost no ammonia or CO_2, would have a pH (at 25 °C) of 8.70. Morpholine would in that case still provide a better protection against low pH in the low pressure turbine than ammonia, because it is as volatile as water. However, other amines with higher stability and basicity (such as cyclohexylamine) might be even more interesting.

It has previously been mentioned that the chemical composition of metal surfaces has influence on the degradation kinetics. Because this is an indication of a heterogeneous process in which the surface area participates, the surface:volume (S:V) ratio will have an influence as well. Segond et al. (2002) investigated the ammonia oxidation rate in sub- and supercritical water in an almost identical flow reactor as used in this study, but they used two stainless steel tube diameters (1.56 and 3.18 mm outer diameter). They concluded that the global oxidation rate constant of ammonia decreases with around 40%, when the $S{:}V$ ratio is doubled. Although this study does not deal with an oxidation process, it is likely that the metal

surface has a similar effect. A 1/16 inch (1.56 mm) stainless steel tube has an S:V ratio of 4 mm^{-1}, while a superheater tube of 20 mm in diameter has an S:V ratio of 0.5 mm^{-1}. Therefore, it is reasonable to assume that degradation kinetics in this study have been overestimated. Future studies should therefore focus on the influence of the metal surface and the difference between homogeneous and heterogeneous degradation kinetics. A strong influence of metal surface would mean that superheaters would become even more dominant in determining the thermal stability of alkalizing amines in steam-water cycles, because S:V ratios of boiler are in the 10^{-3} mm^{-1} order of magnitude. The results of Rossiter et al. (1985) show that the small tubing could be an intrinsic flaw of the experimental flow reactor that was used in this study. This can also be an explanation for the lower degradation rate of morpholine found by Gilbert & Lamarre (1991). If that were to be corrected, the flow reactor remains a good tool for simulating processes in the steam water cycle.

3.5 Conclusions

This study has led to the following conclusions:

- Thermolysis of morpholine at superheater conditions is higher than hydrothermolysis at boiler conditions.
- Degradation kinetics of morpholine thermolysis under superheater conditions were well described by a first order relationship. Anionic/acidic degradation products increased linearly with time.
- Degradation kinetics of morpholine in superheated steam increased with temperature and decreased with increasing pressure.
- In the stainless steel flow reactor with S:V ratio 4 mm^{-1}, E_a, $\ln(A)$ and V_a were 160 ($\pm$2.0) $kJmol^{-1}$, 21.7 ($\pm$0.663) s^{-1} and 896 ($\pm$36) cm^3mol^{-1} respectively. The resulting model produced degradation rate constants with a maximum error of 23% from the empirical result.

Care must be taken when using the model results to give an indication of morpholine stability in the steam-water cycle based on boiler and superheater retention times, because effects during (hydro)thermolysis require further investigation.

References

Gilbert, R., & Lamarre, C. (1989). Thermal stability of morpholine additive in the steam-water cycle of CANDU-PHW nuclear power plants. *Canadian Journal of Chemical Engineering*, *67*(4), 646-651.

Gilbert, R., & Lamarre, C. (1991). Identification and distribution of the morpholine breakdown products in the different cteam-condensate cycles of the CANDU-PHW nuclear power plants. *EPRI Workshop on Use of Amines in Conditioning Steam-Water Circuits*, Palo Alto, CA.

Laidler, K. (1987). *Chemical kinetics* (3rd Edition ed.). New York, NY: Harper Collins Publishers Inc.

Mori, S., Sato, T., & Shimura, Y. (2012). Characterization of amines under high temperature conditions and their use for boiler water treatment. *Corrosion*, Salt Lake City, UT.

Nguyen, M. T. (2011). Pressure-temperature degradation of (6R,S) 5-methyltetrahydrofolic acid: a kinetic study. *Vietnamese Journal of Science and Technology*, *49*(6A), 330-340.

Rossiter, W., Godette, M., Brown, P., & Galuk, K. G. (1985). An investigation of the degradation of aqueous ethylene glycol and propylene glycol solution using

ion chromatography. *Solar Energy Materials*, *1985*(11), 455-467.

Segond, N., Matsumare, Y., & Yamamoto, K. (2002). Determination of ammonia oxidation rate in sub- and supercritical water. *Industrial Engineering Chemistry Research*, *41*(24), 6020-6027.

Shenburger, D., Zupanovitch, J., & Walker, J. (1992). Loop testing of alternate amines for all-volatile treatment control in pwr's. *EPRI Report*, *TR-100756*, Palo Alto, CA.

4

Role of Metal Surface Catalysis in the Thermolysis of Amines

This chapter is based on:

Moed, D.H., Verliefde, A.R.D. and Rietveld, L.C. **(2014)** Role of Metal Surface Catalysis in the Thermolysis of Morpholine and Ethanolamine under Superheater Conditions. *Industrial & Engineering Chemistry Research*, 53(50), 19392-19397.

Abstract

Metal catalysis of amine thermolysis caused by oxides on the inner surface of superheater tubes has been investigated by using a flow-reactor and metal tubes of varying sizes and elemental composition. Kinetics of morpholine and ethanolamine thermolysis decreased as the tube size increased. The relation between the S:V ratio and the degradation rate constant k was linear. Heterogeneous thermolysis accounted for 82–92% of the value of the degradation rate constant k at an S:V ratio of 4.65 mm^{-1}. This decreased to only 6–17% at an S:V ratio of 0.4 mm^{-1}. Although results varied between the two applied materials, there is no consistent trend that can link thermolysis kinetics to tube wall composition. Organic acid anion production was weakly related to amine structure, temperature and tube diameter, but strongly related to metal oxide composition, with formate and acetate altering as dominant organic acid anion. A distinction between homogeneous and heterogeneous thermolysis has been made, but results indicate that a lab study with a large enough tube diameter will lead to more reliable predictions.

4.1 Introduction

In Chapter 3 morpholine (MOR) degradation kinetics were found to be first order, increasing with temperature and decreasing with pressure. The tubes used in the flow reactor in Chapter 3 were only 1.5 mm in diameter though, making the surface:volume (S:V) ratio much bigger than in a full scale fossil fired plant, of which the tube diameter is at least 10 times larger. Degradation studies in a similar flow reactor revealed the importance of the S:V ratio during ammonia oxidation (Segond et al., 2002). The study of Segond et al. assumes a linear relation between S:V ratio and the degradation rate constant (k), but bases this finding on measurements with just 2 tube diameters. Except for the S:V ratio, the composition of the tube could have an influence as well, as is shown in metal oxide catalysis studies (Jackson & Hargreaves, 2009).

In this chapter, a more thorough investigation of amine degradation under fossil fired plant conditions was carried out. MOR and ethanolamine (ETA) were selected to investigate the influence of temperature, amine structure, S:V ratio and metal surface composition on the kinetics of the thermolysis of amines at superheater conditions. This was done by installing four different tube diameters in two different materials (so eight combinations in total) in the flow reactor used in Chapter 3. The influence of temperature on MOR and ETA degradation was tested at 500 and 530 °C. Pressure was kept at a constant 13.5 MPa pressure, to ensure pressure would not influence the results as was observed in Chapter 3. The condensed steam was sampled and analyzed for amines and organic acid anion concentrations, the latter being measured because of its importance in practical situations. The resulting data was used to find a relation between S:V ratio and amine degradation kinetics, thereby showing the importance of the metal surface and its potential catalytic effects when degradation reactions occur. Parameters that can introduce uncertainty such as oxygen and heat-up/cooling issues were minimized.

4.2 Methods & Materials

4.2.1 Flow reactor

The flow reactor used in this study is an adaptation of the flow reactor used in Chapters 2 and 3 and is shown in Figure 4.1. Instead of a liquid salt bath, a fluidized sand bath was used for heat transfer, which is safer and easier to heat, cool and control. A glass vessel containing the solution of interest was equipped with a pH and oxygen meter, to monitor the influent quality. The vessel also contained a tube for argon sparging to remove oxygen and an HPLC pump inlet equipped with a filter. This HPLC pump provided the pressure to send the water through stainless steel tubing inside a fluidized sand bath at a fixed flow rate to rapidly heat the feedwater. Instead of a liquid salt bath, a fluidized sand bath was used for heat transfer. The fluidized sand bath was an Omega (Stamford, CT, USA) FSB-3 containing fine aluminum oxide for heat transfer. The fluidized sand bath temperature was regulated by a 4838 Parr (Frankfurt am Main, Germany) temperature controller. Temperature feedback was provided by a thermocouple from the fluidized sand bath to the controller. Upon leaving the sand bath, this water was immediately cooled in a cooling spiral that was submerged in a beaker with water, which was kept at 20($\pm$2) °C by letting tap water run through it. Back pressure was controlled by an adjustable relief valve (BPR) (Swagelok, Waddinxveen, the Netherlands).

The volume of the tubes inside the reactor differed per tube material and diameter. Since water and steam increase in volume at higher temperatures, the retention time in the tubing is a function of both flow velocity and fluidized sand bath temperature.

4.2.2 Procedure and conditions

At the beginning of each experiment, the relief valve was first set to the desired pressure and the temperature controller at the right temperature. The glass vessel was filled with ultrapure water (Elga Purelab Ultra, Veolia WS, Ede, The Netherlands) and sparged with argon until oxygen was below 20 ppb O_2, after which 9 ppm of the amine of interest was added. Then carbohydrazide (Sigma Aldrich, 99% trace metal basis) was dosed at 0.1 ppm to scavenge any remaining oxygen, after which the solution was again briefly sparged with argon. During the remainder of the experiment, the solution was kept under a nitrogen blanket, to prevent oxygen intrusion. When temperature was stable, the experiment was started and a 4 mL sample was taken at the desired contact time. This was repeated for all the conditions listed in Table 4.1 and executed in duplicate (64 experiments in total, with 4 retention times tested during each experiment).

The outer diameters of the tubes were 1.59, 3.18, 6.35, and 12.7 mm, with a wall thickness of 0.36, 0.71, 0.89 and 1.27 mm respectively. The inside of the tubes had to have a metal oxide layer before the experiments started, to ensure this did not change during the run. To create a metal oxide layer on a new tube before starting experiments, the tubing was pre-treated by flushing for 24 hours with a 17 ppm (1 M) NH_3 solution at 300 °C and 10.0 MPa while maintaining 10–20 ppb oxygen in the influent. Table 4.2 shows the elemental composition range for 316 stainless steel (SS) and Hastelloy C-276 (C276) in percentages.

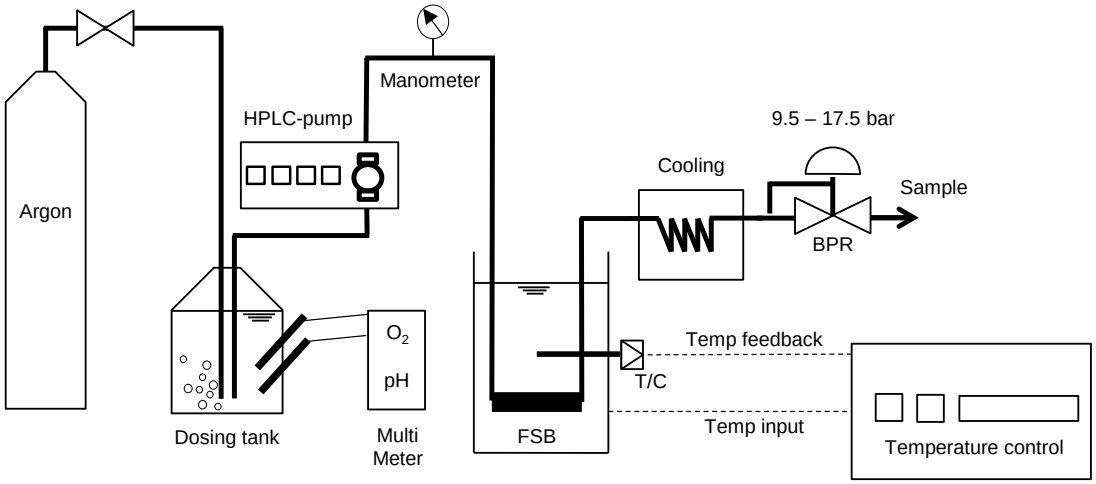

Figure 4.1: Schematic of the flow reactor used for the thermolysis of amines

Table 4.1: Conditions applied during the experiments for both MOR and ETA

Materials	S:V **ratios**	T	P	t
Stainless Steel 316	4.65 mm^{-1}	500 °C	13.5 MPa	0 – 5 s
Hastelloy C276	2.32 mm^{-1}	530 °C		5 – 10 s
	0.89 mm^{-1}			10 – 20 s
	0.4 mm^{-1}			20 – 30 s

Table 4.2: Elemental composition range of the 316 Stainless Steel and Hastelloy C-276 Alloy in percentages. For elements with an asterisk the maximum value is given

	Fe	**Cr**	**Ni**	**Mo**	**W**	**Co***	**Mn***	**Si***	**C***	**S***
SS	62 – 68	16 – 18	11 – 14	2 – 3	-	-	2	0.75	0.035	0.03
C276	4 – 7	14.5 – 18.5	51.5 – 60	15 – 17	3 – 4.5	2.5	1	0.08	0.01	0.03

4.2.3 Analyses

Analysis of organic acid anions was performed using a Metrohm (Schiedam, The Netherlands) 881 ion chromatography system. A Metrohm A Supp 16 4.0/250 anion column was operated at 67 °C with eluent containing 7.5 mM Na_2CO_3 + 0.75 mM NaOH in ultrapure water. The suppressor was regenerated with 50 mM H_2SO_4 and the limit of detection was 1 ppb. For cation analysis a Metrohm C5 cation column was used, with 3 mM HNO_3 as an eluent, for which the limit of detection of MOR and ETA was 5 ppb.

The surface composition of the larger tubing was analyzed with X-Ray Diffraction (XRD). The samples were fixed with plasticine on the holder. The instrument used was a Bruker D8 Advance diffractometer, Bragg-Brentano geometry with graphite monochromator and Vantec position sensitive detector. Co K radiation was applied, with a divergence slit 1 mm, 45 kV / 35 mA and no sample spinning. The scatter screen position was lowered on the wall of the tube, preventing the X-ray beam on the wall reaching the detector. Data was evaluated with Bruker software Diffrac.EVA version 3.1.

The tubing with an outer diameter (OD) of 3.18 and 1.59 mm was too small for successful XRD analysis and therefore Scanning Electron Microscopy (SEM) and Energy Dispersive Spectroscopy (EDS) were employed to obtain the chemical composition of the inner surfaces exposed. The micrographs were obtained from a JEOL JSM 6500F using an electron beam with energy of 15 keV and beam current of approximately 200 pA. The micrographs obtained were acquired in secondary electron image mode (SEI) and back scattered electron image mode (BEI). EDS was performed with an Thermo-Fisher Ultradry Solid State Drift detector (SSD) and processed with Noran System 7 software. The compositions of point measurements were determined semi-quantitatively using computer stored reference spectra of the pure elements with an acquisition time of 30 seconds.

4.2.4 Temperature and S:V relations

First order isobaric degradation kinetics as a function of absolute temperature were modeled according to the Equations in Section 3.2 of this thesis. By investigating degradation at different surface to volume ratios, both homogeneous and heterogeneous degradation kinetics of the amines can be calculated. Segond et al. (2002) provided evidence for a linear relation between the $S{:}V$ ratio and k according to:

$$k(T) = A_H e^{\frac{-E_{a;H}}{RT}} + A_W e^{\frac{-E_{a;W}}{RT}} \frac{S}{V} \qquad (4.1)$$

where:

A_H	=	prefactor for homogeneous degradation (s^{-1})
$E_{a;H}$	=	activation energy for homogeneous degradation ($Jmol^{-1}$)
A_W	=	prefactor for heterogeneous degradation (s^{-1})
$E_{a;W}$	=	activation energy for heterogeneous degradation ($Jmol^{-1}$)

Results in this study show whether assuming such a linear relation can be justified. It will also show to what extent the surface area of the reaction is important.

4.3 Results & Discussion

During all experiments degradation behavior was investigated at several retention times and each experiment led to plots as shown in Figure 4.2, which represent the experimental degradation curves for MOR thermolysis at 530 °C and 13.5 MPa in SS tubes of four different diameters. Because the different curves are represented quite well by first-order kinetic models, the value of the kinetic rate constant k for each experiment could be derived from the exponential regression line through the data points and $t = 0$, $C/C_0 = 1$.

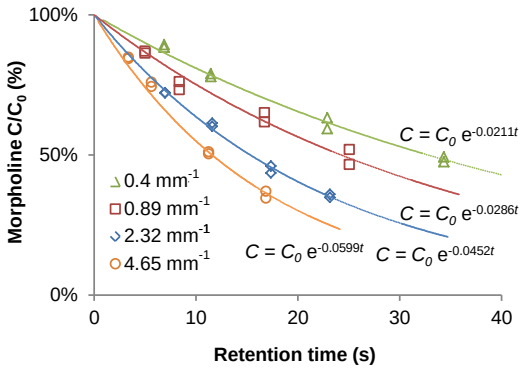

Figure 4.2: C/C_0 vs. retention time for morpholine degradation at 530 °C and 13.5 MPa on stainless steel for four tube sizes

The resulting k values from the different experiments with the different amines at the range of temperatures were combined for the two metals, and were used to determine the slope and y-intercept of the S:V ratio plotted against k, which is shown in Figure 4.3 (A and B). A linear relation between k and S:V ratio was found for both ETA and MOR for both materials, with k increasing as the S:V ratio increased, although some variation in k value for the same experiment can be observed. MOR was more stable than ETA at both tested temperatures. The metal oxide catalysis effect of the tube wall surface appeared to be bigger for the thermolysis of ETA than MOR (since the slope of k as a function of S:V ratio is steeper for ETA). As the S:V ratio approaches 0 (i.e. the tube diameter becomes infinitely large), there is only homogeneous thermolysis occurring and degradation kinetics (k) are not influenced by metal oxide catalysis any more.

No large difference between experiments with SS and C276 were seen, although it can be seen from the graphs that the homogenous part of k, derived from the y-intercept, was different for the tubes made of SS and C276 for ETA at 500 °C. The stronger effect of metal surface catalysis on ETA has an influence on the reproducibility. Although no consistent differences in kinetic rate constant between the two materials were found, the XRD analysis of the surface composition of the tubes revealed large differences in oxide composition for each metal tube. The SEM/EDS results obtained for the smaller diameters reveal that, by weight, there were more oxides formed on the SS tubes than on the C276 tubes. However, the XRD analysis did not detect much chromium or nickel oxides on the C276 tubes, while the SEM/EDS results suggest that this should have been the case. The surface compositions were distinctly different, both visually and chemically, and vary even for the same material, but there was no consistent difference noticeable in the k-values for first order thermolysis that can be attributed to the metal oxide composition. To illustrate this, the Relative Standard Deviations (RSDs) for

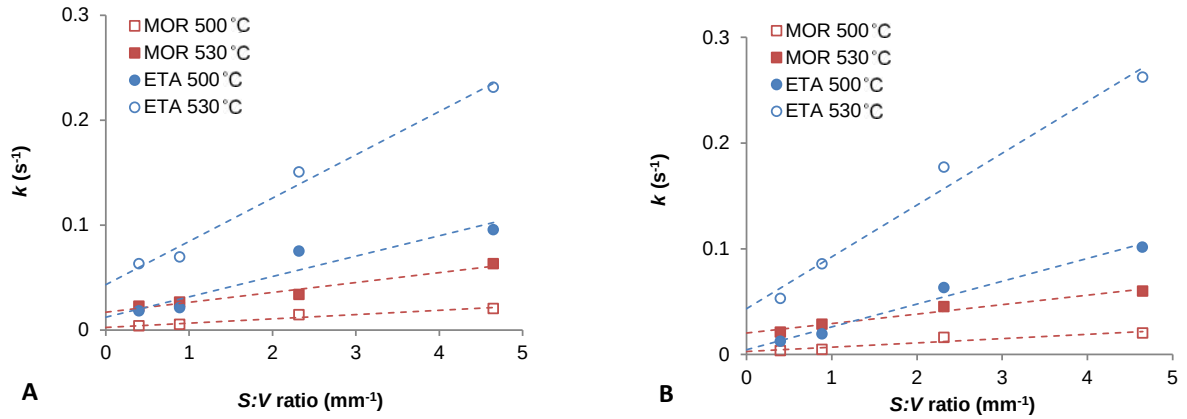

Figure 4.3: Calculated values of k plotted against the S:V ratio at 500 and 530 °C and 13.5 MPa for C276 (A) and SS (B)

values found for k found for SS and C276 at the same conditions have been plotted in Figure 4.4. Each $S{:}V$ ratio was used in four experiments for each combination of amine and temperature.

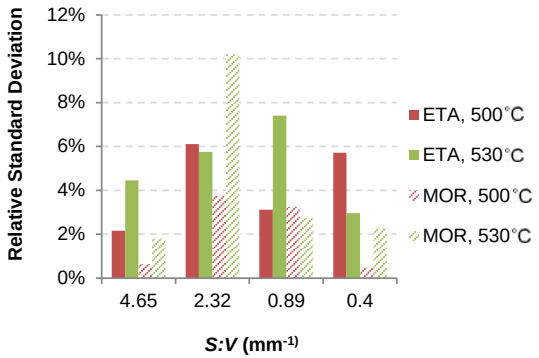

Figure 4.4: RSD for values of k found for the same experiment with SS compared to C276, executed in duplicate

If the surface composition had a strong influence on the uncertainty in degradation kinetics, the RSDs found would have decreased along with the $S{:}V$ ratio. The highest differences in k value between SS and C276 were noticeable for ETA and it is not certain that this can be attributed to differences in surface composition, since this was not observed during MOR thermolysis. There may be other effects that impact the results (change of surface during experiment, differences between the macroscopic and microscopic surface size), which are not included in this simple model.

The homogeneous and heterogeneous Arrhenius constants as determined from the experimental data using Equation 4.1 are shown in Table 4.3. The value calculated from these constants for k at 510 °C and 13.5 MPa of 0.044 s^{-1} is in the same order of magnitude as the 0.051 s^{-1} found in Chapter 3. The previously discussed errors found between the results for metal surface catalysis of SS and C276 during ETA thermolysis, are reflected

in the Arrhenius constants found for the homogeneous part of the equation. The errors combined caused the linear regression lines of ETA degradation at 500 °C to cross the y-axis at 0.0124 and 0.062 s^{-1} for C276 and SS respectively. This 50% difference causes a 45% difference between the homogeneous activation energies found for both materials and is also reflected in a 47% difference between the natural logarithms of the homogeneous prefactors A_H. Differences in degradation kinetics for MOR were smaller which is again reflected in the Arrhenius constants.

The large effect of errors over the whole set of experiments on the homogeneous Arrhenius constants for ETA indicates that trying to account for wall effects when modeling amine thermolysis in superheaters introduced more uncertainty. The data show that at the lowest investigated S:V ratio, catalytic wall effects accounted for only 6–17% of the total value of k, while at the highest S:V ratio this went up to 82–92%. Therefore, thermolysis of amines at superheater conditions should be investigated in a laboratory setting, using a tube large enough to represent an actual superheater.

From the above results, it can be concluded that results of previous studies with smaller tube diameters have given an overestimation of degradation kinetics during amine thermolysis at superheater conditions. To make predictions of amine longevity in fossil fired power plants and industrial steam-water cycles possible, a data set with a larger tube diameter (1.25 mm or more) has to be created for all amines that are currently being applied, covering a large temperature and pressure range. Extrapolation to only homogeneous catalysis based on different S:V ratios is not recommended, as this introduces large errors.

Another factor of uncertainty that will be introduced when translating experimental data to full-scale steam-water cycles, is that heating will not be as instantaneous as in the lab. There is a temperature profile over the length of the superheater tube and retention times at a certain temperature can be uncertain. On top of that, the tube wall will be hotter than the steam and the exhaust temperature is regulated. Therefore wall effects could start to play an increasing role again.

4.3.1 Organic acid anion formation

As stated in the introduction, potential organic acid anion formation during amine thermolysis is currently preventing the wider acceptance of amines for application in steam-water cycles. The thermolysis of ETA and MOR in this study led to the formation of mostly acetate and formate, although some traces (up to 20 ppb) of glycolate were found for both amines and traces of propionate were found after MOR degradation. Figure 4.5 shows the relation between the highest achieved degradation percentage and the formate and acetate production during each experimental run, for MOR and ETA.

The highest concentrations of organic acid anions were measured for ETA, but this was also the amine that reached the highest degradation percentages. The spread was high and there were some severe outliers for both amines for both acetate and formate. There does not seem to be a clear relationship between organic acid anion production, amine structure and degradation percentage. When the same data for organic acid anion formation is sorted by tube OD it can be seen that experiments

Table 4.3: Calculated homogeneous and heterogeneous Arrhenius constants for ETA and MOR thermolysis at 13.5 MPa

	$E_{a;H}$ **(kJmol^{-1})**	$\ln(A_H)$ **(s^{-1})**	$E_{a;W}$ **(kJmol^{-1})**	$\ln(A_W)$ **(s^{-1})**
ETA on C276	215.3	29.11	150.7	19.37
ETA on SS	389.3	55.18	131.1	16.51
MOR on C276	324.0	44.45	179.5	22.32
MOR on SS	343.1	47.49	137.0	15.66

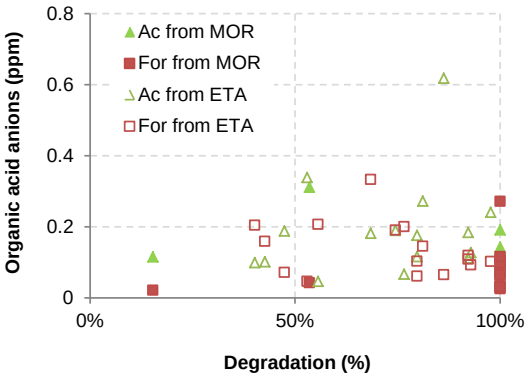

Figure 4.5: Maximum degradation vs. formate (For) and acetate (Ac) production from 9 ppm MOR and ETA for all temperatures, tube sizes and materials

performed with larger tube diameters produced more organic acid anions (plot not shown). Higher temperatures on average produce more acetate and less formate (plot not shown), which was also concluded in Chapter 2.

A more obvious relation was observed when plotting the same data for formate and acetate sorted by used tube material (Figure 4.6). Experiments performed with tubes made of SS produced more acetate than formate, while the exact opposite was observed for tubes made of C276.

Although no large influence of surface composition was found for larger diameters when it comes to degradation kinetics, catalytic effects of the wall did have an influence on the type of organic acid anions produced for all tube sizes. The material composition of the wall surface had more influence on the degradation pathway than the temperature, tube diameter or amine composition.

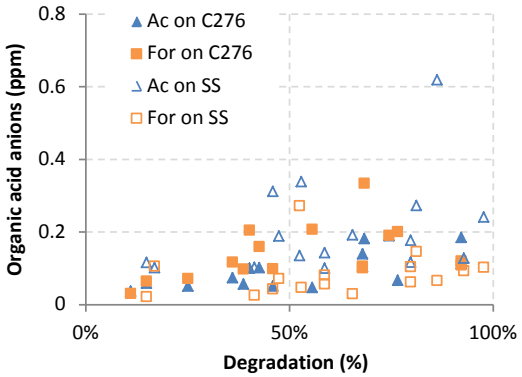

Figure 4.6: Maximum degradation during an experiment vs. formate (For) and acetate (Ac) production on SS and C276 for all temperatures, tube sizes and amines

The concentrations for ETA used in this paper are exaggerated, because much less is needed to maintain suf-

ficiently high pH in a steam-water cycle (1.51 ppm for a pH of 9.2 at 25 °C). MOR concentrations in practice are around 10 ppm to maintain the same pH in the condensate because of the low pK_a of MOR (8.94 ppm for a pH of 9.2 at 25 °C). Therefore MOR thermolysis in a superheater will in practice produce more organic acid anions than ETA, based on the concentrations at which they are applied.

The higher stability of MOR does give it a slight advantage when it comes to organic acid anion production, but ETA's better basicity at high temperature, lower concentration to maintain sufficient pH and the resulting lower organic acid anion concentrations will make ETA more attractive for use as an alkalizing amine in steam-water cycles than MOR. There will be a maximum temperature for both amines to be applied though, for which more research is necessary.

4.4 Conclusions

This chapter has led to the following conclusions:

- There was an influence of the metal oxides on the inner tube wall on amine thermolysis kinetics, with degradation rate increasing as the tube size decreased.
- The relation between the S:V ratio and the degradation rate constant k was linear.
- Metal surface catalysis during thermolysis of MOR and ETA accounted for 82–92% of the value of the degradation rate constant k at an S:V ratio of 4.65 mm^{-1}. This decreased to only 6–17% at an S:V ratio of 0.4 mm^{-1}.
- Although results varied between the two applied materials, there is no consistent trend that can link thermolysis kinetics to tube wall composition.
- A distinction between homogeneous and heterogeneous thermolysis has been made, but results indicate that a lab study with a large enough tube diameter will lead to more reliable predictions.
- Organic acid anion production was weakly related to amine structure, temperature and tube diameter, but strongly related to metal oxide composition. More formate was found when using C276 tubes and more acetate when using SS tubes.
- The higher stability of MOR seems to give it an advantage when it comes to organic acid anion production, but ETA's higher basicity at high temperature (thus lower concentration to maintain sufficient pH) and the resulting lower organic acid anion concentrations will make ETA more attractive for use as an alkalizing amine in steam-water cycles than MOR.
- There is a maximum combination of temperature and retention time for both amines to be applied at, for which more research is necessary.

References

Jackson, S. D., & Hargreaves, J. S. J. (2009). *Metal oxide catalysis* (1st Edition ed.). Hoboken, NJ: Wiley Publishing.

Segond, N., Matsumare, Y., & Yamamoto, K. (2002). Determination of ammonia oxidation rate in sub- and supercritical water. *Industrial Engineering Chemistry Research*, *41*(24), 6020-6027.

5

Effects of Temperature and Pressure on the Thermolysis of five Alkalizing Amines

This chapter is based on:

Moed, D.H., Verliefde, A.R.D. and Rietveld, L.C. **(2015)** Effects of Temperature and Pressure on the Thermolysis of Morpholine, Ethanolamine, Cyclohexylamine, Dimethylamine, and 3-Methoxypropylamine in Superheated Steam. *Industrial & Engineering Chemistry Research*, 54 (10), 2606-2612

Abstract

Morpholine, ethanolamine, cyclohexylamine, dimethylamine and 3-methoxypropylamine were exposed to 500, 530 and 560 °C at 9.5, 13.5 and 17.5 MPa to investigate the influence of temperature and pressure on amine thermolysis kinetics. The surface:volume ratio of the reactor tube was 0.4 mm^{-1}, close to the value of superheater tubes in steam-water cycles. All amines thermolyzed by first order kinetics, with the exception of dimethylamine. The Arrhenius constants E_a, $\ln(A)$ and V_a were obtained from the experimental data for all investigated amines. The influence of pressure on thermolysis kinetics was less pronounced than in previous studies and was different for each amine. Dimethylamine did not degrade below 20 and 10% at 500 and 530 °C respectively, in spite of longer retention times being applied, suggesting synthesis may occur. Limited practical data showed some promise for the applicability of the model to steam-water cycles. More plant data is necessary to fully validate the model. In all cases, thermolysis of the amines led to the formation of between 150 and 600 ppb organic acid anions. In most cases the concentrations increased linearly with increasing degradation percentage. Acetate and formate were found as major degradation products, with some propionate and traces of glycolate. Cationic degradation products were ammonia and some amines, meaning that the complete thermolysis of an amine does not necessarily lead to acidic conditions.

5.1 Introduction

Amine degradation kinetics were found in Chapter 3 to be first order, increasing with temperature and decreasing with pressure. The tubes used in the flow reactor in Chapter 3, however, were only 1.5 mm in diameter, making the surface:volume (S:V) ratio of 4.65 mm^{-1} much higher than in full scale fossil fired plants, of which the tube diameters are typically at least 10 times larger. The metal oxide layer on the surface of the tubes appeared to also influence thermolysis kinetics. Chapter 4 provides a relation between S:V ratio and thermolysis kinetics, and makes a distinction between homogeneous (in the bulk steam) and heterogeneous (on the metal surface) thermolysis. Although heterogeneous thermolysis accounted for 82 - 92% of the value of the degradation rate constant k for tubing with an S:V ratio of 4.65 mm^{-1}, this was only 6 - 17% at an S:V ratio of 0.4 mm^{-1}. This led to the conclusion that an amine thermolysis study is best conducted with larger metal tubes, preferably 0.4 mm^{-1} or less, in order to approximate superheater tube sizes.

In this study, temperature and pressure dependence of the thermolysis of five amines that are being applied in steam-water cycles (morpholine (MOR), ethanolamine (ETA), dimethylamine (DMA), cyclohexylamine (CHA) and 3-methoxypropylamine (MOPA)) were studied in a flow reactor equipped with a Hastelloy C-276 tube with an S:V ratio of 0.4 mm^{-1}. The data was used to construct a predictive model to assess the thermal stability of amines in high temperature and pressure steam-water cycles. The organic acid anions and ammonia that are produced during amine thermolysis are discussed and an explanation is given as to why DMA does not degrade according to first order kinetics.

5.2 Methods & Materials

5.2.1 Setup and conditions

The experimental setup used in this study is identical to that described in Section 5.2 of this thesis. An HPLC pump sends the solution of interest through Hastelloy C-276 tubing inside a fluidized sand bath at a fixed flow rate. The tube inside the fluidized sand bed has a 12.5 mm external diameter with a volume of 6.2 ml and an internal diameter of 10 mm, thus having an $S{:}V$ ratio of 0.4 mm^{-1}.

The amine solutions of interest were tested at the conditions listed in Table 5.1 and experiments were executed in duplicate. Retention times were varied by adjusting the HPLC pump flow to 0.75, 1.0, 1.5 or 2.5 mL/min and the flow was checked for accuracy before every run. Because water and steam increase in volume at higher temperatures, the retention time in the tubing is a function of flow, temperature and pressure inside the tube. Therefore applied retention times are listed in ranges. Oxygen was removed with argon and 0.1 ppm carbohydrazide was dosed to eliminate any remaining traces of oxygen.

Table 5.1: Conditions applied during the experiments for both MOR and ETA

Amines	T	P	t
MOR	500 °C	9.5 MPa	0 – 5 s
ETA	530 °C	13.5 MPa	5 – 10 s
DMA	560 °C	17.5 MPa	10 – 20 s
CHA			20 – 30 s
MOPA			

5.2.2 Analyses

Analysis of organic acid anions was performed using a Metrohm (Schiedam, The Netherlands) 881 ion chromatography system. A Metrohm A Supp 16 4.0/250 anion column was operated at 67 °C with eluent containing 7.5 mM Na_2CO_3 + 0.75 mM NaOH in ultrapure water. The suppressor was regenerated with 50 mM H_2SO_4 and the limit of detection was 1 ppb. For cation analysis a Metrohm C5 cation column was used, with 3 mM HNO_3 as the eluent, for which the limit of detection of MOR, ETA, MOPA and DMA was 5 ppb, and 50 ppb for CHA. The detection limit for ammonia was 1 ppb.

5.2.3 Temperature and pressure relations

Amine thermolysis was modeled according to the equations in Section 3.2 of this thesis. Combining Equations 3.3 and 3.4, the reaction rate as a function of temperature and pressure can be written as:

$$r = k(T,P)[C] = e^{ln(A) - \frac{-E_a}{RT} - \frac{-V_a}{RT}(P - P_{ref})}[C] \quad (5.1)$$

In order to find the experimental values for k, an integrated first-order rate law was fitted to the experimentally determined decrease in concentration of the amines upon degradation. First order is assumed because this was found to be the case for amine degradation in most previous studies (Domae & Fujiwara, 2009; Gilbert & Lamarre, 1989) and in Chapters 3 and 4 of this thesis.

5.3 Results & Discussion

5.3.1 Temperature and pressure relations

Degradation curves were constructed from the obtained data. The thermolysis of all amines led to first order regression curves, with the exception of DMA which will be discussed in more detail. First order kinetics applied to degradation percentages over 90% as well, showing concentration independency in the range 1-9 ppm. This range could be bigger, but the data cannot validate such a claim. The values for k resulting from the degradation curves were used to create the Arrhenius plots for the temperature relation. An example of such a plot is given in Figure 5.1, which shows the relation between $\ln(k)$ and $1/T$ for the thermolysis of ETA in dry steam. The linear regression lines given for each pressure enabled the calculation of the activation energy E_a (by using the slope) and the prefactor A (by using the y-intercept). The average of the resulting three E_a and $\ln(A)$ values was used in the model. The same data have been used to plot $\ln(k)$ against P for each temperature (see Figure 5.2) from which V_a was calculated, by using the slope of the linear regression lines at each temperature. The average for the three temperatures is the value of V_a used in the proposed model.

The Arrhenius plots for the other four amines can be found in Appendix Section 5.5. In the appendix, Figure 5.8, Figure 5.11 and Figure 5.14 show the pressure relation of $\ln(k)$ for MOR, MOPA and CHA and have almost horizontal regression lines. Figure 5.7, Figure 5.10 and Figure 5.13 show their temperature relation of $\ln(k)$,

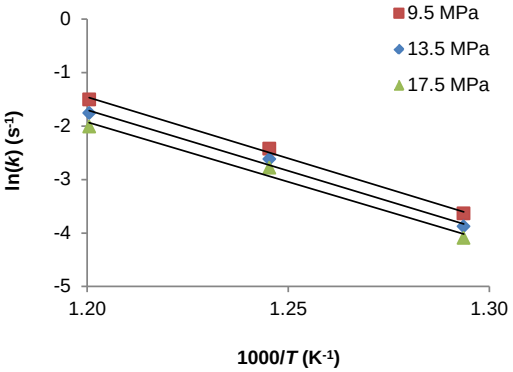

Figure 5.1: Arrhenius plot of the relation between ln(k) and 1/T for the thermolysis of ETA in dry steam at 500, 530 and 560 °C

of which the regression lines are close together. MOR, MOPA and CHA therefore show no clear pressure dependency. All values found for E_a, A and V_a are summarized in Table 5.2, including the errors. The activation volumes of MOR, MOPA and CHA have been highlighted in gray, because of their apparent lack of pressure dependency.

It must be noted that higher activation energy does not necessarily imply higher thermal stability of a compound, as thermal stability also depends on the prefactor A. The activation energy indicates the amount of energy that is required to start the degradation reaction, but the prefactor A determines how quickly the amine degrades as a function of temperature. For example, the thermolysis of CHA in dry steam has a high activation energy at 500 °C, resulting in a higher value for k than for MOR, making CHA more stable than MOR at that temperature. However, the high prefactor determines that the rate constants of CHA and MOR are almost the same at

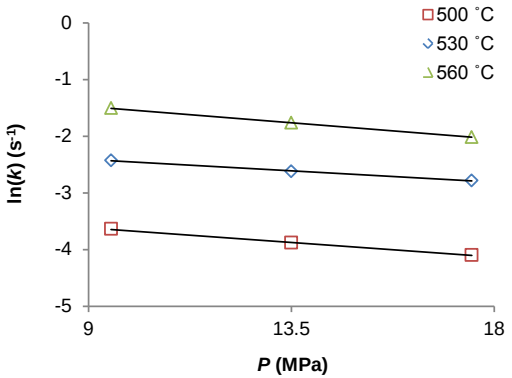

Figure 5.2: Plot of the relation between ln(k) and P for the thermolysis of ETA in dry steam at 9.5, 13.5 and 17.5 MPa

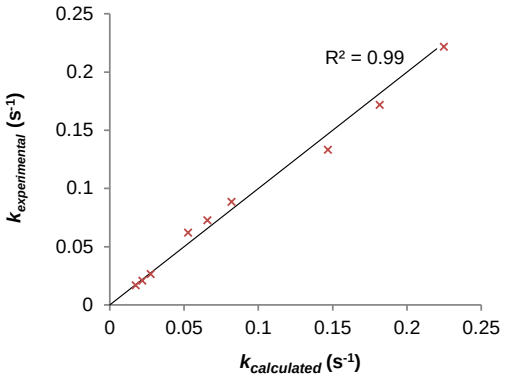

Figure 5.3: Calculated values of k plotted against the experimentally obtained values of k for all experiments conducted with ETA

560 °C and 13.5 MPa (0.074 and 0.072 s^{-1} respectively).

In Chapter 3 calculated MOR thermal stability was much lower, but that study was executed with a smaller (S:V = 4.65 mm^{-1}) stainless steel tube, resulting in a large contribution of catalytic wall effects in the thermolysis. This emphasizes the importance of the S:V ratio when studying thermal degradation in conditions resembling full-scale plants, as was shown in Chapter 4. In order to compare the experimentally obtained values of k to those calculated using Equation 5.1 and the results in Table 5.2, the experimental k was plotted against the calculated k. The coefficient of determination R^2 was used as a measure for goodness of fit. As an example, the relation between measured and calculated values of k for ETA is shown in Figure 4. The figures for all other amines are provided in the Appendix in Section 5.5 (Figure 5.9, Figure 5.12, Figure 5.15 and Figure 5.18). The coefficients of determination of the modelled compared to the experimental data for ETA, MOR, MOPA, CHA and DMA are 0.99, 0.97, 0.97, 0.92 and 0.99, respectively.

5.3.2 Dimethylamine

DMA requires special attention among the studied amines because it was the only compound that did not degrade by first-order kinetics in all situations. The previously discussed Arrhenius plots and model calculations for DMA have been made with k values derived from the shortest retention times (Figure 5.4A), but when DMA was exposed to longer retention times, first order kinetics did not apply anymore. At 500 °C, thermal degradation stopped when DMA was at around 20%, as shown in Figure 5.4B. At 530 °C, the DMA concentration did not drop below 10%. At 560 °C, the DMA concentration went down to less than 2% within a few seconds, but the compound never fully degraded. In some cases, DMA concentrations measured for longer retention times were

Table 5.2: Summary of E_a, ln(A) and V_a found for each amine, including the Standard Deviation (SD) and Relative Standard Deviation (RSD)

Amine	Constant	Mean	SD	RSD	Unit
ETA	E_a	189	1	1%	($kJmol^{-1}$)
	$\ln(A)$	25.5	0.4	2%	(s^{-1})
	V_a	369	59	16%	(cm^3mol^{-1})
MOR	E_a	295	15	5%	($kJmol^{-1}$)
	$\ln(A)$	40.2	2.2	5%	(s^{-1})
	V_a	137	134	98%	(cm^3mol^{-1})
MOPA	E_a	254	16	6%	($kJmol^{-1}$)
	$\ln(A)$	35.6	2.4	7%	(s^{-1})
	V_a	6	151	2343%	(cm^3mol^{-1})
CHA	E_a	409	12	3%	($kJmol^{-1}$)
	$\ln(A)$	56.9	1.7	3%	(s^{-1})
	V_a	272	112	41%	(cm^3mol^{-1})
DMA	E_a	100	3	3%	($kJmol^{-1}$)
	$\ln(A)$	13.6	0.4	3%	(s^{-1})
	V_a	346	19	6%	(cm^3mol^{-1})

even higher compared to shorter retention times and a clear increasing trend was observed. For instance, at 500 °C and 17.5 MPa, 15% DMA remains after 14 seconds in the reactor. After 43 seconds at the same conditions, 23% DMA is left. This increase cannot be explained through the error of detection of the ion chromatograph.

Longer retention times do not allow degradation of DMA below 20% at 500 °C, suggesting that the DMA thermolysis reaction is reversible. This can only be the case if DMA is synthesized from the breakdown products. Mochida et al. (1983) investigated the synthesis of DMA and methylamine from ammonia and methanol over metal oxides at 300 450 °C which could yield up to 50%. A patent by Ashina et al. (1986) describes almost the same process, but claims that higher selectivity for DMA can be obtained by exposing methanol and ammonia to steam at 250 700 °C. During the experiments, ammonia was a degradation product and the presence of methanol is plausible. Methylamine was also found as a degradation product in all DMA experiments, and its concentration remained constant at higher retention times. Although all this is speculative, the synthesis of DMA in a superheater, or perhaps in the condensing stages, is plausible.

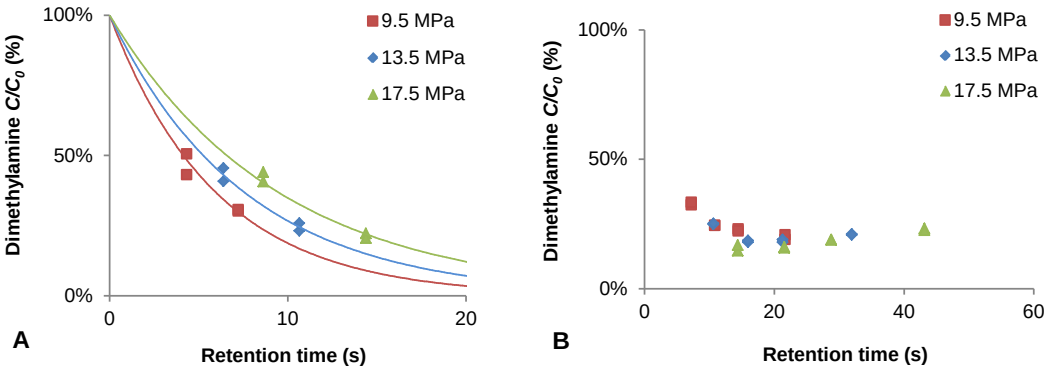

Figure 5.4: Degradation percentage vs. retention time for the thermolysis of DMA at 500 °C for shorter (A) and longer (B) retention times. First order degradation does not apply to longer retention times.

5.3.3 Organic acid anion formation

Potential organic acid anion formation during amine thermolysis is currently preventing the general acceptance of amines for application in steam-water cycles. In Chapter 4, formate and acetate were found to be the major anionic degradation products of MOR and ETA. In addition, glycolate was measured as a degradation product of MOR and ETA. In the current study, however, also propionate was found in samples from MOR degradation. All organic acid data from MOR thermolysis experiments conducted in the current study, is summarized in Figure 5.5. Formate was the major degradation product, which does not correspond to the findings in the previous study with a higher $S{:}V$ ratio. This indicates that the surface of the tubes does not only have an influence on the degradation kinetics, but also on what degradation product is preferably formed. Formate, acetate and propionate all increased with increasing degradation (despite the increasing temperature), while glycolate was only found at trace levels throughout all MOR thermolysis experiments.

The other organic acid plots for all amines can be found in the Appendix in Section 5.5 (Figure 5.19, Figure 5.20, Figure 5.21 and Figure 5.22). It is seen that formate and acetate from ETA degradation were found at similar concentrations (by mass) and their concentrations increased linearly up to 290 ppb for 100% amine degradation. Glycolate concentrations after ETA degradation seem to decrease with increasing ETA degradation, but also decreased with increasing temperature, which indicates low thermal stability of glycolate. For MOPA the highest concentration found for the degradation products were those of formate (up to 242 ppb), and acetate (up to 120 ppb). Propionate concentrations increased with increasing MOPA degradation, but did not exceed 17 ppb.

The highest total organic acid anion concentration during CHA thermolysis was less than 200 ppb. Acetate

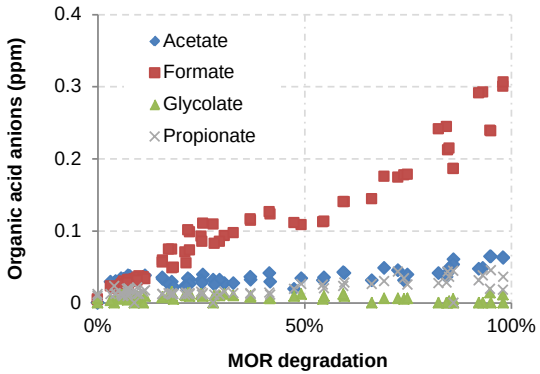

Figure 5.5: Acetate, formate, glycolate and propionate formation vs. degradation percentage during thermolysis of MOR at 500, 530 and 560 °C and 9.5, 13.5 and 17.5 MPa

concentrations from CHA were slightly higher than formate concentrations, which were slightly higher propionate concentrations. All three organic acid anions increased proportional to CHA degradation. An offset of 5 ppb formate and 10 ppb acetate can be seen for low degradation percentages. This is caused by organic carbon contamination (from e.g. air or plastic pump interior), which is hard to prevent, even in full-scale plants. This is also the reason that DMA thermolysis seems to produce small amounts of acetate, which cannot be the case. DMA produced almost exclusively formate, which can be attributed to its small molecule structure, making formation of other organic acid anions improbable, unless synthesis would occur. Formate was also observed to be the only anionic degradation product by Bull (2013) when using DMA as an ammonia replacement for a secondary circuit.

Although acetate and propionate concentrations did not fluctuate, the formate concentrations went up and down for all amines, even under similar conditions and degradation percentages. This can be seen mostly for ETA, MOPA and DMA, where formic acid concentrations for high degradation percentages vary between 159 - 271 ppb, 51 - 242 ppb and 62 - 299 ppb, respectively. What causes the formate concentrations to be so unpredictable is further discussed in Chapter 6. Over the entire study, 1-15% of the carbon released by degraded amines could be traced back as organic acid anions (by mass), meaning that a large proportion of the amines degraded to neutral compounds.

In all cases, thermolysis of the amines led to the formation of organic acid anions. In most cases the concentrations increased linearly with increasing degradation percentage. Organic acid anions are a concern in power plant regions with two-phase flow, because organic acids are less volatile than ammonia. This means that when applying amines there might be a point at which the acidity of the degradation products has enough influence on the water phase that magnetite (the protective oxide layer found at power plant conditions) solubility increases. In practice, not all amines would be dosed at the same concentration, since their dosage will depend on their basicity. An amine that requires a lower dose to maintain sufficiently high pH in a steam-water cycle, will also form fewer organic acid anions. It also has to be noted that amines and organic acid anions in a power plant will cycle through the system, so the thermal stability of organic acids in superheated steam matters as well. Regardless, the protection an amine offers is a combination of its thermal stability and tendency to produce

organic acid anions.

5.3.4 Nitrogen balance

As an amine breaks down, the cationic degradation products could still offer some protection. Ammonia and other cationic degradation products were measured in this study to determine the percentage of nitrogen that can be found as cations providing alkalinity. This has been expressed as a percentage of the total organic nitrogen in the influent. For MOR, which degraded into ammonia and small traces of ETA (up to 229 ppb), the results of cationic degradation products are shown in Figure 5.6. Not all nitrogen could be traced back as ammonia or other cationic degradation products. This is probably due to the degradation of the amines and/or ammonia to inorganic nitrogen, or to the loss of ammonia during grab sampling, due to its volatility. A blank run with only 0.1 ppm carbohydrazide revealed that 33 (±15) ppb ammonia came from the carbohydrazide. Results have been corrected for this.

For other amines a higher degree of scattering is seen in the nitrogen recovery plots, which is shown in the Appendix in Section 5.5 (in Figure 5.23, Figure 5.24, Figure 5.25 and Figure 5.26). In some cases, 100% of the nitrogen can be accounted for, usually at the lower temperatures or lower degradation percentages. In all cases the dominant cationic degradation product was ammonia. For DMA, traces of methylamine (up to 236 ppb) were found as decomposition products as well, while MOPA also degraded to some hydroxyl propylamine (up to 204 ppb).

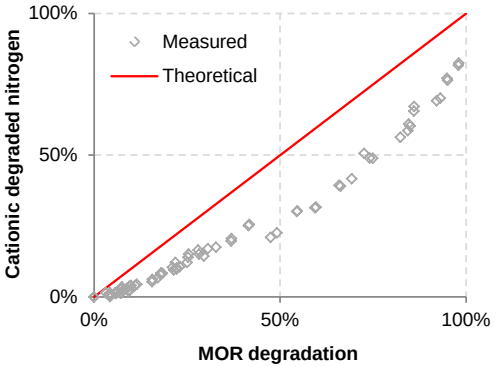

Figure 5.6: The percentage of the total nitrogen measured as cationic degradation products (theoretical and measured) for MOR at 500, 530 and 560 °C and 9.5, 13.5 and 17.5 MPa

With most nitrogen always being converted to ammonia or another amine, the thermolysis of an amine in a power plant does not necessarily have to lead to a hazardous pH drop, as the pH effect by formation of organic acids will mainly be countered by the alkalizing effect of the ammonia. As stated in the previous section, this could still imply a lower degree of protection in two-phase flow, as some organic acids are less volatile than ammonia and prefer the liquid film which covers the metal surface.

5.3.5 Comparison with practical data

Practical data in literature that can be used to verify the model is almost non-existent, mostly due to the lack of information on retention times in superheaters and reheaters. Some general comparisons can be made though. Layton & Daniels (2010) reported a power plant survey on amine usage which showed detailed data for

ETA degradation in several parts of two plants (A and B), while in plant B CHA was also dosed. The third plant (C) ran (partially) on MOPA dosing. The superheater and reheater temperatures of plant A, B and C were 540, 566 and 538 °C, with pressures of 17.9, 13.1 and 13.1 MPa, respectively.

Retention times could not be calculated from the reported data, so degradation percentages can only be compared relative to each other. Similarity was found between their results and this study, in the stability of CHA relative to ETA. Layton and Daniels showed a loss of CHA and ETA over the superheater and reheater, but also showed that CHA is more stable than ETA at 551 °C. The average loss percentages of CHA and ETA were 47(±7)% and 60(±11)% respectively at a 551 °C reheater steam temperature. According to the model presented in this paper, a 47% decrease in CHA at 551 °C and a pressure of 13.1 MPa corresponded to a 70% loss of ETA at similar conditions. The findings corroborate practical data (within the degree of accuracy of the plant data). When applying the same retention time to the conditions found in plant C (a Heat Recovery Steam Generator like plant B), the model predicts a 70% loss of MOPA, which is close to the highest degradation percentage of MOPA found in that specific plant of 66%.

It should be kept in mind that comparisons between model data based on lab-scale experiments and full-scale data need to be handled with care. Amines in a plant do not stay at a fixed temperature for a few seconds, but follow a profile of temperatures. Determining retention times and temperature profiles in superheater and reheaters is a challenge. However, making these kinds of comparisons is important for assessing the applicability of amine thermal stability modelling.

A difference in model and plant data is found in the organic acid anions formation in plant A, where ETA is being dosed. There was almost no formate measured at this location, which is different from what was measured in plant B and the observations during the ETA degradation in this study. This underlines the unpredictable behavior of formate. Plant B shows a formate to acetate ratio close to what was experimentally obtained in this lab-scale study. In plant C organic acid concentrations were very low, but the MOPA was dosed at only 20 ppb.

5.4 Conclusions

This study has led to the following conclusions:

- All amines thermolyzed by first order kinetics, with the exception of dimethylamine.
- The obtained Arrhenius constants were:

	E_a **(kJmol^{-1})**	$\ln(A)$ **(s^{-1})**	V_a **(cm^{3}mol^{-1})**
ETA	189	25.5	369
MOR	295	40.2	137
MOPA	254	35.6	6
CHA	409	56.9	272
DMA	100	13.6	346

- The influence of pressure on thermolysis kinetics was much less pronounced than in previous studies, which can probably be attributed to the low $S{:}V$ ratio in this study, which was applied to come closer to superheater conditions.

- Dimethylamine did not degrade below 20 and 10% of the initial concentration at 500 and 530 °C respectively, in spite of longer retention times being applied. This suggests that synthesis may occur, either at high temperature or in the condensing stages. Further studies are necessary to clarify this phenomenon.
- In all cases, thermolysis of the amines led to the formation of organic acid anions. In most cases, the concentrations increased linearly with increasing degradation percentage. Acetate and formate were found as major degradation products, with some propionate and traces of glycolate.
- Cationic degradation products consisted of mostly ammonia and some amines, meaning that the complete thermolysis of an amine does not necessarily lead to acidic conditions. Not all nitrogen could be traced back to these cationic degradation products, suggesting that some other inorganic nitrogen species were formed, or ammonia was lost during sampling.
- Comparing the model to some limited practical measurements of amines in power plants shows some promise in the model applicability. A larger dataset and more information on superheater retention times are necessary to validate the model proposed in this paper, which should try to focus on retention times in the hottest sections of power plants.

References

Ashina, Y., Fujita, T., Fukatsu, M., & Yagi, J. (1986). Process for producing dimethylamine in preference to mono- and trimethylamines by gas phase catalytic reaction of ammonia with methanol. *US 4582936*, April 15.

Bull, A. (2013). Dimethylamine as a replacement for ammonia dosing in the secondary circuit of an advanced gas-cooled reactor power station. *16th International Conference on the Properties of Water and Steam*, London, United Kingdom.

Domae, M., & Fujiwara, K. (2009). Thermal decomposition of 3-methoxypropylamine as an alternative amine in PWR secondary systems. *Journal of Nuclear science & Technology*, *46*(2), 210-215.

Gilbert, R., & Lamarre, C. (1989). Thermal stability of morpholine additive in the steam-water cycle of CANDU-PHW nuclear power plants. *Canadian Journal of Chemical Engineering*, *67*(4), 646-651.

Layton, K. F., & Daniels, D. G. (2010). Interim guidance - amine treatments in fossil power plants. *EPRI Report*, *1019636*, Palo Alto, CA.

Mochida, I., Yasutake, A., Fujitsu, H., & Takeshita, K. (1983). Selective synthesis of dimethylamine from methanol and ammonia over zeolites. *Journal of Catalysis*, *82*(2), 313-321.

5.5 Appendix

5.5.1 Supporting graphs: temperature-pressure relations

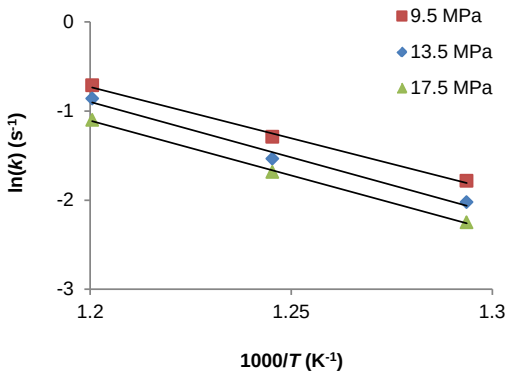

Figure 5.7: Arrhenius plot of the relation between ln(k) and 1/T for the thermolysis of DMA in dry steam at 500, 530 and 560 °C

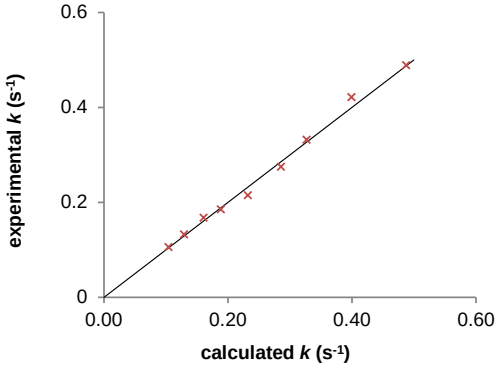

Figure 5.9: Calculated values of k plotted against the experimentally obtained values of k for all experiments conducted with DMA

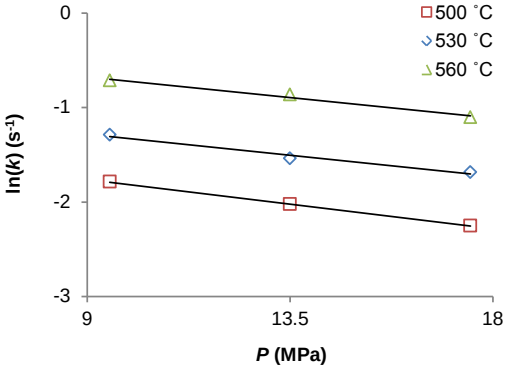

Figure 5.8: Plot of the relation between ln(k) and P for the thermolysis of DMA in dry steam at 9.5, 13.5 and 17.5 MPa

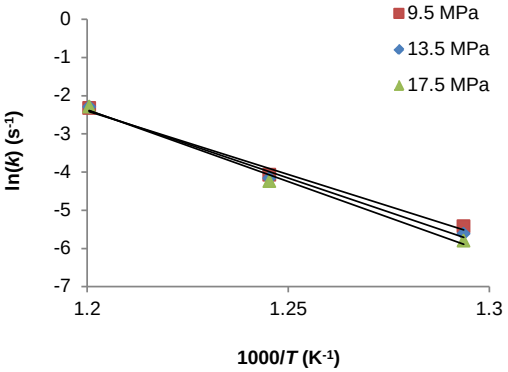

Figure 5.10: Arrhenius plot of the relation between ln(k) and 1/T for the thermolysis of MOR in dry steam at 500, 530 and 560 °C

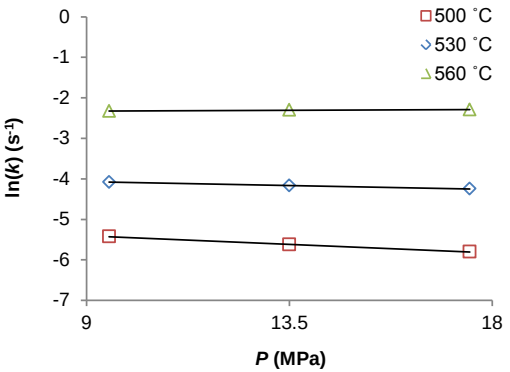

Figure 5.11: Plot of the relation between ln(k) and P for the thermolysis of MOR in dry steam at 9.5, 13.5 and 17.5 MPa

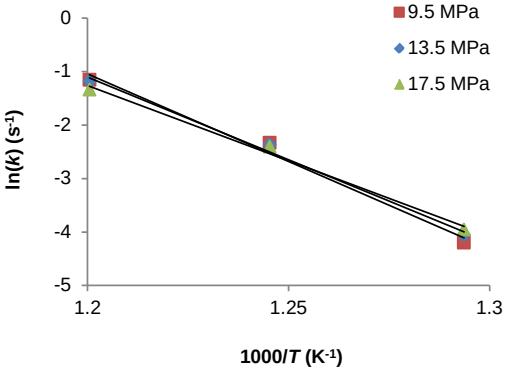

Figure 5.13: Arrhenius plot of the relation between ln(k) and 1/T for the thermolysis of MOPA in dry steam at 500, 530 and 560 °C

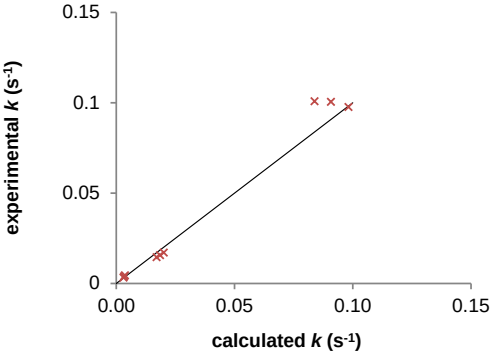

Figure 5.12: Calculated values of k plotted against the experimentally obtained values of k for all experiments conducted with MOR

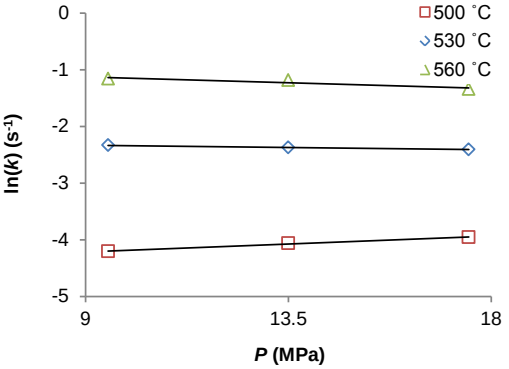

Figure 5.14: Plot of the relation between ln(k) and P for the thermolysis of MOPA in dry steam at 9.5, 13.5 and 17.5 MPa

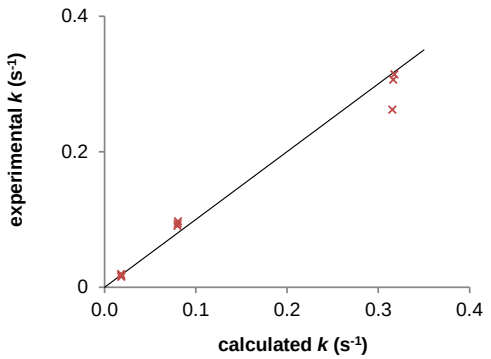

Figure 5.15: Calculated values of k plotted against the experimentally obtained values of k for all experiments conducted with MOPA

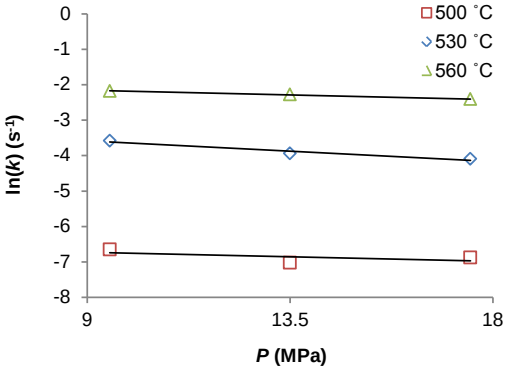

Figure 5.17: Plot of the relation between ln(k) and P for the thermolysis of CHA in dry steam at 9.5, 13.5 and 17.5 MPa

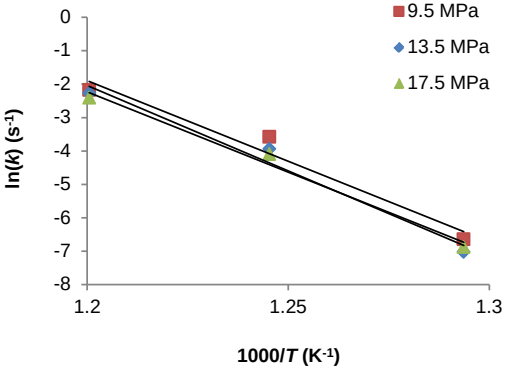

Figure 5.16: Arrhenius plot of the relation between ln(k) and 1/T for the thermolysis of CHA in dry steam at 500, 530 and 560 °C

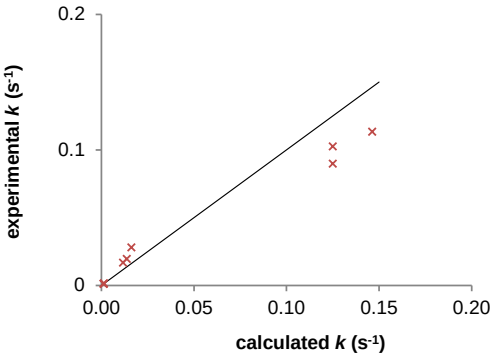

Figure 5.18: Calculated values of k plotted against the experimentally obtained values of k for all experiments conducted with CHA

5.5.2 Supporting graphs: organic acid anions

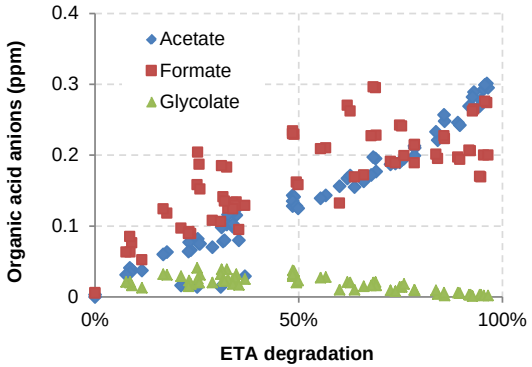

Figure 5.19: Acetate, formate and glycolate formation vs. degradation percentage during thermolysis of ETA at 500, 530 and 560 °C and 9.5, 13.5 and 17.5 MPa

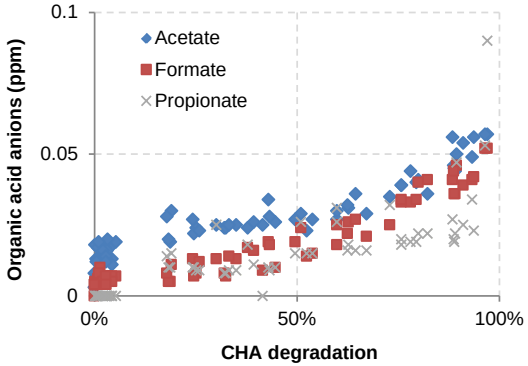

Figure 5.21: Acetate, formate and propionate formation vs. degradation percentage during thermolysis of CHA at 500, 530 and 560 °C and 9.5, 13.5 and 17.5 MPa

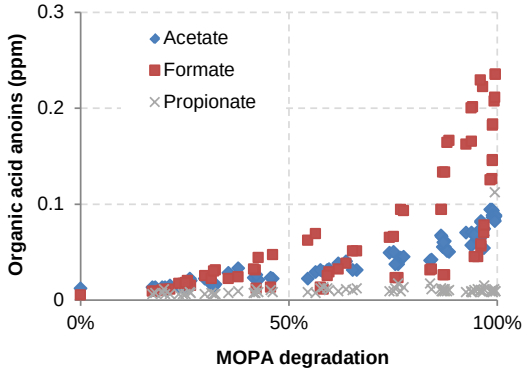

Figure 5.20: Acetate, formate and propionate formation vs. degradation percentage during thermolysis of MOPA at 500, 530 and 560 °C and 9.5, 13.5 and 17.5 MPa

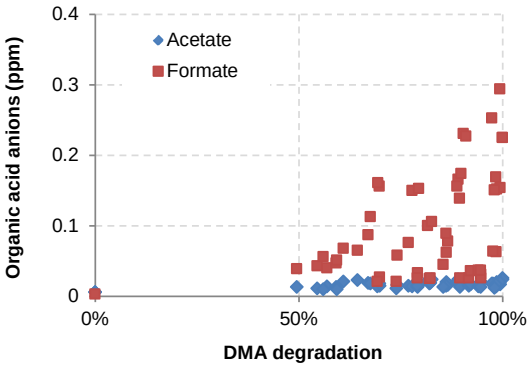

Figure 5.22: Acetate and formate formation vs. degradation percentage during thermolysis of DMA at 500, 530 and 560 °C and 9.5, 13.5 and 17.5 MPa

5.5.3 Supporting graphs: nitrogen recovery

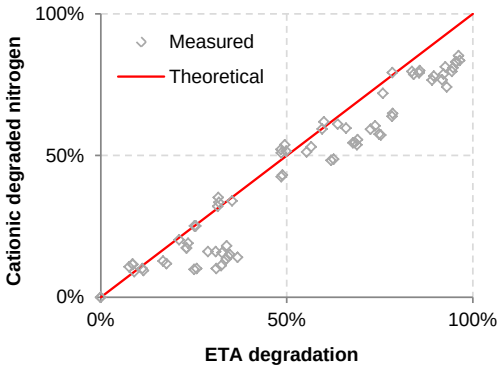

Figure 5.23: The percentage of total nitrogen measured as cationic degradation products for ETA at 500, 530 and 560 °C and 9.5, 13.5 and 17.5 MPa

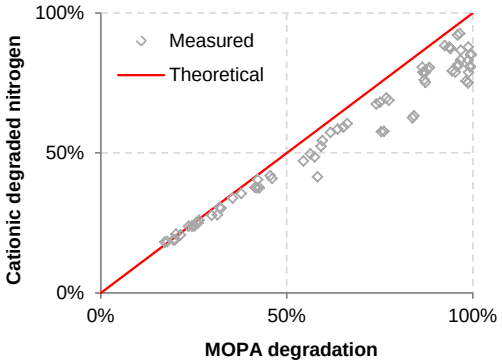

Figure 5.24: The percentage of total nitrogen measured as cationic degradation products (theoretical and measured) for MOPA at 500, 530 and 560 °C and 9.5, 13.5 and 17.5 MPa

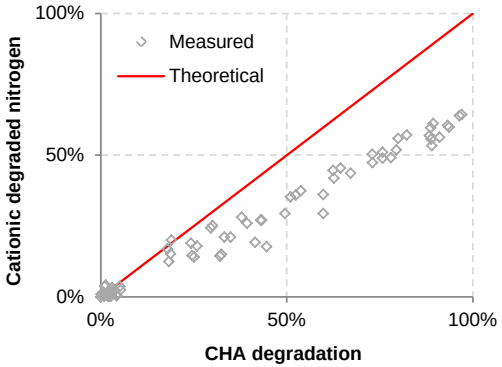

Figure 5.25: The percentage of total nitrogen measured as cationic degradation products (theoretical and measured) for CHA at 500, 530 and 560 °C and 9.5, 13.5 and 17.5 MPa

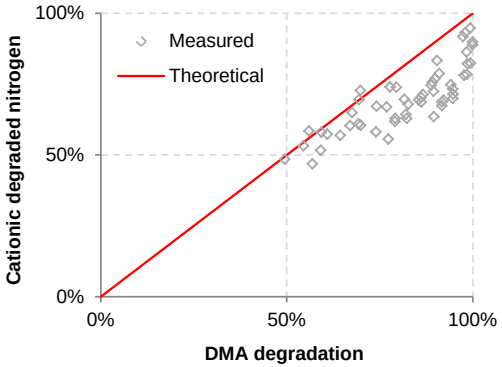

Figure 5.26: The percentage of total nitrogen measured as cationic degradation products (theoretical and measured) for DMA at 500, 530 and 560 °C and 9.5, 13.5 and 17.5 MPa

6

Anionic Organic Contamination in Petrochemical Steam-Water Cycles

This chapter is based on:

Moed, D.H., Verliefde, A.R.D., Muller, E. and Rietvel,d L.C. **(2015)** Sources of Anionic Organic Contamination in Petrochemical Steam-Water Cycles. *Industrial Water Treatment*, 32 (2), 33-42

Abstract

This study investigates the degree to which possible contaminants in petrochemical steam-water cycles can produce organic acid anions and the thermal stability of formic and acetic acid with a flow reactor. This has been done in high temperature water at 275 °C (6.0 MPa) and 375 °C (13.5 MPa) and in superheated steam at 510 °C (13.5 MPa). The (hydro)thermolysis of 10 ppm organic carbon as ethylene glycol and slurry oil produced up to a few hundred ppb acetate and formate. The (hydro)thermolysis of 10 ppm organic carbon as polyethylene glycol produced a high variety and quantity of organic acid anions, that could only partially be determined to be in the lower ppm range. The (hydro)thermolysis of 10 ppm organic carbon as the water dissolvable fraction of gasoil, naphtha and hydro wax led to organic acid anion concentrations that only slightly exceeded the blank results. A concentration of 10 ppm methyl ethyl ketoxime thermally degraded into several organic acid anions and nitrite in the higher ppb or lower ppm range. The species and quantity of anionic degradation products was strongly dependent on temperature and retention time for all tested compounds. Formate was dominant at the lowest temperatures, whereas acetate (and for methyl ethyl ketoxime also propionate) was highest in quantity at the highest tested temperatures. Formic acid is very unstable under steam water cycle conditions. It is still found in high temperature and pressure steam-water cycles though and therefore could be synthesized in the condensing stages at the right conditions. Acetic acid has high thermal stability and is therefore the dominant organic acid anion at high temperatures. The Arrhenius constants for acetic acid thermolysis in a superheater are: $E_a = 162.7\ (\pm 4.4)$ kJmol^{-1}, $\ln(A) = 20.1\ (\pm 0.9)$ s^{-1} and $V_a = 617.5\ (\pm 27.1)$ cm^{3}mol^{-1}.

6.1 Introduction

No work has been published on the sources of anionic contaminants found in petrochemical steam-water cycles. In these cycles, Total Organic Carbon (TOC) concentrations might increase due to a lack of feedwater treatment, by insufficiently treated return condensate from process steam or through condenser and heat exchanger leaks. There is also the possibility that organic treatment chemicals (designed to improve cycle chemistry) are applied at a temperature at which they thermally decompose to (amongst others) organic acid anions. As shown in the amine thermolysis studies, the application of water treatment chemicals can lead to anionic contamination as well. The oxygen scavenger methyl ethyl ketoxime (MEKO) has therefore been included in this study. Acetate is frequently reported as the dominant organic acid anion arising from organic compound breakdown at higher temperatures, while formate is found mostly in low temperature systems, which has also been verified in Chapter 2. Being the most prominent anionic contaminants in steam-water cycles, their thermal stability is assessed in this Chapter as well.

This chapter investigates the degree to which the (hydro)thermolysis of possible organic contaminants and MEKO can produce organic acid anions under steam-water cycle conditions. The investigated contaminants were mono ethylene glycol (MEG), polyethylene glycol (PEG) and the water dissolvable fractions of gasoil, naphtha, slurry oil and hydro wax. On top of that,

the thermal stability of acetic and formic acid as most commonly found degradation products of TOC in steam-water cycles, was investigated. Because the presence of acetic acid is one of the biggest concerns in all types of steam-water cycles, its thermal stability was quantified for a bigger range of high temperatures and pressures.

6.2 Methods & Materials

The Experimental setup used in this study is almost identical to that described in Section 5.2 of this thesis, although nitrogen was used instead of argon for oxygen removal.

6.2.1 Procedure and conditions

At the beginning of each experiment, the BPR was first set to the desired pressure and the temperature controller at the right temperature. The glass vessel was filled with ultrapure water (Elga Purelab Ultra, Veolia WS, Ede, The Netherlands) and sparged with nitrogen until oxygen was below 20 ppb O_2, after which the organic contaminant/chemical of interest was added. Then, carbohydrazide was dosed at 0.1 ppm to scavenge any remaining oxygen, and also ammonia was dosed at 0.5 ppm to protect the setup from corrosion due to acid conditions. Ammonia was not added during the study of formic and acetic acid thermal decomposition, to ensure that the thermal stability of the organic acid species and not that of the ammonium salt was investigated. After dosing, the solution was again briefly sparged with nitrogen. During the remainder of the experiment, the solution was kept under a nitrogen blanket, to prevent oxygen intrusion. When temperature was stable, the experiment was started and a 4 mL sample was taken at the desired contact time. This was repeated for all the conditions and solutions listed in Table 6.1 and all experiments were executed in duplicate.

These conditions were chosen to replicate the conditions in intermediate (6.0 MPa) and high (13.5 MPa) pressure boiler systems with high superheater temperatures (510 °C). Low pressure boiler conditions were applied to MEKO, because it is often applied in low pressure systems. A lower superheater temperature was applied to formic and acetic acid to get a better idea at which temperature they start degrading. In addition to the conditions mentioned in Table 6.1, acetic acid was also exposed to 500, 530 and 560 °C at 9.5, 13.5 and 17.5 MPa in order to quantify its high thermal stability. The model applied to results of acetic acid decomposition is the same as in Section 3.2.

6.2.2 Analyses

Analysis of organic acid anions was performed using a Metrohm (Schiedam, The Netherlands) 881 ion chromatography system. A Metrohm A Supp 16 4.0/250 anion column was operated at 67 °C with eluent containing 7.5 mM Na_2CO_3 + 0.75 mM NaOH in ultrapure water. The suppressor was regenerated with 50 mM H_2SO_4 and the limit of detection was 1 ppb. TOC was measured as Non-Purgable Organic Carbon (NPOC) on a Shimadzu ('s-Hertogenbosch, the Netherlands) TOC-V analyzer with high sensitivity catalyst. The online measurements for O_2 and pH were done with WTW (Weilheim, Germany) probes and multi-meter.

Table 6.1: Feed solutions for experiments with their corresponding concentration. Listed temperature/pressure combinations and retention times have been applied to all contaminants, except those printed in italic

Solution	**C (ppm)**	$T - P$	t
MEG	10 (as TOC)	**In water**	
PEG	10 (as TOC)	*210 °C – 2.0 MPa*[a]	60 – 300 s
Gasoil	10 (as TOC)	275 °C – 6.0 MPa	300 – 600 s
Naphtha	10 (as TOC)	335 °C – 13.5 MPa	600 – 1200 s
Slurry oil	10 (as TOC)		
Hydro wax	10 (as TOC)	**In steam**	
MEKO	10	*400 °C – 13.5MPa*[b]	5 – 10 s
Formic acid	10	510 °C – 13.5 MPa	10 – 20 s
Acetic acid	10		20 – 40 s

[a] 210 °C and 2.0 MPa has only been applied to MEKO

[b] 400 °C and 13.5 MPa has only been applied to formate and acetate

6.2.3 Preparation of solutions

MEKO, formic and acetic acid are measured on a ppm/ppb basis in industry. Therefore, these were dosed directly into the glass dosing bottle at 10 ppm. The other contaminants are measured as TOC in a practical situation. Therefore 10 ppm TOC solutions were created for each contaminant. For MEG and PEG the TOC content of a 100 ppm sample was determined. NPOC content was 23.5 and 55.0 ppm for MEG and PEG respectively. This information was used to create a 10 ppm solution. Gasoil, naphtha, slurry oil and hydro wax were supplied by Shell. These hydrocarbons do not dissolve well and only come in contact with hot steam and condensate. Therefore 100 mL of each was dosed into a 2000 mL borosilicate glass bottle, heated to 95 °C and stirred for 24 hours. The resulting NPOC concentrations for gasoil, naphtha, slurry oil and hydro wax were 44.4, 21.2, 2.5 and 8.56 ppm respectively. These results were used to create 10 ppm TOC solutions. For slurry oil and hydro wax the dosed amount of hydrocarbon had to be increased in order to create a solution of 10 ppm TOC.

6.3 Results & Discussion

6.3.1 (Hydro)thermolysis of contaminants

The results of the (hydro)thermolysis of MEG, PEG, gasoil, naphtha, slurry oil and hydro wax are shown in Table 6.2. The first run was a blank run with demineralized water only. Ultrapure water is easily contaminated by TOC from the laboratory atmosphere or from plastic parts (i.e. the pump membrane) and even a 100 ppb increase in TOC content can lead to organic acid anion formation at boiler or superheater conditions as was shown in Chapter 2. The results for the blank run are at the

top of the table and show what levels of organic acid anions can be considered background concentrations. The error on organic acid anion concentrations between the duplicate runs was up to 50% for the blank, another indication that these concentrations are a consequence of contamination. A few samples showed traces of glycolate (1-3 ppb), but there was no consistency in those results.

When thermally degraded, gasoil, naphtha and hydro wax produced only slightly more organic acid anions than the blank. In some cases the measured acetate and formate concentrations after degradation were even lower than those for the blank run. Where slightly higher values are found, these could be attributed to more TOC contamination from the laboratory environment. Errors for these results varied greatly and could be as high as 75%, which points even more towards (varying) TOC contamination. The water dissolvable fractions of gasoil, naphtha and hydro wax are therefore unlikely sources of acetate and formate in a petrochemical steam-water cycle.

The thermal degradation of slurry oil produced organic acid anion concentrations that were an order of magnitude higher than the blank. Therefore, it was the only hydrocarbon fraction coming in contact with process steam or condensate, of which the water dissolvable fraction might be suspect of contaminating the steam-water cycle. As with previous TOC degradation studies, there was more formate measured after lower temperature degradation and more acetate at the higher temperatures. Retention times had little effect on concentrations, except for acetate at 510 °C, where tripling the retention time led to a 54% increase in acetate. Traces of glycolate were detected at 335 °C (up to 21 ppb). Results for slurry oil (hydro)thermolysis were reproducible, with the exception of acetate production at 275 °C for 364 seconds, for which the error was 25%.

Organic acid anion measurements after MEG (hydro)thermolysis showed a similar trend as for slurry oil. Acetate concentrations increased and those of formate decreased with temperature. Formate concentrations were higher at high pressure superheater than high pressure boiler conditions though. With 1,670 ppb acetate at 510 °C, PEG produced by far the most organic acid anions on a ppm basis. The results for the thermal degradation of PEG could only be interpreted for superheater conditions. At boiler conditions PEG produced such a larger amount of different anionic species, that the chromatogram (normally a set of peaks) showed a big hump of anions. Even after dilution this could not be turned into a set of peaks. It can be concluded that a PEG contamination would lead to the largest increase in anions in the cycle. MEG and PEG results were all well reproducible, with the biggest error being a single 15% and most around 1-10%. Other organic and inorganic by-products will most definitely have formed, but since they were not anionic species, these were not considered important enough to be measured in this study. It is likely though, that smaller organic and inorganic species play an important role in the occurrence of organic acid anions. This is explained in more detail in Section 6.3.3.

MEG or PEG are both cooling water additives that would find their way into a steam-water cycle through a condenser leak, so condenser leaks are a likely factor in TOC (organic acid anion) contamination. Alternatively they could also enter the condensate system in case of

Table 6.2: Concentrations of organic acid anions (in ppb) after the (hydro)thermolysis of organic contaminants at boiler and superheater conditions for several retention times

	T	275 °C			335 °C			510 °C		
	P	6.0 MPa			13.5 MPa			13.5 MPa		
	t	121 s	364 s	911 s	101 s	303 s	760 s	7 s	13 s	23 s
Blank	Acetate	1	3	2	2	5	7	9	9	18
	Formate	6	10	20	4	5	6	2	0	2
MEG	Acetate	81	81	76	72	65	72	127	162	196
	Formate	127	135	148	29	12	11	53	40	16
PEG	Acetate	N/A	N/A	N/A	N/A	N/A	N/A	725	1144	1670
	Formate	N/A	N/A	N/A	N/A	N/A	N/A	70	180	28
Gasoil	Acetate	0	4	6	1	1	5	34	32	34
	Formate	17	18	30	12	13	18	0	0	0
Naphtha	Acetate	6	11	15	4	3	5	8	17	14
	Formate	23	25	32	8	8	8	12	10	9
Slurry oil	Acetate	182	200	207	175	189	172	245	343	378
	Formate	396	406	413	112	95	102	32	46	46
Hydro Wax	Acetate	19	28	38	14	24	26	24	23	27
	Formate	26	26	27	8	14	14	5	5	6

contaminated return condensate at a PEG/MEG production facility. Insufficient treatment of return condensate that has been in contact with slurry oil is another probable cause.

6.3.2 (Hydro)thermolysis of MEKO

The results of the (hydro)thermolysis of MEKO have been summarized in Table 6.3. Although MEKO is dosed into steam-water cycles to protect the system from corrosion, it produces more anions when thermally degraded than any of the previously discussed hydrocarbons (with the exception of PEG). Acetate is not formed from MEKO until superheater conditions are reached, while some formate was present in collected samples at both low and higher temperatures. Almost no glycolate was found, but the propionate concentrations reached 349 ppb at high temperatures. Unlike previously discussed hydrocarbons, the thermal degradation of MEKO produced less anionic by-products at longer superheat retention times. Errors went down as organic acid concentrations increased.

The biggest difference from other hydrocarbons is that MEKO produced inorganic anion species, namely nitrate and nitrite. This is a consequence of the ketoxime group in MEKO's molecular structure. The highest measured nitrate concentration was only 113 ($\pm$ 40) ppb, while for nitrite that was 1,716 ($\pm$ 83 ppb), meaning that 33.5% of nitrogen from the MEKO was found as inorganic anionic decomposition products (see bottom row of Table 6.3). Nitrite concentrations even went up to 3.94 ppm when pushing retention times at 335 °C to over 1500 seconds. This means that in the most extreme case 75% of nitrogen in the MEKO had been converted to nitrite. Another 4% was present as nitrate. Whether nitrate was actually a decomposition product, or was formed as the sample was taken (and therefore exposed to oxygen) is hard to say.

No published research is available on nitrite and high temperature corrosion of metals, but nitrite acts as an oxidant in anoxic water and nitrous acid is a weak acid with a pK_a of 3.3. By comparison, the pK_a of acetic acid is only 4.76. Dosing 10 ppm of an oxygen scavenger is very excessive (a typical dosage is in the ppb range), so the concentrations in Table 6.3 will not be found in an actual steam-water cycle. Guidelines for anion concentrations are strict though, so it will not take much MEKO to cause a chemical upset. On the other hand, in an online publication, a supplier of MEKO presented data which indicated that MEKO inhibits corrosion when dosed at low ppb levels by enabling the formation of an iron oxide layer more resistant to FAC than magnetite DeWitt & Rondum (2000). A complicating factor is that oxidation (instead of hydrothermolysis) of MEKO could lead to less harmful breakdown products. If that is the case, only overdosing would be an issue. Where steam quality regulations are strict, MEKO might not be the ideal oxygen scavenger.

6.3.3 (Hydro)thermolysis of acids)

The thermal stability of acetic and formic acid has also been tested, the results of which are shown in Table 6.4. All errors for formic and acetic acid (hydro)thermolysis were below 3%, making the dataset reproducible. Acetic

Table 6.3: Concentrations of anions (in ppb) after the (hydro)thermolysis of MEKO at boiler and superheater conditions for several retention times

T	210 °C			275 °C			335 °C			510 °C		
P	2.0 MPa			6.0 MPa			13.5 MPa			13.5 MPa		
t	138 s	415 s	1038 s	121 s	362 s	910 s	101 s	303 s	760 s	7 s	13 s	23 s
Acetate	0	2	5	2	7	12	19	10	39	608	440	254
Formate	53	74	75	26	19	14	18	7	6	38	54	38
Propionate	0	0	0	8	15	19	15	14	10	349	194	60
Glycolate	0	0	0	0	0	0	11	6	7	0	0	0
Nitrate	0	0	0	0	0	0	110	113	78	43	35	26
Nitrite	125	220	251	791	923	835	1241	1167	1716	635	416	239
% N of Total	2.4%	4.2%	4.7%	15.0%	17.5%	15.8%	25.0%	23.6%	33.5%	12.6%	8.4%	4.9%

acid did not start degrading notably until the highest tested temperature was reached. Formic acid started degrading at 275 °C and was almost completely thermolyzed within 10 seconds at 400 °C superheat. This supports findings of Maiella & Brill (1998), which in Chapter 2 were attributed to a lack of sparging. In fact, the thermal degradation kinetics they match the findings of the results presented in this chapter.

Acetic acid thermal stability was thus indeed found to be much higher than that of formate, which explains why it is the dominant organic acid anion at higher temperatures. What cannot be explained from this dataset is why there is any formate present in steam-water cycles with superheaters. Even at 530 °C superheat (at 9.5 17.5 MPa), formic acid can still be found in laboratory (Chapters 2, 3, 4 and 5 of this thesis) and case studies Mathews et al. (2010). An explanation could be that formic acid is synthesized from other degradation products as temperature decreases. This could, for instance, happen in the condensing stages. The degradation of formic acid was found to be reversible at conditions found in steam-water cycles by Yasaka et al. (2008):

$$HCOOH \leftrightarrow CO_2 + H_2 \tag{6.1}$$

$$HCOOH \leftrightarrow CO + H_2O \tag{6.2}$$

The presence of a base stabilizes the formate by neutralizing it. This could explain why formate was allowed to degrade completely in the case of formic acid and still be formed when TOC or an organic treatment chemical is degraded in the presence of ammonia. Both in a case study and laboratory studies described in this thesis, measured formate concentrations after (hydro)thermolysis of organic material were unpredictable. This can also be a consequence of formate only being present under the right conditions and dependent on concentrations of gases and bases. Acetate is much more

Table 6.4: The remaining percentage of 10 ppm acetic and formic acid after exposure to the listed temperatures, pressures and retention times

T	275 °C			335 °C			400 °C			510 °C		
P	6.0 MPa			13.5 MPa			13.5 MPa			13.5 MPa		
t	121 s	362 s	729 s	101 s	304 s	608 s	9 s	18 s	44 s	7 s	13 s	33 s
Acetic acid	100%	99%	97%	95%	100%	99%	98%	97%	97%	93%	90%	86%
Formic acid	101%	98%	93%	33%	25%	21%	2%	0%	0%	0%	0%	0%

predictable and being the dominant organic acid anion its thermal stability needs to be better understood.

6.3.4 Thermolysis model for acetic acid

First order degradation plots have been made for acetic acid for 500, 530 and 560 °C to investigate the thermal stability more closely. Figure 6.1 shows this plot for 560 °C for 9.5, 13.5 and 17.5 MPa, with the first order relationships.

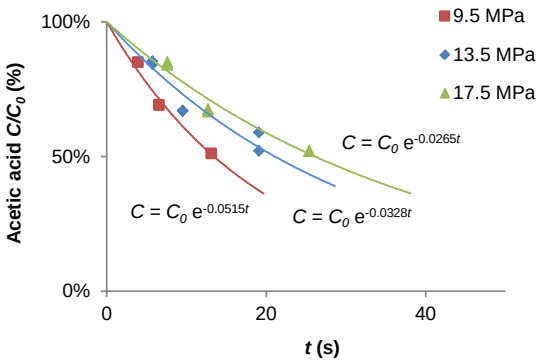

Figure 6.1: Degradation plot of acetic acid at 560 °C for 9.5, 13.5 and 17.5 MPa with first order relationships

The reaction rate constant k was derived from these plots for each combination of temperature and pressure. As was discussed in Section 2.5, plotting $\ln(k)$ against pressure (in MPa) and the reciprocal of temperature (in K^{-1}) results in the Arrhenius plots necessary to determine the Arrhenius constants. Based on the results shown in Figure 6.2, the activation energy E_a = 162.7 (±4.4) $kJmol^{-1}$, the natural logarithm of the prefactor $\ln(A)$ = 20.1 (± 0.9) s^{-1} and the activation volume V_a = 617.5 (± 27.1) cm^3mol^{-1} could be determined.

The results of this acetic acid thermolysis study indicate that acetic acid will decompose at superheater conditions, although not very fast. In most cases, its formation from TOC breakdown will thus overwhelm its decomposition rate. The calculated Arrhenius constants can be used to determine whether acetic acid will persist in a steam-water cycle, or degrade to some degree.

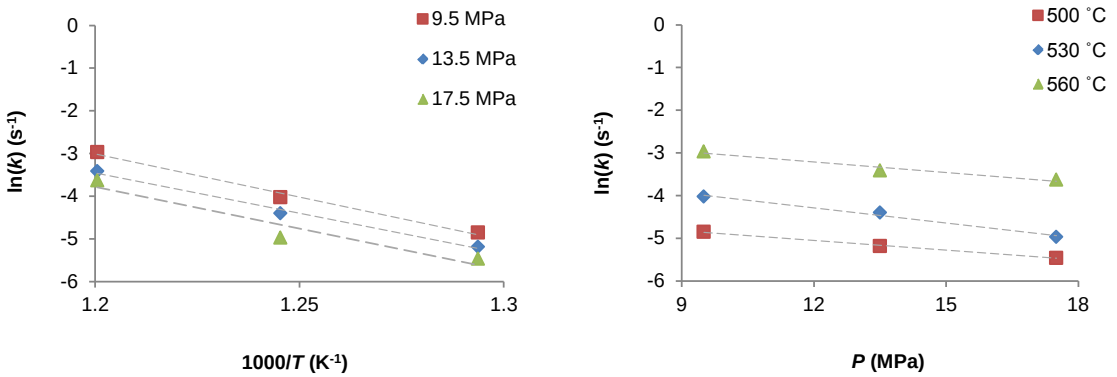

Figure 6.2: Plots of ln(k) vs. temperature and pressure for the thermolysis of acetic acid

6.4 Conclusions

This study has led to the following conclusions:

- The (hydro)thermolysis of 10 ppm TOC as MEG and slurry oil produced up to a few hundred ppb acetate and formate.
- The (hydro)thermolysis of 10 ppm TOC as PEG produced a high variety and quantity of organic acid anions, that could only partially be determined to be in the lower ppm range.
- The (hydro)thermolysis of 10 ppm TOC as the water dissolvable fraction of gasoil, naphtha and hydro wax led to organic acid anion concentrations that only slightly exceeded the blank results.
- Condenser leaks and insufficiently treated return condensate (from slurry oil) are both a likely source for TOC and organic acid anion contamination.
- 10 ppm MEKO thermally degraded into several organic acid anions and nitrite in the higher ppb or lower ppm range. MEKO overdosing has to be prevented at all times.
- The species and quantity of anionic degradation products was strongly dependent on temperature and retention time for all tested compounds. Formate was dominant at the lowest temperatures, whereas acetate (and for MEKO propionate) was highest in quantity at the highest tested temperatures.
- Formic acid is very unstable under steam water cycle conditions. It is still found in high temperature and pressure steam-water cycles though and therefore could be synthesized in the condensing stages at the right conditions.
- Acetic acid has high thermal stability and is therefore the dominant organic acid anion at high temperatures. The Arrhenius constants for acetic acid thermolysis in a superheater are E_a = 162.7 (±4.4) kJmol^{-1}, ln(A) = 20.1 (±0.9) s^{-1} and V_a = 617.5 (±27.1) cm^{3}mol^{-1}.

References

DeWitt, D., & Rondum, K. D. (2000). The impact of methyl ethyl ketoxime. *Chemical Online*, http://www.chemicalonline.com/doc/the-impact-of-methyl-ethyl-ketoxime-0001.

Maiella, P. G., & Brill, T. B. (1998). Evidence of wall effects in decarboxylation kinetics of 1.00 m HCO_2X (X = H, Na) at 280-330 °C and 275 bar. *Journal of Physical Chemistry A*, *102*(29), 5886-5891.

Mathews, J., Ball, M., Bursik, A., Cutler, F., Sadler, M., & Foutch, G. (2010). Assessment of amines for fossil plant applications. *EPRI Report*, *1017475*, Palo Alto, CA.

Yasaka, Y., Yoshida, K., Wakai, C., Matubayasi, N., & Nakahara, M. (2008). Kinetics and equilibrium of the reversible formic acid decomposition in hot water. *15th International Conference on the Properties of Water and Steam*, Berlin, Germany.

7

Ethanolamine and Two-Phase Flow Accelerated Corrosion

This chapter is based on:

Moed, D.H., Weerakul, S., Lister, D.H., Leaukosol, N., Rietveld L.C. and Verliefde, A.R.D. **(2015)** Effect of Ethanolamine, Ammonia, Acetic Acid and Formic Acid on Two-Phase Flow Accelerated Corrosion in Steam-Water Cycles. *Industrial & Engineering Chemistry Research*, 54 (36), 8963-8970

Abstract

Effects of ethanolamine, ammonia, acetic and formic acid on two-phase flow-accelerated corrosion were investigated in an experimental loop simulating the conditions found in a water-steam cycle. Results indicate that the effects of acetic acid and ethanolamine on the corrosion rate neutralize each other. The effect of acetic acid on the corrosion rate was most pronounced at the highest tested steam quality. A model simulation for liquid film pH at 90% steam quality suggests that at very high steam qualities the protection ethanolamine provides increases, while the protection provided by ammonia goes down. A linear relation between calculated liquid film pH and the measured corrosion rate was found for 24% steam quality within a pH range from 5.6 to 6.3. Formic acid was thermally unstable at the tested temperatures and had no effect on the corrosion rate.

7.1 Introduction

The knowledge obtained on amine thermolysis and organic acid anion formation from the previous chapters is used to design flow-accelerated corrosion (FAC) experiments. Lertsurasakda et al. (2013) used a small scale steam-water cycle and found that the corrosion rate was flow velocity dependent, thereby verifying that the investigated corrosion phenomenon was FAC. They also showed that ethanolamine (ETA) does indeed offer much better protection against two-phase FAC than NH_3 at the same flow velocity. ETA has limited thermal stability and the main decomposition products of ETA are NH_3, acetic acid (AA) and formic acid (FA) as was shown in Chapters 4 and 5 of this thesis and by Layton & Daniels (2010). The two-phase FAC rate in a high temperature system applying ETA will therefore be influenced by the volatility, concentration and basicity/acidity of these compounds. Other important factors influencing FAC are the steam quality (the relative mass fraction of water in the vapor phase), pipe geometry and flow rate, because these parameters together dictate the flow velocity through a pipe.

As the ETA concentration in the cycle decreases due to thermal degradation, and acidic by-products concentration increases, the protection against two-phase FAC that ETA normally provides will thus decrease. In early condensation or very high evaporation where a majority of the water is in the steam phase, pH depressions have been noted from acetate and formate in the presence of NH_3 (EPRI, 1999). In addition, recent corrosion work in the phase transition zone (EPRI, 2014) has validated these earlier findings of a pH reduction associated with acetate and formate in the early condensate. Studies of corrosion product transport from condensate samples (EPRI, 2014) have also supported those findings. In these cases, increases in pitting and/or corrosion product transport showed correlations with early condensate pH calculations based on the composition of the steam and/or condensate samples.

This chapter aims to validate how the FAC rate is affected by the decomposition of ETA and the increase of the concentration of NH_3, AA and FA. The two-phase FAC rate in ETA containing systems is therefore investigated using a carbon steel probe at 200 °C and a flow rate of 0.56 L/min, for varying chemical compositions

and steam qualities. Because of the maximum temperature the feedwater heater could reach, the highest applied steam quality is 24%.

The objectives of this chapter are twofold:

- To investigate the effect of AA on two-phase FAC, in the presence of NH_3 and ETA, at steam qualities of 3.6% and 24%.
- To study the difference between two-phase FAC rates of a mixture of AA and FA and NH_3, with and without ETA at 24% steam quality.

7.2 Methods & Materials

7.2.1 FAC loop

The loop and probe that have been used in this study, have been thoroughly described before by Lertsurasakda et al. (2013) and Lister et al. (2013). Therefore, only the essentials will be explained here. A schematic diagram of the loop is shown in Figure 7.1.

The feedwater in the reservoir was ultrapure water that was conditioned to the desired chemistry after purging with argon to remove oxygen and CO_2. From there, the feed water is pumped through electrical heaters (preheater, main heater) to raise the temperature to the desired level. The heated feed is then flashed to a two-phase mixture by a pneumatic valve where an isenthalpic throttling process occurs (throttle valve). By controlling pressure and temperature upstream of the throttle valve and pressure downstream, a wide range of steam qualities can be applied. The two-phase mixture goes through the corrosion test section, where the corrosion rate is measured using a carbon-steel probe, before exiting the high-pressure section of the loop via a full-flow condenser, and a pneumatic back-pressure regulator that maintains the downstream pressure. In the low-pressure return line to the reservoir, the flow passes through 0.2 μm filters and a flow meter before being returned to the reservoir. Oxygen is measured using an Orbisphere oxygen analyzer in a separate loop to avoid interference from bubbles of gas that fail to re-dissolve in the final condenser. To facilitate overall fluid movement, the two-phase stream between the throttle valve and the main condenser outlet flows downwards.

Anionic and cationic impurities that might still be in the loop from previous experiments were removed by strong-acid/strong-base ion-exchange resins before starting a corrosion experiment, by running the system with deionized water only. Chemistry in the loop is then altered by chemicals injected through a septum (in the Orbisphere by-pass in Figure 7.1) located on the return line just before the entry point of feed water to the reservoir. Before dosing chemicals, the ion exchange columns are by-passed, to prevent them from removing the injected compounds.

7.2.2 Probe for resistance measurements

The test section contains an electrical resistance probe for on-line resistance measurements, from which corrosion rates can be determined. The probes are made of Type A-106 Grade B carbon steel. They are 85 mm long with a bore of 1.6 mm. A schematic diagram of the probe is shown in Figure 7.2. The steel composition is presented

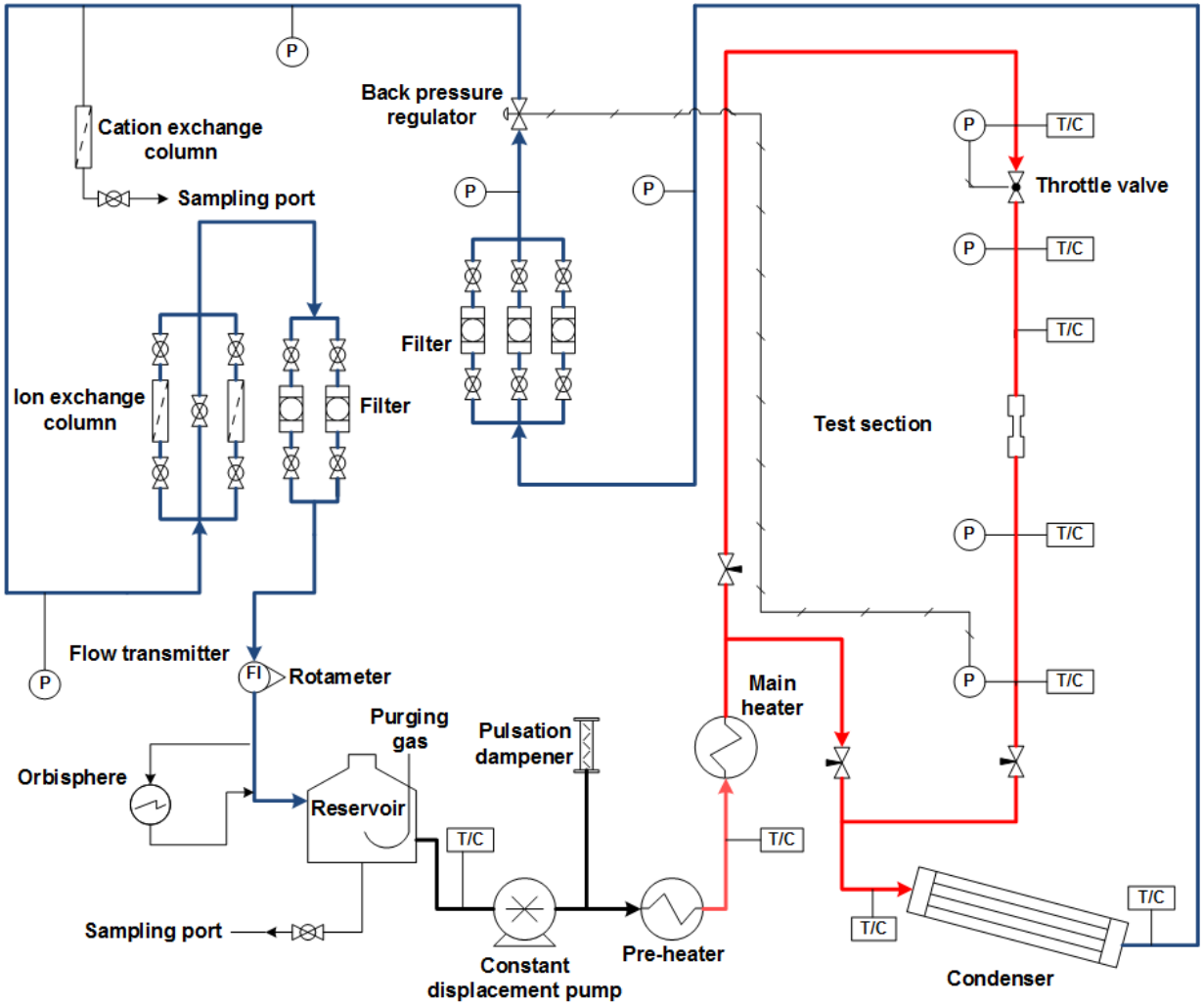

Figure 7.1: Schematic diagram of the two-phase FAC experimental loop

in Table 7.1. The steel composition is presented in Table 7.4 in Appendix Section 7.5.

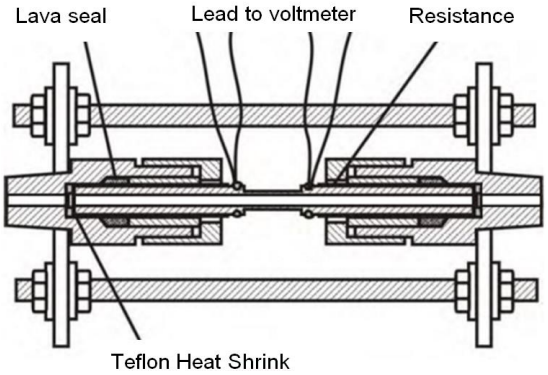

Figure 7.2: Schematic diagram of the corrosion probe

The temperature-compensating resistance correlation for a probe was determined in the test loop before the start of an experiment. The relation between measured resistance and the probe wall thickness was originally derived from:

$$R = \frac{\rho L}{A} \tag{7.1}$$

where:

R	=	electrical resistance (Ω)
ρ	=	resistivity of carbon steel (Ω)
L	=	length of the probe (m)
A	=	cross-sectional area (m^2)

The probes are not completely homogeneous though. There is a silver solder shoulder where the probe is connected to the voltameter, which is corrected for by introducing the initial end-effect (E^0). The initial-end effect is temperature dependent. Since the probes are hand-made, there are some inconsistencies in fabrication (i.e. human cause or accuracy of machinery), which is corrected for by introducing the geometry correction factors (α and β). The correlation of measured resistance and the wall thickness has therefore been determined to be (Lister et al., 2013):

$$R(T) = \rho\left(\frac{L}{A} + E^0(T) + \alpha T + \beta\right) \tag{7.2}$$

where:

E^0	=	initial end-effect (m^{-1})
α	=	geometrical temperature coef. (m^{-1} °C^{-1})
β	=	geometrical correction term (m^{-1})
T	=	temperature (°C)

The initial end-effects (E^0) at various temperatures were obtained at the beginning of each experiment, then the E^0 as a function of temperature was inserted into Equation 7.2. The resulting equation therefore improves accuracy of the FAC measurement. The probe wall thickness was calculated using the following equation:

$$w = \frac{D}{2} - \sqrt{\frac{D^2}{4} - \frac{A}{\pi}} \tag{7.3}$$

where:

w	=	probe wall thickness (m)
D	=	probe diameter (m)

Combining Equations 7.2 and 7.3, the probe wall thickness as a function of resistance and temperature could be calculated with:

$$w = \frac{D}{2} - \sqrt{\frac{D^2}{4} - \frac{L}{\pi\left(\frac{R}{\rho} - E^0 - \alpha T - \beta\right)}} \tag{7.4}$$

7.2.3 Conditions and concentrations

If ETA were to decompose (i.e. in the superheater) this would form NH_3, AA and FA, the concentrations of which depend on various parameters. For the sake of comparison, ammonia was always kept at around 500 ppb, because this solution has a pH of 9.2 at 25 °C, which is a common pH value for power plants to maintain. The applied concentrations for AA were 50 and 100 ppb. FA occurs at lower concentrations in steam-water cycles (as was found in Chapter 2 and 5) and was dosed at 50 ppb only. These organic acid concentrations are slightly exaggerated compared to what can be expected in steam-water cycles, but for the purpose of this study. The ETA concentration was varied (as it varies in power plants, based on the degree of decomposition).

Run 1 investigated the effects of changes in AA concentration and steam quality, in the presence of NH_3 and ETA. After determining a baseline corrosion rate at neutral conditions (deionized water, no chemical conditioning), the experimental run was started with 500 ppb NH_3 and 100 ppb ETA at 24% steam quality. After a stable corrosion rate was determined, the AA concentration was increased two times with 50 ppb and the change in corrosion rate was investigated for both 3.6% and 24% steam quality. The last part of the run took place under single phase conditions (0% steam quality, or liquid water), without changing water chemistry.

The entire second run was performed at 24% steam quality. After establishing a constant corrosion rate under neutral conditions, 500 ppb NH_3 was dosed. When a stable corrosion rate was determined 100 ppb of AA and after that 50 ppb of FA were added, to study how much protection NH_3 can offer in a steam-water cycle containing organic acids without ETA. Then, ETA was added in two consecutive steps of 100 ppb each, and then a final addition of 200 ppb, increasing the ETA concentration to 400 ppb.

After every change in chemistry or operational condition, the system was run until a stable corrosion rate was obtained before changing another parameter. The conditions and chemistries used throughout the experiments can also be found in Table 7.1 and 7.2, where the results are presented. In this study, an automated needle valve was utilized as a throttling device (see Lister et al. (2013) for details). The input to the valve was under-saturated, high temperature water from the heater, and the downstream pressure was set low enough for free expansion to occur. With the assumption of an ideal isenthalpic process, steam quality could be determined from the upstream enthalpy and downstream temperature at the test section as follows:

$$\chi = \frac{H_{TS} - H_L}{H_G - H_L} \tag{7.5}$$

where:

χ	=	steam quality (-)
H_{TS}	=	enthalpy at test section (J)
H_L	=	enthalpy of liquid water (J)
H_G	=	enthalpy of steam (J)

The use of different steam qualities causes velocities through the probe to change. At 0.56 L/min and 200 °C, the average velocity through the probe is 5.3, 35 and 20101 m/s, for 0%, 3.6% and 24% steam quality respectively.

7.2.4 Analytical measurements

The parameters that were continuously measured were probe resistance, temperature (at several points, indicated by T/C in Figure 7.1), pressure (at several points, indicated by P in Figure 7.1) and oxygen. Ionic content was measured by a Dionex Ion chromatograph, with a CS 17 cation column and an AS 18 anion column. Detection after the columns was done by conductivity measurement, of which the signal was suppressed, for both anions and cations, by stripping the counter-ions from the eluent before detection.

7.2.5 Liquid film pH model

In order to calculate the liquid film pH at the corresponding temperature, chemical compound concentrations and steam quality values, a model was made. The model assumes that the temperature in the liquid film is the same as the average temperature across the probe. Dissolved compounds are divided between the vapor phase and the liquid phase according to their relative volatility. The concentration in the liquid includes the ionized species.

$$RV = \frac{[C]_G}{[C]_L} \tag{7.6}$$

where:

RV	=	relative volatility
$[C]_G$	=	concentration of the compound in the vapour
$[C]_L$	=	concentration of the compound in the liquid (ionic and nonionic)

When considering steam quality, the total concentration of a compound in the liquid and gas phase can be expressed as:

$$[C] = (1 - \chi)[C]_L + \chi[C]_G \tag{7.7}$$

Combing Equations 7.6 and 7.7, the concentration in the liquid phase as a function of total concentration, relative volatility and steam quality can be calculated. The model assumes that only the undissociated compounds are distributed between vapor and liquid, while ions stay in the liquid. Therefore, the relative volatility of compounds is influenced by the dissociation degree of the compounds, i.e. the acid/base strength. The dissociation degree can be determined from the base dissociation constant and the pH. This means that the relative volatility of a compound is a function of its volatility, dissociation and concentration. Therefore, the relative volatility is not constant, but the ratio between the relative volatility and the degree of dissociation is constant. This complies with Nernst's distribution law:

$$K_D = \frac{RV}{1 - d} = \frac{[C]_G}{C_{L;u}} \tag{7.8}$$

where:

K_D	=	distribution coefficient
d	=	degree of dissociation
$[C]_{L;u}$	=	concentration of the undissociated compound in the liquid

Both K and K_D are temperature dependent. In Table 7.4 (in the Appendix), the values of the dissociation constants and distribution coefficient of the four compounds of interest and water have been listed for 200 °C and 1.1 MPa, with their respective sources.

The model starts by assuming that the relative volatility is equal to K_D for each compound and then calculates the concentration of the compounds in the liquid. With these concentrations in the liquid, the charge balance is solved for H^+. From the H^+ concentration, the ionization of each compound and the corresponding new relative volatilities are calculated, which are put back into the model. This is iterated to converge to the correct liquid film pH. The models code (made in Matlab) can be found in the Appendix Section 7.5.3.

7.3 Results & Discussion

7.3.1 FAC rates

During run 1, the loop was stable and there were no upsets in temperature and pressure. Oxygen went up to 40 ppb for about an hour, because of a defect in the argon sparging. The NH_3 concentration decreased by 8% over the course of three weeks, from 500 to 460 ppb, due to the sparging with argon causing volatilization in the feed vessel. Temperature, pressure and concentration profiles during the first run can be found in the Appendix section 7.5.2. The calculated wall thickness from measured electrical resistance as a function of time can found in Figure 7.3. The corrosion rates were calculated from the slope of each set of conditions, obtained by linear regression. After each injection of a compound, the data of the first five hours after injection were not taken into consideration to let the water chemistry stabilize. After a steam quality change, the slope determination was started after a day or more, to allow for temperature and pressure to stabilize. A slight influence of fluctuating room temperature can be seen in the wall thickness plot. Especially at single-phase flow at the end of the run, the fluctuation in wall thickness seems to be a consequence of the fluctuation in room temperature.

The corrosion rate at neutral chemistry determined from the slopes at 24% steam quality during run 1 was 2.0 mm/y. Adding 500 ppb NH_3 and 100 ppb ETA caused the rate to drop to 0.57 mm/y. The first 50 ppb AA addition that followed caused the rate to increase again to 0.69 mm/y, a 21% relative increase that showed an effect of AA on two-phase FAC. After the runs at 24%, the steam quality was changed to 3.6%. This caused the measured FAC rate to drop to 0.33 mm/y. The lower FAC at lower steam quality does not necessarily relate to changes in distribution between the liquid film and steam, since steam quality also affects fluid velocity through the probe. At 0.56 L/min and 200 °C, the average velocity through the probe is 5.3, 35 and $20 \cdot 10^1$ m/s, for 0%, 3.6% and 24% steam quality respectively. This does not represent the velocity of the liquid film, because the liquid layer moves slower than the saturated steam, especially at higher steam qualities and velocities

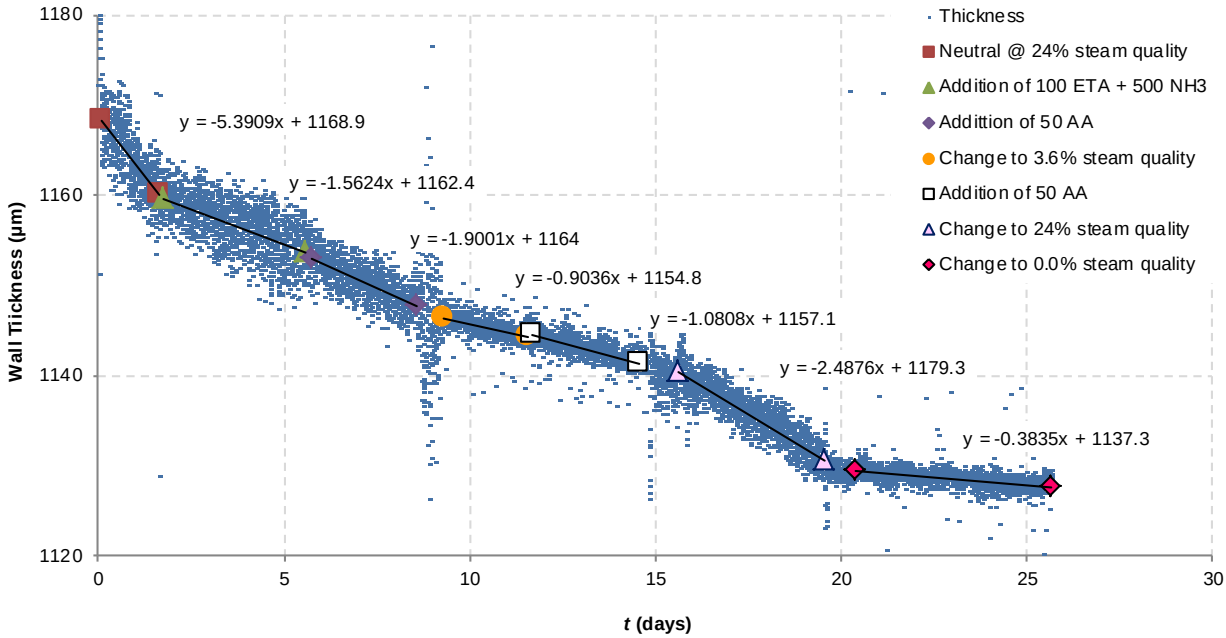

Figure 7.3: Wall thickness vs. time for run 1. Chemical additions are given in ppb.

Table 7.1: Summary of calculated FAC rates for run 1 with their statistical properties

T (°C)	NH_4 (ppb)	ETA (ppb)	AA (ppb)	SQ (%)	pH @ 25 °C -	r (mm/y)	R^2 (-)	SE (mm/y)	RSE (-)
200	0	0	0	24	7	1.96	0.28	0.12	6%
200	500	100	0	24	9.2	0.57	0.35	0.02	3%
200	500	100	50	24	9.19	0.69	0.49	0.02	3%
200	500	100	50	3.6	9.19	0.33	0.27	0.02	5%
200	500	100	100	3.6	9.17	0.39	0.4	0.01	3%
200	500	100	100	24	9.17	0.91	0.8	0.01	1%
200	500	100	100	0	9.17	0.14	0.1	0.01	6%

(Fujie, 1963). This is also a reason why the velocity is 6 times higher at 24% than at 3.6%, while the two-phase FAC rate only doubles.

Adding another 50 ppb AA at this steam quality, again had an effect on the FAC rate, which increased to 0.39 mm/y, an 18% increase. After changing the steam quality back to 24%, the corrosion rate increased to 0.91 mm/y after the second AA injection. This shows that acetic acid does indeed have an effect on two-phase FAC. The influence of AA on the FAC rate at 3.6% steam quality was lower than at the higher steam quality. When the steam quality was reduced to 0% at the end of the run, the average flow velocity dropped from 35 to 5.3 m/s, which was the most prominent cause for the corrosion rate to drop from 0.39 to 0.14 mm/y. The influence of a change in flow velocity on the corrosion rate was higher than for the previous change in steam quality.

The calculated rates for each change in chemistry and conditions have been summarized in Table 7.1, with the coefficient of determination (R^2), standard error (SE) and relative standard error (RSE). Judging from the (relative) standard errors on the estimated slope, the measured changes in FAC rate are statistically relevant, in spite of a few low coefficients of determination.

The probe wall thickness gradually decreased from 1170 μm to 1126 μm, meaning the probe radius increased by 44 μm. This caused the average velocity through the probe to decrease by 10%. As previously shown, the velocity of the liquid film is lower than that of the saturated steam and the relation between flow velocity and the corrosion rate is not linear. It is therefore estimated that the gradual reduction in corrosion rate due to probe thinning over the course of the entire experiment at 24% steam quality is around 2 to 3%. At 0% steam quality this could be up to 5%.

During run 2 there was an upset of the loop, between day 12 and 15 of the run. For unknown reasons, the temperature across the probe started dropping a few degrees. In order to maintain 200 °C at the probe, the back pressure had to be increased. The temperature upset and the resulting change in back pressure can be found in the Appendix section 7.52. There were no upsets in oxygen concentration. NH_3 was added periodically to prevent the concentration from dropping as it did during run 1. FA concentrations decreased immediately after dosing, due to a lack of thermal stability of FA. This observed low thermal stability matches the findings presented in Chapter 6. The changes in chemistry throughout the run can be found in the Appendix Section 7.5.2. The calculated wall thickness of the probe, based on measured resistance as a function of time can been seen in Figure 7.4. From the slopes in this graph, the corrosion rates can be determined. During the upset, the corrosion rates were not calculated.

The initial neutral corrosion rate, measured for run 2, was 1.45 mm/y, 26% lower than the neutral rate of run 1. Whether this was caused by a difference in chromium content of the probe or a different probe diameter remains unclear. Upon adding 500 ppb NH_3 the corrosion rate decreased to 0.67 mm/y, and then increased again to 0.73 mm/y after adding 100 ppb AA.

After that there was the upset, causing the rate to drop. Unexpectedly, after the upset and the corresponding change in back pressure, the corrosion rates had changed

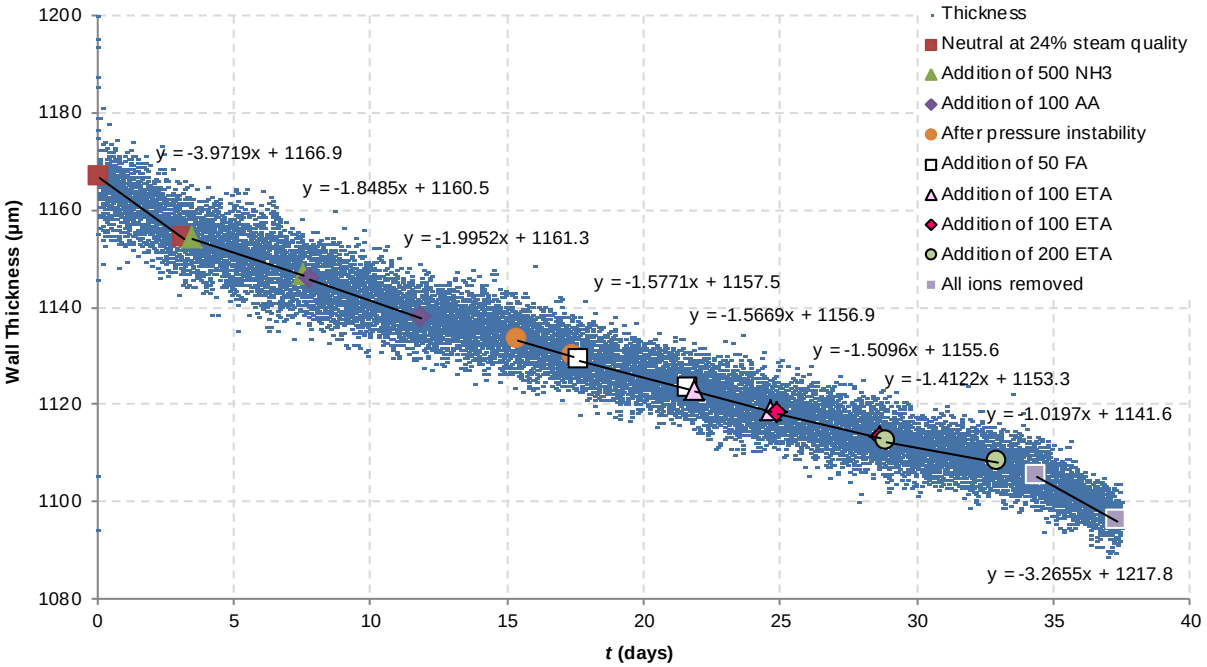

Figure 7.4: Wall thickness vs. time for run 2. Chemical additions are given in ppb.

Table 7.2: Summary of calculated FAC rates for run 2 with their statistical properties

T (°C)	NH_4 (ppb)	ETA (ppb)	AA (ppb)	FA (ppb)	SQ (%)	pH @ 25 °C -	r (mm/y)	R^2 (-)	SE (mm/y)	RSE (-)
200	0	0	0	0	24	7.00	1.40	0.17	0.08	6%
200	500	0	0	0	24	9.19	0.67	0.17	0.03	5%
200	500	0	100	0	24	9.15	0.73	0.24	0.03	4%
200	500	0	100	0	24	9.15	0.58	0.05	0.09	15%
200	500	0	100	50	24	9.13	0.57	0.20	0.03	5%
200	500	100	100	50	24	9.15	0.55	0.12	0.03	7%
200	500	200	100	50	24	9.17	0.51	0.15	0.02	6%
200	500	400	100	50	24	9.21	0.37	0.11	0.02	6%
200	0	0	0	0	24	7.00	1.10	0.32	0.05	4%

compared to the rates before the upset. The second rate measurement of AA + NH_3 was 0.58 mm/y, which is 21% less than what was measured a few days before under nominally the same conditions. The FA addition did not have much of an effect, which is probably caused by the fact that FA is not thermally stable under the applied conditions in the feedwater heater. The slight decrease of the corrosion rate is statistically not relevant. Later in the run, it seemed as if there was always an unpredictable trace amount of FA left (15 ± 5 ppb), but the effect on the FAC rate is probably not detectable within the experimental error.

The first addition of 100 ppb ETA did not have a pronounced effect on the measured FAC rate, which dropped only slightly to 0.55 mm/y, a 5% decrease. The dosed ETA will have neutralized the AA in the liquid film, leaving only NH_3 for protection. The second addition of 100 ppb ETA (total of 200 ppb) made the rate drop to 0.51 mm/y and the last 200 ppb ETA (total of 400 ppb) to 0.37 mm/y, which are both a consequence of the increase in liquid film pH. Finally, the ion exchange columns were valved back into the loop to remove all ions. As a result, the neutral rate after the upset could be determined, which was calculated at 1.19 mm/y. As previously observed, the FAC rate is lower after the upset than before. The calculated rates for each change in chemistry have been summarized in Table 7.2. Judging from the (relative) standard errors on the estimated slope, the measured changes in FAC rate are statistically relevant, except for the decrease in FAC rate after the addition of FA and the first 100 ppb ETA.

The probe wall thickness gradually decreased from 1170 μm to 1097 μm, meaning the probe radius increased by 73 μm. This caused the average velocity through the probe to decrease by 15%. As previously shown, the velocity of the liquid film is lower than that of the saturated steam and the relation between flow velocity and the corrosion rate is not linear. It is therefore estimated that the gradual reduction in corrosion rate due to probe thinning over the course of the entire run 2 is around 2 to 3%.

7.3.2 Adjusted FAC rates and liquid film pH

FAC rates obtained under the same conditions have proven to be different. Three times the neutral rate was calculated at 24% steam quality and all three times a different corrosion rate was found. Lertsurasakda et al. (2013) also used the same probes in the same setup and found a different neutral FAC rate at 24% steam quality as well. In an attempt to compare results, the rates were adjusted with the following correction factor:

$$f = \frac{r_{N;1}}{r_{N;x}} \tag{7.9}$$

Where $r_{N;1}$ is the neutral rate of the first run of this study and $r_{N;x}$ is the neutral rate of (part of) the run that the results are to be adjusted for. The chemical dosing in this study at 24% with the corresponding adjusted FAC rates are shown in Table 7.3. The adjusted rate for 550 ppb NH_3 and 1500 ppb ETA were taken from Lertsurasakda et al. (2013). The last columns show the calculated liquid film pH at 24% and 90% steam quality and 200 °C.

Figure 7.5 shows the calculated pH in the liquid phase versus the adjusted FAC rate from Table 7.3 for all 24% steam quality tests at 200 °C. There is a seemingly linear relationship between the FAC rate and the calculated

Table 7.3: Adjusted FAC rates at 24% steam quality (SQ) and 200 °C and calculated liquid film pH at 24 and 90% steam quality

NH_3	ETA	AA	FA	pH @ 25 °C	r_a	pH @ 24% SQ	pH @ 90% SQ
(ppb)				(-)	(mm/y)	(-)	(-)
0	0	0	0	7.00	1.97	5.64	5.64
550	0	0	0	9.20	0.80	6.12	5.90
0	1500	0	0	9.20	0.31	6.33	6.56
500	100	0	0	9.20	0.57	6.13	6.05
500	100	50	0	9.19	0.69	6.10	5.97
500	100	100	0	9.17	0.91	6.07	5.90
500	0	0	0	9.19	0.91	6.09	5.89
500	0	100	0	9.15	0.96	6.02	5.71
500	0	100	15±6	9.13	0.94	6.01	5.67
500	100	100	15±6	9.15	0.91	6.05	5.87
500	200	100	15±6	9.17	0.84	6.09	6.01
500	400	100	15±6	9.21	0.61	6.16	6.18

liquid film pH over the investigated liquid film pH range. It is unlikely that a linear relationship exists over an extended pH range, because it would lead to a negative corrosion rate at higher liquid film pH values. The errors for the calculated (adjusted) FAC rates lead to scattering in the plot.

The results of Lertsurasakda et al. (2013) for 550 ppb NH_3 at 24% steam quality gave an adjusted FAC rate of 0.80 mm/y, which is close to the 0.91 mm/y found for 500 ppb NH_3 in this study. The adjusted rates during run 2 for 500 ppb NH_3 and 100 ppb AA before and after the upset are 0.99 and 0.96 mm/y respectively. These findings suggest that the proposed process to adjust rates was reasonable.

Based on the (adjusted) FAC rates, it can be observed that the addition of 50 or 100 ppb AA to a mix of 100 ppb ETA and 500 ppb NH_3 causes the FAC rate to go up from 0.57 to 0.69 and then further to 0.91 mm/y (at 24% steam quality, the same as the FAC rate with 500 ppb NH_3). This indicates that excessive amine decomposition, if it occurs in steam-water cycle in practice, will lead to an increase in FAC rate. The AA neutralizes mostly the ETA (because of the lower K and K_D) in the liquid film, leaving NH_3 for protection against FAC.

During run 2, addition of 100 ppb AA to 500 ppb NH_3 made the adjusted FAC rate increase from 0.91 to 0.99 mm/y, while the neutral rate was 1.97 mm/y. This indicates a very minor effect of AA on a steam water mixture that only contains NH_3 for corrosion protection at a steam quality of 24%. So the pH in the liquid film seems to be above neutral even after 100 ppb AA is added. This is confirmed by the model calculations; at this steam

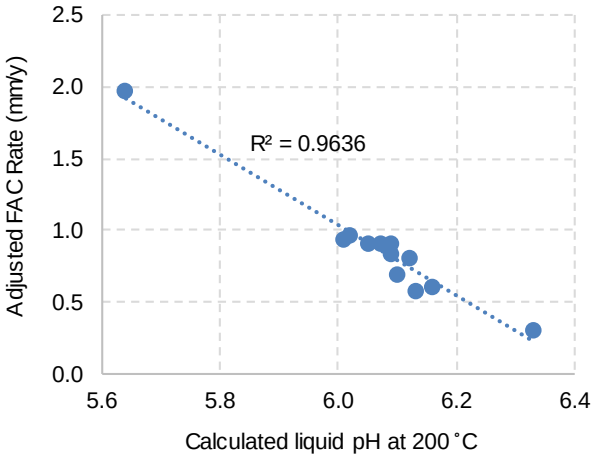

Figure 7.5: The calculated liquid film pH vs. the corresponding corrected FAC at 200 °C and 24.2% steam quality

quality NH_3 is not depleted in the liquid film and acidic conditions do not occur.

However, these results are only for the evaporative or flashing case of two-phase plug flow and not necessarily indicative of the reverse early condensation (such as would be experienced in the phase transition zone of a turbine or through the early parts of a condenser or heater shell). In addition, a higher steam quality could still lead to low pH in the liquid film pH in the absence of ETA.

To show what the theoretical effect of a much higher steam quality would be on the FAC rate, the liquid film pH model was used to calculate the liquid film pH for 90% steam quality. The results can be compared with results for 24% steam quality for all water chemistries in the last two columns of Table 7.3. From modelled results with NH_3 or ETA only, it can be concluded that the protection that NH_3 provides goes down with increasing steam quality, while for ETA the opposite happens. The liquid film pH when applying 500 ppb NH_3 at 200 °C and 90% steam quality is only 5.89, even without the presence of AA. The addition of 50 and 100 ppb AA decreases the liquid film pH further to 5.79 and 5.71 respectively. The subsequent addition of only 100 ppb ETA to the feedwater increases the protection against two-phase FAC and raises the liquid film pH by around 0.2. This theoretical approach for estimating high steam quality two-phase FAC indicates that the highest achievable steam quality in this study of 24% is not high enough to investigate the critical areas of a steam-water cycle.

The experimental and modelled results indicate that there are advantages of using ETA over NH_3 for pH control in steam-water cycles as long as ETA does not fully decompose under the conditions it is applied in. They also show that the presence of organic acid anions in a

steam-water cycle is more problematic when pH control is provided by NH_3 alone.

7.4 Conclusions

Based on the work shown in this chapter, the following conclusions can be drawn:

- FAC rates between separate runs or after an upset in conditions can vary, probably due to differences in conditions, probe diameter and/or metal composition of the probe.
- Adjusting FAC rates based on the rates found under defined (in this case neutral) conditions for each run provides a way to compare FAC rates that otherwise cannot be compared.
- The effect of acetic acid on the FAC rate was most pronounced at 24% steam quality.
- The addition of 100 ppb acetic acid to a feedwater containing 500 ppb NH_3 did not lead to acid conditions in the liquid layer film at 24% steam quality. The FAC rate increased by only 8% and was still well below the rate found under neutral conditions.
- Modelled results for liquid film pH at 90% steam quality suggests that at very high steam qualities the protection ETA provides increases, while the protection provided by NH_3 goes down and a steep liquid film pH drop may occur. This needs to be verified by studying two-phase FAC at around 90% steam quality as well.
- A linear relation between liquid film pH and the (adjusted) two-phase FAC rate at 24% steam quality and 200 °C is found in the pH range between 5.6 and 6.5.
- Therefore, mitigating two-phase FAC is a matter of maintaining sufficiently high liquid film pH.
- There are clear advantages of using ETA over NH_3 for pH control in steam-water cycles as long as ETA does not fully decompose under the conditions it is applied in.
- The presence of organic acid anions in a steam-water cycle is more problematic when pH control is provided by NH_3 alone.
- Formic acid was not stable at the temperatures that were reached in the feedwater heater, and decomposed too fast to observe an effect on the corrosion rate.

References

Bandura, A., & Lvov, S. (2006). The ionization constant of water over wide ranges of temperature and density. *Journal of Physical and Chemical Reference Data*, *35*(1), 15-30.

Bell, J., Wesolowski, D., & Palmer, D. (1993). The dissociation quotients of formic acid in sodium chloride solutions to 200 °C. *Journal of Solution Chemistry*, *22*(2), 125-136.

Cobble, J., & Lin, S. (1989). Chemistry of steam cycle solutions: Properties. In P. Cohen (Ed.), *The asme handbook on water technology for thermal power systems* (p. 551-658). New York, NY: ASME.

Cobble, J., & Turner, P. (1992). PWR advanced all-volatile treatment additives, by-products, and boric acid. *EPRI Report*, *TR-100755*, Palo Alto, CA.

EPRI. (1999). Steam, chemistry and corrosion in the two-phase transition zone of steam turbines. *EPRI Report*, *TR-108184-V1*, Palo Alto, CA.

EPRI. (2014). Control of corrosion in the steam turbine phase transition zone. *EPRI Report*, *3002000593*, Palo Alto, CA.

Fujie, H. (1963). A relation between steam quality and void fraction in two-phase flow. *AlChE Journal*, *10*(2), 227-232.

Hitch, B., & Mesmer, R. (1976). The ionization of aqueous ammonia to 300c in kcl media. *Journal of Solution Chemistry*, *5*(10), 667-680.

Layton, K. F., & Daniels, D. G. (2010). Interim guidance - amine treatments in fossil power plants. *EPRI Report*, *1019636*, Palo Alto, CA.

Lertsurasakda, C., Srisukvatananan, P., Liu, L., Lister, D., & Mathews, J. (2013). The effects of amine on flow-accelerated corrosion in steam-water systems. *PowerPlant Chemistry*, *15*(3), 181-189.

Lister, D. H., Lertsurasakda, C., & Srisukvatananan, P. (2013). Investigation of flow-accelerated corrosion under two-phase flow conditions. *EPRI Report*, *1023845*, Palo Alto, CA.

Mesmer, R., Patterson, C., Busey, R., & Holmes, H. (1989). Ionization of acetic acid in NaCl(aq) media: A potentiometric study to 573 K and 130 bar. *Journal of Physical Chemistry*, *93*(21), 7483-7490.

7.5 Appendix

7.5.1 Supporting tables

Table 7.4: Elemental composition of the Type A-106 Grade B carbon steel used for the probe in weight %

C	**Si**	**Mn**	**P**	**S**	**Cr**	**Mo**	**Fe**
0.20	0.31	0.62	0.020	0.012	0.019	0.004	98.815

Table 7.5: Relevant dissociation and distribution coefficients at 200 °C

Compound	K		K_D	
Acetic acid	$3.273 \cdot 10^{-6}$ (Mesmer et al., 1989)	(molL^{-1})	0.347 (Cobble & Lin, 1989)	(-)
Formic acid	$3.698 \cdot 10^{-6}$ (Bell et al., 1993)	(molL^{-1})	0.457 (Cobble & Lin, 1989)	(-)
Ammonia	$1.975 \cdot 10^{-6}$ (Hitch & Mesmer, 1976)	(molL^{-1})	6.918 Cobble & Lin (1989)	(-)
Ethanolamine	$8.984 \cdot 10^{-7}$ (Cobble & Turner, 1992)	(molL^{-1})	0.240 (Cobble & Turner, 1992)	(-)
Water	$5.591 \cdot 10^{-12}$ (Bandura & Lvov, 2006)	($\text{mol}^2\text{L}^{-2}$)		

7.5.2 Supporting figures

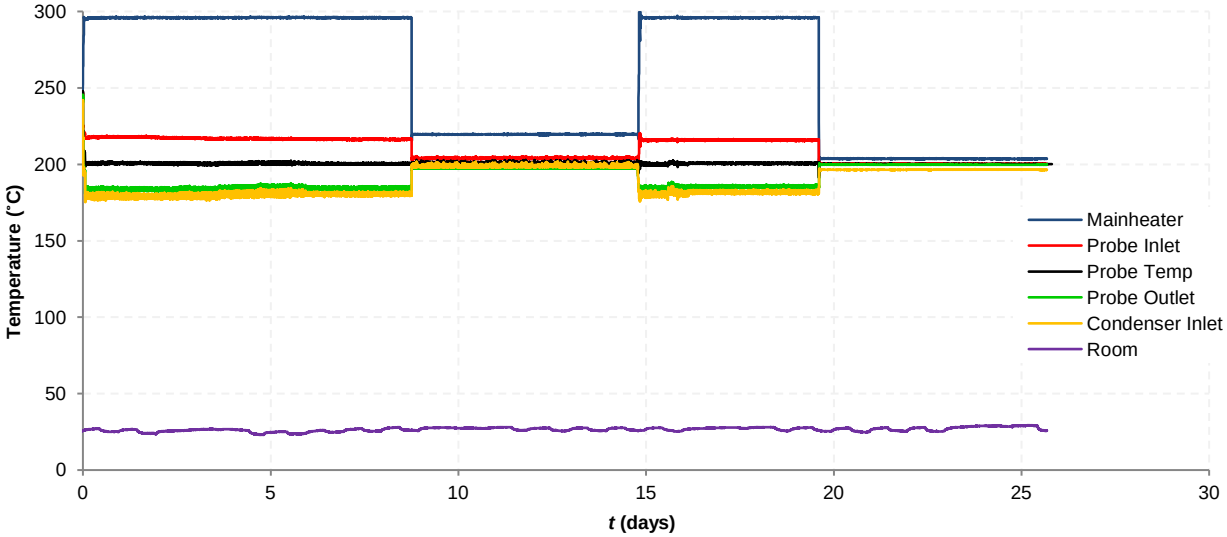

Figure 7.6: Temperature profile during run 1

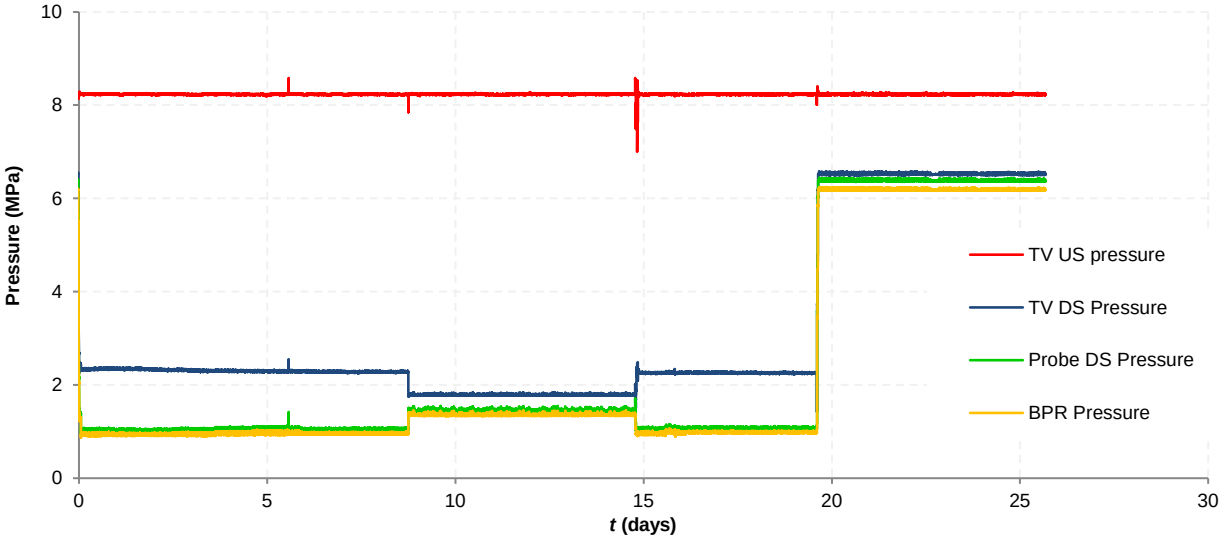

Figure 7.7: Pressure profile during run 1. TV = Throttle valve, DS = downstream, BPR = back pressure regulator

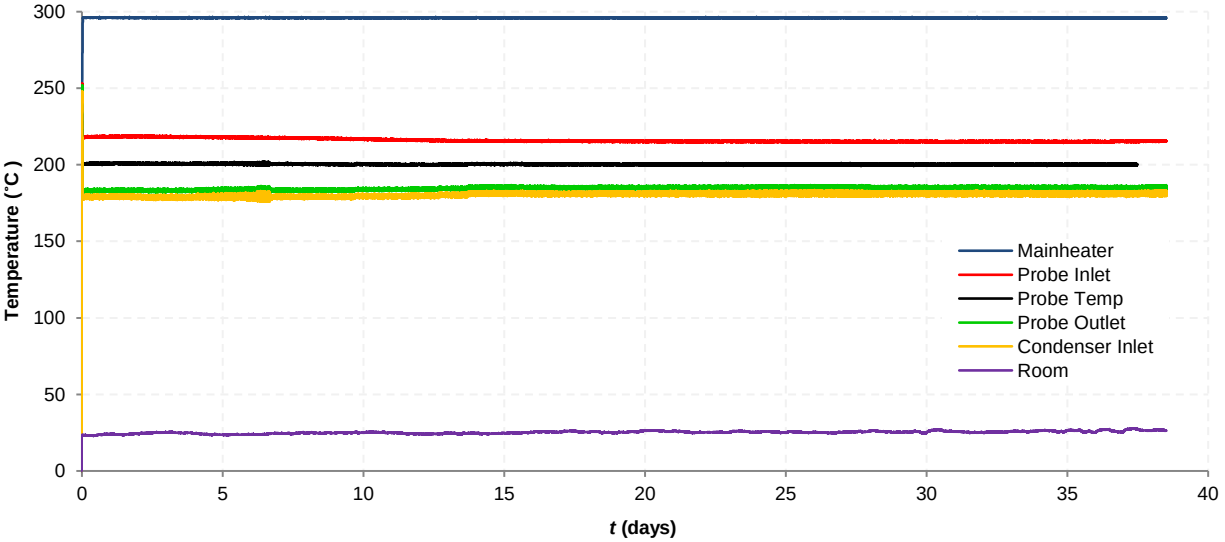

Figure 7.8: Temperature profile during run 2

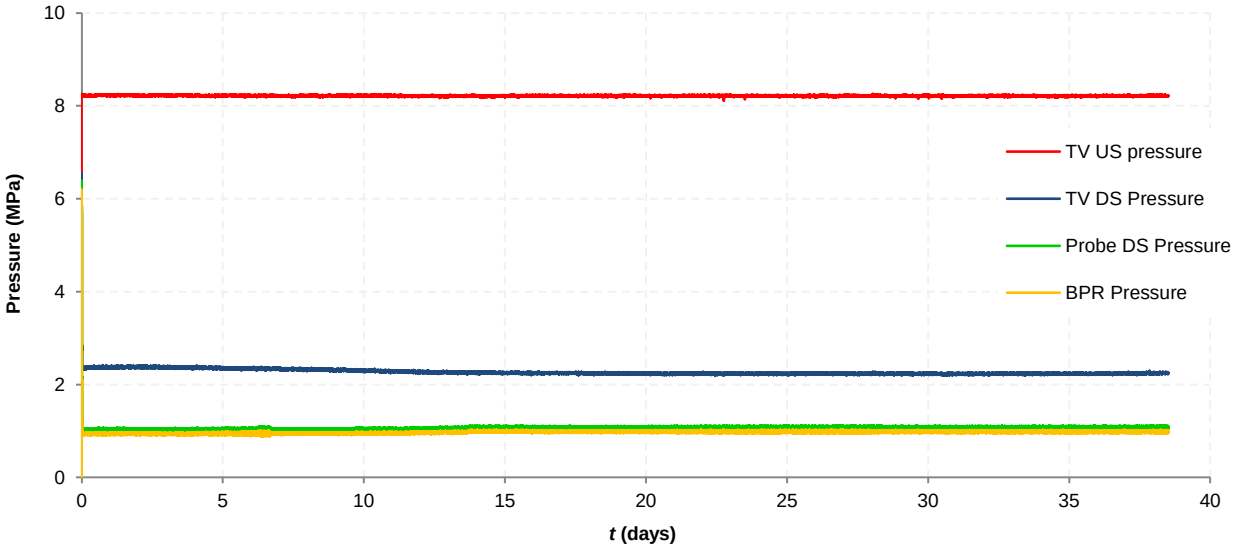

Figure 7.9: Pressure profile during run 2. TV = Throttle valve, DS = downstream, BPR = back pressure regulator

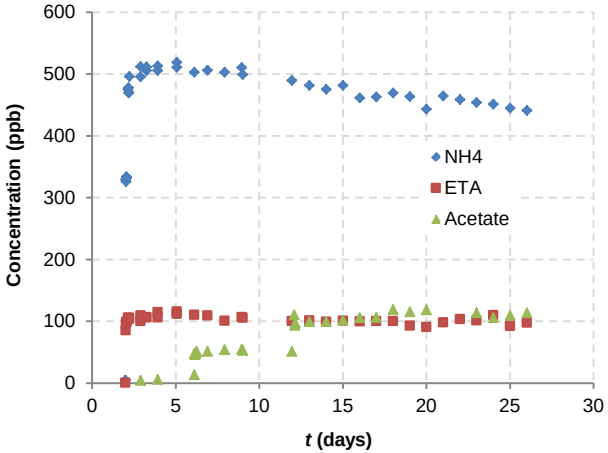

Figure 7.10: Concentrations of ions during run 1

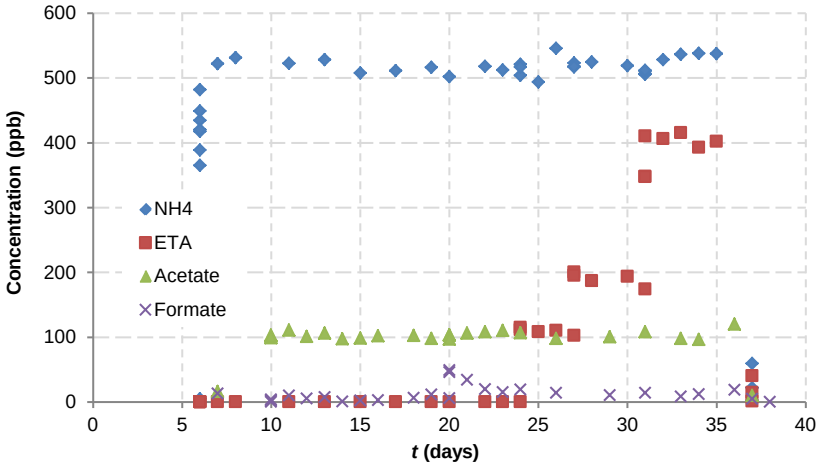

Figure 7.11: Concentrations of ions during run 2

7.5.3 Code for calculating pH in two-phase flow

```
% LiqpHcalcIterative.m
%
% This file takes concentrations (in ppb) and steam quality from a
% text file and uses it as input to calculate liquid film pH at 200 C.
% The result is printed in the same text file behind the concentrations.
%
% Build by D. Moed - April 2015
clc; clear all; close all;

%% INTPUT
filename = 'LiqpHcalcIterative.csv';

%% READ TEXT FILE
fid = fopen(filename);
HDRS = textscan(fid,'%s %s %s %s %s %s',1, 'delimiter',',');
DATA = textscan(fid,'%.10f %.10f %.10f %.10f %.10f %.10f','delimiter',',');
fclose(fid);

for ii = 1:size(DATA{1},1)

%% DEFINITIONS:

pKw = 11.28;
Kw = 10^(-pKw);

% Ammonia
pKb_Am = 5.241;
Kd_Am = 6.91831;
ppb_Am = DATA{1}(ii);
ppb_Am = max(ppb_Am,10^(-10));
MM_Am = 17.031;
C_Am = ppb_Am/(1000000*MM_Am);
```

```
Kb_Am = 10^(-pKb_Am);

% Ethanolamine
pKb_E = 5.206;
Kd_E = 0.240;
ppb_E = DATA{2}(ii);
ppb_E = max(ppb_E,10^(-10));
MM_E = 61.08;
C_E = ppb_E/(1000000*MM_E);
Kb_E = 10^(-pKb_E);

% Acetic acid
pKa_Ac = 5.522;
Kd_Ac = 0.347;
ppb_Ac = DATA{3}(ii);
ppb_Ac = max(ppb_Ac,10^(-10));
MM_Ac = 60.05;
C_Ac = ppb_Ac/(1000000*MM_Ac);
Ka_Ac = 10^(-pKa_Ac);

% Formic acid
pKa_F = 4.591;
Kd_F = 0.457;
ppb_F = DATA{4}(ii);
ppb_F = max(ppb_F,10^(-10));
MM_F = 46.03;
C_F = ppb_F/(1000000*MM_F);
Ka_F = 10^(-pKa_F);
%
SQ = DATA{5}(ii);
H = sqrt(Kw);

%INITIAL VOLATILITY:
```

```
RV_Am = Kd_Am;
RV_E = Kd_E;
RV_Ac = Kd_Ac;
RV_F = Kd_F;


%% Iteration
for k = 1000;

%CONCENTRATIONS:

C_Am_L = C_Am/(1-SQ+RV_Am*SQ);
C_E_L = C_E/(1-SQ+RV_E*SQ);
C_Ac_L = C_Ac/(1-SQ+RV_Ac*SQ);
C_F_L = C_F/(1-SQ+RV_F*SQ);

%CHARGE BALANCE SOLVER:

syms H
S = H + Kb_Am /(Kw/H + Kb_Am)*C_Am_L + Kb_E /(Kw/H + Kb_E)*C_E_L - Kw/H - Ka_Ac/(H + Ka_Ac)*C_A
solS = solve (S,H);
SolH = solS(solS>0);

%ION CONCENTRATIONS AND NEW VOLATILITIES

Am_ion = C_Am_L*Kb_Am/(Kw/SolH+Kb_Am);
RV_Am = Kd_Am*(1-(Am_ion/C_Am_L));
E_ion = C_E_L*Kb_E/(Kw/SolH+Kb_E);
RV_E = Kd_E*(1-(E_ion/C_E_L));
Ac_ion = C_Ac_L*Ka_Ac/(SolH+Ka_Ac);
RV_Ac = Kd_Ac*(1-(Ac_ion/C_Ac_L));
F_ion = C_F_L*Ka_F/(SolH+Ka_F);
RV_F = Kd_F*(1-(F_ion/C_F_L));
```

```
end

pH =-log10(SolH);
DATA{6}(ii)=pH;

end

%% WRITE TO FILE
fid = fopen(filename,'w+');
%write header
for ii=1:length(HDRS)
if ii>1
fprintf(fid,',');
end
fprintf(fid,'%s',char(HDRS{ii}));
end
% write data
for ii=1:size(DATA{1},1)
for jj=1:size(DATA,2)
if jj==1
fprintf(fid,'\n');
else
fprintf(fid,',');
end
if jj==size(DATA,2)
fprintf(fid,'%.2f',DATA{jj}(ii));
else
fprintf(fid,'%i',DATA{jj}(ii));
end
end
end
fclose(fid);
}
```

8

Concluding remarks

8.1 Organic contaminants degradation and organic acid formation

By using natural organic matter concentrate, the hydrothermolysis of organic contaminants found in virtually any steam-water cycle was investigated. As temperature increased, acetate became the dominant degradation product, due to its higher thermal stability than that of the other organic acids. Shorter retention times and lower temperatures led to more variety and quantity of organic acid anions, because the thermally less stable acids do not have sufficient time (and temperature) to degrade. The presence of oxygen decreased the stability of organic acids because oxidation is faster than hydrothermolysis (this was found to be the case for amines as well). A linear decrease in organic matter input did not lead to a linear decrease in organic acids; relatively more organic acid anions were formed at lower organic matter influent concentrations. This could mean that decomposition kinetics of natural organic matter are not of the first order. It could also mean that there was a background concentration of organic carbon contamination in the influent.

When testing the thermal stability and decomposition kinetics of acetic acid in the superheater at 500, 530 and 560 °C and 9.5, 13.5 and 17.5 MPa, it had the highest thermal stability of all investigated chemicals. This again underlines the reason why acetate is the dominant organic acid anion in high temperature and high pressure systems. The thermal stability of formic acid was determined in this study as well, and was lower than expected. At 335 °C and 13.5 MPa it took only 101 seconds for 67% of formic acid to degrade, while at 400 °C and 13.5 MPa it took less than 9 seconds until only 2% of the dosed formic acid concentration remained. Therefore, it is surprising that formic acid can be found in the experiments conducted in this thesis and in full-scale high-temperature steam-water cycles. The fact that formic acid is found can only be explained by formation during the condensing stages, from CO_2 and H_2 or CO and H_2O. This is also an explanation why formic acid is reported to be present in inexplicably varying concentrations in power plants. Using these laboratory results, rough estimations of quantity and quality of the organic acids formed from organic matter hydrothermolysis can be made, based on the operating temperatures and organic carbon concentration in a steam-water cycle.

A laboratory study with contaminants found in petrochemical steam-water cycles was also performed, under both superheater and boiler conditions. The contaminants monoethylene glycol, polyethylene glycol and slurry oil led to an increase in organic acid anion concentrations. Therefore, condenser leaks and insufficiently treated return condensate are both a possible source for organic carbon and organic acid anion contamination. The (hydro)thermolysis of the water dissolvable fraction of gasoil, naphtha and hydro wax led to organic acid anion concentrations that only slightly exceeded the blank results. The obtained results can be used by the petrochemical industry to evaluate which sources of organic contamination in their steam-water cycles should be prevented.

Methyl ethyl ketoxime thermally degraded into several organic acid anions and nitrite in the higher ppb or lower ppm range. Where steam quality needs to be high, methyl ethyl ketoxime has to be applied with care. The

species and concentration of the different formed anionic degradation products was strongly dependent on temperature and retention time for all tested compounds. Formate was dominant at the lowest temperatures, whereas acetate (and in one case propionate) was highest in quantity at the highest tested temperatures.

8.2 Amine (hydro)thermolysis

The investigation of amine thermolysis at steam-water cycle conditions consisted of three parts. The first part of the study started with investigating the suitability of the flow reactor for investigating amine decomposition kinetics by testing the thermal stability of morpholine at both boiler and superheater conditions. The experimental setup proved to provide accurate control of temperature, pressure and retention time, enabling the investigation of kinetic reactions. It was also concluded that thermolysis in the superheater is more important than in the boiler, which matches observations from practice. In addition, kinetics of morpholine thermolysis under superheater conditions were of first order. Degradation kinetics increased with temperature and decreased with increasing pressure, while concentrations of acidic degradation products increased linearly with the morpholine degradation percentage. Morpholine decomposition kinetics were higher than expected based on accounts in the literature. It was hypothesized that catalytic effects of the metal surface in the flow reactor increased morpholine thermolysis. The metal tubes used in the flow reactor were small, with a surface:volume ratio of 4.56 mm^{-1}, at least 10 times larger than in a full-scale installation.

The second part of the study on amine thermal stability tested the hypothesis of the metal surface having a catalytic effect on amine thermolysis, by applying four different tube diameters made of two different materials. All 8 tubes were tested with ethanolamine, morpholine and at two different superheat temperatures. Results showed that there was indeed an influence of the metal oxides on the inner tube wall on amine thermolysis kinetics, with degradation rates decreasing as the tube size increased. The relation between the surface:volume ratio and the degradation rate constant k was linear. Metal surface catalysis during thermolysis of MOR and ETA accounted for 82-92% of the value of the degradation rate constant at a surface:volume ratio of 4.65 mm^{-1}. The contribution of the metal surface catalysis decreased to only 6-17% at a surface:volume ratio of 0.4 mm^{-1}. A distinction between homogeneous and heterogeneous thermolysis could be made, but results indicated that a lab study with a small enough surface:volume ratio will lead to more reliable predictions of thermolysis in practice, because results obtained with larger surface:volume ratios produced larger errors. Although results varied between the two applied tubing materials, there was no consistent trend that can link thermolysis kinetics to tube wall composition. Still, organic acid production was weakly related to amine structure, temperature and tube diameter, but strongly related to metal oxide composition, with formate and acetate altering as dominant organic acid anion.

The third study on amine thermolysis produced the Arrhenius constants necessary to model amine decomposition in steam-water cycles. This was done by using the flow reactor with tubes with a small

surface:volume ratio and testing the more commonly applied alkalizing amines: ethanolamine, morpholine, 3-methoxypropylamine, cyclohexylamine and dimethylamine at 500-560 °C and 9.5-17.5 MPa. All amines showed first order thermolysis kinetics, with the exception of dimethylamine. Activation energy, the pre-exponential factor and activation volume were determined from reproducible data. The influence of pressure on thermolysis kinetics was less pronounced than in the study that used a much smaller tube diameter. Whether that is a consequence of the smaller surface:volume ratio remains unclear. Still, pressure is a variable to take into consideration when assessing the applicability of alkalizing amines in steam-water cycles. The obtained degradation rate constants of morpholine and ethanolamine at 500 °C and 13.5 MPa were close to what was expected based on results in Chapter 4. Any further attempts to compare data from Chapter 5 with Chapters 3 and 4 has not been made, because the different surface:volume ratios caused to much uncertainty. Dimethylamine did not degrade completely (in fact, degradation percentages did not surpass 80 and 90% at 500 and 530 °C respectively, in spite of longer retention times being applied compared to those of other tested amines). This suggests that synthesis of dimethylamine may occur, either at high temperature or in the condensing stages, for instance from ammonia and methanol. If this is the case, dimethylamine can be suitable for power plant applications despite its low thermal stability.

In all cases, thermolysis of the amines led to the formation of organic acid anions. In most cases, the concentrations increased linearly with increasing amine degradation percentage. Acetate and formate (the latter despite its low thermal stability) were found as major degradation products, with some propionate and traces of glycolate present. Most of the nitrogen from decomposed amines could be traced back to cationic degradation products consisting of mostly ammonia and some amines. This means that the complete thermolysis of an amine does not necessarily lead to acidic conditions. Only where the molar concentration of organic acids exceeds that of ammonia, or in two-phase flow, acidic conditions will occur. Not all nitrogen could be traced back to these cationic degradation products, suggesting that some other inorganic nitrogen species were formed, or ammonia was lost during sampling.

The obtained activation energy, the pre-exponential factor and activation volume were used to create a model for amine decomposition in steam-water cycles. Comparing the model to scarcely available practical measurements of amines in power plants shows promise of the model applicability to full-scale steam-water cycles. The results in this study can also be used to get an indication of which organic acid anion by-products can be expected in practical applications.

8.3 Organics and two-phase FAC

To investigate the impact of the (hydro)thermolysis in steam-water cycles, two-phase FAC experiments were conducted with varying chemistries and steam qualities. Results showed a linear relation between liquid film pH and the two-phase FAC rate at a steam quality of 24%. Expanding the liquid film pH model to higher steam qualities gave an idea of the dangers of high acetate concentrations in steam-water cycles. If the acetate concentration exceeds the ethanolamine concentration, for example

due to excessive thermolysis in the superheater, alkalinity in the two-phase zone would be provided by ammonia only. This means that the maximum allowable percentage of ethanolamine decomposition can be determined, which in turn could be linked to superheat temperature based on the model for amine thermolysis described in this thesis. When conventional all-volatile treatment is applied in a steam-water cycle, acetic acid should be kept at a minimum, to prevent low liquid film pH in moisture transition zones.

8.4 Methods for investigating (hydro)thermal reactions

Different methods can be envisaged to investigate hydrothermal reactions (simulating boilers), and one of the objectives of this thesis was to determine which methods are most suitable for investigating hydrothermal organic reactions in dilute solutions. Most studies on amine stability found in the literature used autoclaves. Although an autoclave might seem like the most reasonable way to simulate a process in a boiler due to its simplicity, the heating rate and large dead volumes during sampling can make it hard to determine kinetics of reactions that occur very fast. It was found that a lower heating rate of the autoclave gives more organic acid anions as degradation products, both in quantity and variety. The autoclave used in this study took over 75 minutes to fully heat the water inside, a time frame which far exceeds the time it takes feedwater to do the same in a boiler in a full-scale plant. Therefore, such an autoclave is not representative for full-scale boilers. The slow heating issue can be addressed by introducing the solution or chemicals of interest to a stirred autoclave when it is already at temperature. However, because it takes more than a few seconds to get a sample out of the autoclave it will still hinder the proper investigation of processes with fast kinetics, like the decomposition of amines. On top of that, an autoclave will be unsuitable for creating superheater conditions. Therefore, an alternative setup was also investigated in this research. The alternative to the autoclave, the flow reactor, was shown in Chapter 2 to provide results that were more representative for steam-water cycles when comparing lab results to a case-study. The morpholine (hydro)thermolysis study in Chapter 3 showed that the flow reactor had sufficiently high heating rate and that temperature, pressure and retention time could be accurately controlled.

8.5 Limitations and uncertainties in this study

Using the results on NOM hydrothermolysis and the thermal stability of acetic and formic acid, rough estimations of quantity and species of the organic acid anions can be made, based on the operating temperatures and organic carbon concentration in a steam-water cycle. However, due to the complex and varying nature of natural organic matter in different source waters, corresponding hydrothermal reactions and the complexity of steam-water cycles, there is a degree of uncertainty to take into consideration. The natural organic matter used in this thesis was all nonionic, but does not distinguish between large and small neutral organic matter. Cycles of concentration in a boiler due to make-up water addition and blowdown, combined with organic acid thermal stability also influence organic acid anion concentrations in a steam-water cycle. The presence of formic acid despite

its limited thermal stability makes matters even more complex. The precise prediction of formation of organic acid anions from organic contaminants will therefore be site specific. No attention has been given to the nonionic decomposition products and their possible impact on the steam-water cycle, but whether they have any relevance is yet to be proven. Knowing which nonionic decomposition products exist, might give deeper insights in the decomposition mechanisms though.

The (hydro)thermolysis of the water dissolvable fraction of gasoil, naphtha and hydro wax led to organic acid anion concentrations that only slightly exceeded the blank results. However, these fractions might not be completely relevant to the real-world situation. In a petrochemical plant it is not the condensate, but the hot steam that comes in contact with the process. The return condensate might therefore be different in nature from the solutions created in the laboratory. The results on which the model for amine thermolysis was based were consistent and reproducible. Unfortunately, due to the limited data for amine stability from full-scale steam-water cycles, the model could not be validated well. A larger dataset and more information on superheater retention times are thus necessary. If such a dataset were available to validate the model, the model could be used to set guidelines for alkalizing amine applications in fossil-fired plants. Wall effects where wall temperature is much higher than that of the bulk fluid also need more attention, because the main difference between the laboratory experiments and amine thermolysis in a full-scale plant is that at full-scale there is a larger temperature gradient over the length of the superheater tube and through the tube wall. Especially in conventional fossil-fired plants, heat flux is high and wall effects could become more dominant than was assumed in this study. Combined cycle plants with duct burners have high heat-flux through the tube wall as well. Despite the fact that the flow reactor is good for mimicking feedwater heater and superheater conditions, it does not directly simulate a large conventional boiler very well, because the tubes in the flow reactor have a higher surface: volume ratio. Therefore, wall effects can play a larger role in the flow reactor than would be the case in a large industrial boiler. This might have influenced results from the NOM and petrochemical contaminant hydrothermolysis study. In addition, volatile decompositions products might have dissipated from samples during grab sampling as soon as the sample comes into contact with air. If the complete reaction mechanism resulting in degradation products, including dissolved gases like CO_2, needs to be understood, grab sampling will no longer suffice because the composition of a sample can change as soon as it is cooled down, exposed to air or when the pressure is reduced. In that case a spectroscopic flow cell can prove very handy, because it enables the direct measurement of a large number of compounds, both neutral and ionic.

The experimental two-phase FAC loop used in this study produced different FAC rates, even when the same operational conditions were applied. This might be related to the composition of the probe, or the probe diameter, which might be slightly different between two individually produced probes. Although for the majority of the 70 days that the loop was running, stable conditions could be maintained, there was also an upset that caused the FAC rate to change while feed water chemistry remained the same, the reasons for which are unknown.

Correcting obtained FAC rates based on the rate found at neutral conditions provided a way of comparing the results of runs conducted under slightly different circumstances, but this is far from ideal. The underlying cause of the lack of reproducibility needs to be understood in the future, before attempts can be made at improving loop stability and reproducibility. Also, the tested steam quality was not high enough to create the conditions in which ammonia provided insufficient protection against acetic acid. Tests with higher steam quality are necessary to validate the findings in this thesis on FAC and liquid film pH.

8.6 Practical implications of the thesis results

The main objective of this thesis was to contribute to well-founded guidelines for organic contaminants and alkalizing amine application in steam-water cycles. Although setting these guidelines solely based on this thesis is not possible, the results that have been presented do have practical implications.

The two-phase FAC experiments and modelling of the pH in the liquid film indicate that at lower steam quality (¡ 25%), pH depressions by acetic acid will hardly occur in a steam-water cycle that uses only ammonia for pH control. At higher steam qualities (the end of a flashing stage or first condensation) the advantages of ethanolamine over ammonia become more evident, because ammonia does not provide proper pH control, even without the presence of acetic acid. Since ammonia is a decomposition product of amines, the application of amines can be justified as long as the remaining molar amine concentration exceeds that of all organic acids in the steam.

Whether the latter is the case can be assessed with the amine stability model proposed in this thesis, which should provide upper limits at which amines can be applied. This is only possible, though, after the model has been validated in practice. What should be considered is that, in this study, ethanolamine and ammonia were both dosed to reach a pH of 9.2 in the feedwater (i.e., at 1500 and 500 ppb respectively). In terms of costs for chemical consumption, the option of increasing the ammonia dosage should also be considered. Although ammonia will still not provide the same protection as ethanolamine in two-phase flow, it will be cheaper and thermally more stable. Making such economic considerations is not an objective of this thesis, but the models for calculating liquid film pH in two-phase and amine stability flow can assist in assessing what is the most cost-efficient treatment while maintaining proper pH control.

When ammonia is the only dosed chemical for pH control, limiting organic contamination in steam-water cycles becomes more important. This thesis describes which organic acid anions can be expected from organic contaminants, based on process conditions and natural organic matter in the feedwater, in more general terms. When playing it safe, reverse osmosis treatment and condensate polishing should be applied for boiler feedwater water to keep organic contamination at a minimum.

In an industrial (petrochemical) steam-water cycle, limiting organic contamination is hard, because of exposure of the steam to the process and the recycling of condensate from these processes, often without proper treat-

ment. Emphasis in practice should therefore be put on either improving condensate polishing or applying more advanced water treatment chemicals. Alternatively, a high percentage of condensate could be discharged instead of going back into the cycle. This will depend on investment and operational costs, but also on demands of (for instance) turbine suppliers. If proven cost-effective, condensate that has been in contact with slurry oil or (poly)ethylene glycol could be treated separately to decrease make-up water requirements. When advanced treatment chemicals are applied, methyl ethyl ketoxime should dosed carefully, because of its limited thermal stability and the release of nitrite and organic acid anions.

8.7 Suggestions for future studies

To further assist the establishment of well-founded guidelines for organic contaminants in boiler make-up and treatment chemicals in steam-water cycles, several phenomena highlighted in this thesis need more research. Laboratory experiments that could further expand the knowledge include:

- Investigating the influence of high heat flux through superheater tubes on amine decomposition, thereby getting a better understanding of wall effects in fossil-fired plants and plants with duct burners. This could be done by making a small scale superheater in which wall and exhaust temperature can be controlled.
- Investigating amine decomposition kinetics in supercritical water. Supercritical water has different properties from sub-critical water and supercritical systems could very well suffer from increased amine decomposition in the boiler. This also gives room for investigating the influence of concentration and pH on the kinetics of hydrothermolysis, something that was not relevant during thermolysis in superheater steam.
- Further determining the decomposition mechanism of dimethylamine and find out if it persists in a steam-water cycle in spite of its apparent low thermal stability, by conducting experiments with a spectroscopic flow cell at high temperature and pressure.
- Studying two-phase FAC at higher steam qualities. This could also provide validation of the model used to predict the pH of the liquid film.
- Investigating the thermal stability of film-forming amines, which have very different properties than alkalizing amines and protect systems by creating a protective film on the metal.

More practical studies that can expand the current knowledge include:

- A plant survey that compares natural organic matter concentrations and fractions in the make-up with organic acid concentrations found in the steam-water cycle, as a function of temperature, retention time and blowdown, could provide a better foundation for an organic carbon guideline in the make-up water.
- A large plant survey amongst steam-water cycles that apply alkalizing amines, in which amine concentrations are monitored in several sections of the plant along with temperature, pressure and retention times, could provide the necessary validation for the amine decomposition model.

List of Publications

van Halem, D., Moed, D.H., Verberk, J.Q.J.C., Amy, G.L., van Dijk, J.C. **(2012)** Cation Exchange During Subsurface Iron Removal. *Water Research*, 46 (2), 307-315

Moed, D.H., Van Halem, D., Verberk, J.Q.J.C., Amy, G.L., Van Dijk, J.C. **(2012)** Influence of Groundwater Composition on Subsurface Iron and Arsenic Removal. *Water Science and Technology*, 66 (1), 173-178

Moed, D.H., Verliefde, A.R.D., Rietveld, L.C. and Heijman, S.G.J. **(2013)** Degradation Kinetics of Six Alkalizing Amines. *16th International Conference on the Properties of Water and Steam*, London, United Kingdom

Moed, D.H., Verliefde, A.R.D., Rietveld, L.C. and Heijman, S.G.J. **(2014)** Organic Acid Formation in Steam-Water Cycles: Influence Of Temperature, Retention Time, Heating Rate and O2. *Applied Thermal Engineering*, 65 (2), 194-200

Moed, D.H., Verliefde, A.R.D., Heijman, S.G.J. and Rietveld, L.C. **(2014)** Thermolysis of Morpholine in Water and Superheated Steam. *Industrial & Engineering Chemistry Research*, 53 (19), 8012-8017

Moed, D.H., Verliefde, A.R.D. and Rietveld, L.C. **(2014)** Role of Metal Surface Catalysis in the Thermolysis of Morpholine and Ethanolamine under Superheater Conditions. *Industrial & Engineering Chemistry Research*, 53 (50), 19392-19397

Moed, D.H., Verliefde, A.R.D. and Rietveld, L.C. **(2015)** Effects of Temperature and Pressure on the Thermolysis of Morpholine, Ethanolamine, Cyclohexylamine, Dimethylamine, and 3Methoxypropylamine in Superheated Steam. *Industrial & Engineering Chemistry Research*, 54 (10), 2606-2612

Moed, D.H., Verliefde, A.R.D., Muller E. and Rietveld L.C. **(2015)** Sources of Anionic Organic Contamination in Petrochemical Steam-Water Cycles. *Industrial Water Treatment*, 32 (2), 33-42

Moed, D.H., Weerakul, S., Lister, D.H., Leaukosol, N., Rietveld L.C. and Verliefde, A.R.D. **(2015)** Effect of Ethanolamine, Ammonia, Acetic Acid and Formic Acid on Two-Phase Flow Accelerated Corrosion in Steam-Water Cycles. *Industrial & Engineering Chemistry Research*, 54 (36), 8963-8970

Curriculum Vitae

David Moed, born on the 7th of May, 1986 in Amersfoort, the Netherlands, completed a Bachelor's degree in civil engineering at the Delft University of Technology between 2005 and 2008. Having a keen interest in water quality and treatment, he went on to do the Master Watermanagement at the same faculty and focused on drinking water and wastewater treatment. When finishing the Masters degree in 2011, a PhD-position at the Watermanagement department of the TU Delft was offered, the subject of which could be anything related to cooling towers or steam-water cycles. The chosen subject, organic contaminants and treatment chemicals in steam-water cycles, has provided David with very specific and broader insights in how water and its constituents behave in these systems. David continues to pursue a career revolving around water technology, both for water consumption and industrial use.